Generation and characterization of new breast cancer mouse models expressing *PIK3CA* mutants

Inauguraldissertation

zur

Erlangung der Würde eines Doktors der Philosophie

vorgelegt der

Philosophisch-Naturwissenschaftlichen Fakultät

der Universität Basel

von

Dominique Stephan Meyer

aus Basel

Leiter der Arbeit: Dr. Mohamed Bentires-Alj

Friedrich Miescher Institute for Biomedical Research, Basel

Basel, 2012

Originaldokument gespeichert auf dem Dokumentenserver der Universität Basel
edoc.unibas.ch

Dieses Werk ist unter dem Vertrag „Creative Commons Namensnennung-Keine kommerzielle Nutzung-Keine Bearbeitung 2.5 Schweiz“ lizenziert. Die vollständige Lizenz kann unter **creativecommons.org/licences/by-nc-nd/2.5/ch** eingesehen werden

Namensnennung-Keine kommerzielle Nutzung-Keine Bearbeitung 2.5 Schweiz

---

Sie dürfen:

das Werk vervielfältigen, verbreiten und öffentlich zugänglich machen

Zu den folgenden Bedingungen:

Namensnennung. Sie müssen den Namen des Autors/Rechteinhabers in der von ihm festgelegten Weise nennen (wodurch aber nicht der Eindruck entstehen darf, Sie oder die Nutzung des Werkes durch Sie würden entlohnt).

Keine kommerzielle Nutzung. Dieses Werk darf nicht für kommerzielle Zwecke verwendet werden.

Keine Bearbeitung. Dieses Werk darf nicht bearbeitet oder in anderer Weise verändert werden.

- Im Falle einer Verbreitung müssen Sie anderen die Lizenzbedingungen, unter welche dieses Werk fällt, mitteilen. Am Einfachsten ist es, einen Link auf diese Seite einzubinden.
- Jede der vorgenannten Bedingungen kann aufgehoben werden, sofern Sie die Einwilligung des Rechteinhabers dazu erhalten.
- Diese Lizenz lässt die Urheberpersönlichkeitsrechte unberührt.

Die gesetzlichen Schranken des Urheberrechts bleiben hiervon unberührt.

Die Commons Deed ist eine Zusammenfassung des Lizenzvertrags in allgemeinverständlicher Sprache: http://creativecommons.org/licenses/by-nc-nd/2.5/ch/legalcode.de

Haftungsausschluss:
Die Commons Deed ist kein Lizenzvertrag. Sie ist lediglich ein Referenztext, der den zugrundeliegenden Lizenzvertrag übersichtlich und in allgemeinverständlicher Sprache wiedergibt. Die Deed selbst entfaltet keine juristische Wirkung und erscheint im eigentlichen Lizenzvertrag nicht. Creative Commons ist keine Rechtsanwaltsgesellschaft und leistet keine Rechtsberatung. Die Weitergabe und Verlinkung des Commons Deeds führt zu keinem Mandatsverhältnis.

Quelle: http://creativecommons.org/licenses/by-nc-nd/2.5/ch/ Datum: 3.4.2009

Genehmigt von der Philosophisch-Naturwissenschaftlichen Fakultät

auf Antrag von

Dr. Mohamed Bentires-Alj Prof. Dr. Nancy Hynes Prof. Dr. Christoph Rochlitz

Basel, den 18.10.2011

Prof. Dr. Martin Spiess

Table of Content

Contents

Table of Content **3**

Abstract **6**

Introduction **7**

1. The Mammary Gland 7

1.1 Mammary gland development and physiology 7

1.2 The mammary gland cell hierarchy 8

2. Breast Cancer 9

2.1 Breast cancer prevalence 9

2.2 Breast cancer classification 10

3. PI3K Signaling 12

3.1 PI3K classification 12

3.2 Structure of Class I PI3Ks 13

3.3 The Growth factor receptor/PI3K/Akt signaling axis 14

3.4 PI3K signaling mediates cell survival and cell cycle progression 16

3.5 PI3K signaling regulates protein synthesis 16

3.6 PI3K signaling controls metabolism 17

4. The PI3K pathway in normal mammary gland physiology 17

4.1 The roles of Akt isoforms in normal mammary gland physiology 17

4.2 The roles of PTEN in normal mammary gland physiology 19

4.3 The effects of p110α on normal mammary gland physiology 19

5. PI3K pathway in mammary gland tumorigenesis 20

5.1 Akt isoforms in mammary gland tumorigenesis 20

5.2 PTEN in mammary gland tumorigenesis 20

5.3 p110α in mammary gland tumorigenesis 21

6. PI3K in breast cancer 21

6.1 PIK3CA mutations are oncogenic 21

6.2 Different mechanisms lead to hyperactivity of p110α hotspot mutants 24

6.3 PIK3CA mutations in human breast cancer 25
6.4 Association of PIK3CA mutations with clinicopathological markers 26
6.5 PIK3CA mutations and patient outcome 28
Rationale and Aims of the Work 29
Part I: *PIK3CA* H1047R Induces Heterogeneous Mammary Carcinomas 30
Results and discussion of the published manuscript "Luminal Expression of *PIK3CA* Mutant H1047R in the Mammary Gland Induces Heterogeneous Tumors" 31
Expression of PIK3CA H1047R in luminal mammary epithelial cells induces carcinomas 31
WAPiCre H1047R and MMTV-Cre H1047R-evoked mammary tumors are heterogeneous 39
Part II: *PIK3CA* E545K and H1047R Induce Mammary Carcinomas with Different Latencies ... 45
Results 46
WAPiCre E545K but not PIK3CA wild-type mice form mammary tumors 46
Discussion and Outlook 47
Part III: Total Body Expression of Mutant *PIK3CA* Results in Premature Death and Alters Mammary Epithelial Cell Properties 49
Results 50
Whole body expression of mutant PIK3CA is lethal 50
CAGS-CreERT2 H1047R-derived mammary epithelial cells exhibit increased sphere-forming capacity 54
Expression of H1047R results in an accumulation of a mammary epithelial cell population enriched in ER-negative cells 55
CAGS-CreERT2 H1047R mutant MECs produce aberrant outgrowths and mammary tumors eventually 57
Discussion and Outlook 58
Summary and Outlook 63
Material and Methods 64
Transgenic Mice 64
Immunohistochemistry 64
Protein Analysis 65
Statistical analysis 65
Southern Blot 65
RT-PCR 65

MEC isolation and mammosphere assay 66

FACS analysis 66

Acknoledgements **67**

References **69**

Appendix **77**

Manuscript: Luminal Expression of PIK3CA Mutant H1047R in the Mammary Gland Induces Heterogeneous Tumors 78

Viewpoint: Can phosphatidylinositol 3-kinase/mammalian target of rapamycin inhibition Erase them all? 88

Frimorfo Report 93

Curriculum Vitae 104

Abstract

The PI3K signaling cascade, a key mediator of cellular survival, growth and metabolism, is frequently altered in human cancer. Activating mutations in *PIK3CA*, which encodes the alpha catalytic subunit of PI3K, occur in ~30% of breast cancers. These mutations result in constitutive activity of the enzyme and are oncogenic but it was not known whether they are sufficient to induce mammary carcinomas in mice. In this work, we generated mice conditionally expressing mutant *PIK3CA* H1047R in the luminal mammary epithelium targeted by either an MMTV or a WAP promoter. We demonstrated that expression of *PIK3CA* H1047R evokes heterogeneous tumors that express luminal and basal markers and are positive for the estrogen receptor. Additionally, we showed that such *PIK3CA* H1047R expression leads to a dramatic delay in mammary gland involution and that parity accelerates *PIK3CA* H1047R-induced carcinogenesis. Our results suggest that the *PIK3CA* H1047R oncogene targets a multipotent progenitor cell and show that this model recapitulates features of human breast tumors with *PIK3CA* H1047R.

We further showed that WAP targeted expression of another *PIK3CA* mutant, E545K, also induces mammary tumors, albeit with a longer tumor latency. Interestingly, luminal expression of wild type *PIK3CA* does not result in tumor formation, demonstrating that the *in vivo* tumorigenicity of mutant *PIK3CA* is caused by the mutation rather than overexpression.

Expression of *PIK3CA* mutations in all cells of the mouse leads to premature death. The mice develop multiple hematomas underneath the skin once they express mutant *PIK3CA*, however, no defect in the blood coagulation cascade or platelets was discovered and the exact cause of death remains unknown.

Mammary epithelial cells (MEC) from *PIK3CA* mutant mice had enhanced sphere-forming capacity with respect to both, size and frequency. In addition, when transplanted into a cleared fat pad, H1047R mutant epithelial cells partially reconstitute the gland and form hyperplasias that progress to carcinomas.

Introduction

1. The Mammary Gland

1.1 Mammary gland development and physiology

Since the human breast is not readily accessible for research only little is known about human breast development (Howard and Gusterson 2000). Therefore, much of our knowledge about mammary gland biology comes from extensive studies on the mouse mammary gland which is thought to be regulated by growth patterns and control mechanisms comparable to those of the human breast (Cardiff and Wellings 1999). A unique feature of the mammary gland with respect to other organs is the fact that much of its developmental processes occur postnatally during puberty and later during reproductive cycles.

After birth the mammary epithelium consists of a rudimentary ductal tree embedded in a stromal environment called the mammary fat pad. With the onset of puberty and the secretion of the ovarian hormones estrogen and progesterone, the tips of this rudimentary ductal system enlarge forming specialized structures called terminal end buds (TEB) which further branch and fill the mammary stroma. TEBs are highly proliferative and a monolayer of stem cells within the cap cells of the TEBs gives rise to the two major cell types of the bi-layered mammary gland epithelium. Luminal epithelial cells form the inner layer and secrete milk during lactation. The luminal cells are surrounded by contractile myoepithelial cells which squeeze the secreted milk (Silberstein 2001).

During pregnancy several hormones including progesterone and prolactin induce massive tissue remodeling characterized by ductal branching and extensive cell proliferation to form the alveoli, the functional units of the mammary gland which secrete milk. By the end of pregnancy the mammary epithelium fills out the whole mammary fat pad (Silberstein 2001; Oakes, Hilton et al. 2006). After lactation the mammary gland undergoes tissue remodeling called involution, during which the secretory alveoli collapse and massive epithelial cell death

occurs while the adipocytes gradually increase in volume (Watson 2006). The involuted mammary gland resembles that of a virgin mouse and is ready to go through another reproductive cycle.

1.2 The mammary gland cell hierarchy

Adult stem cells have the capability to produce all the cell types of a given organ. In the mammary gland adult stem cells have been described by their ability to reconstitute a functional gland when donor mammary tissue fragments or even a single cell was transplanted into an epithelium-free fat pad (Deome, Faulkin et al. 1959; Kordon and Smith 1998; Shackleton, Vaillant et al. 2006; Stingl, Eirew et al. 2006; Sleeman, Kendrick et al. 2007).

Transplantation experiments led to the identification of cells capable of forming either ductal- or lobule-limited outgrowths. While lobuloalveolar progenitors lack cap cells at the tip of TEBs and are therefore unable to penetrate the fat pad, ductal progenitors fill the fat pad but fail to undergo lobuloalveolar development during pregnancy (Kordon and Smith 1998; Bruno and Smith 2010).

The combination of cell surface markers and fluorescence-activated cell sorting (FACS) technology has led to the identification and isolation of distinct mammary epithelial cell subpopulations. Based on the expression levels of the heat stable antigen (CD24) the cells of the mammary gland can be separated into $CD24^{high}$, $CD24^{med}$, and $CD24^{neg}$ cells. The $CD24^{high}$ cell population is enriched in luminal cells and therefore stains almost exclusively for the luminal marker cytokeratin 18 (K18) (Sleeman, Kendrick et al. 2006). The $CD24^{high}$ cells can further be resolved into two subpopulations based on their expression levels of the stem cell antigen 1 (Sca-1). CD24 positive cells expressing Sca-1 ($CD24^{high}/Sca\text{-}1^{+}$) are enriched in luminal cells expressing the estrogen receptor (ER) and do not have mammary gland repopulating activity. In contrast, the $CD24^{high}/Sca\text{-}1^{-}$ cells are mostly ER negative and have potent colony forming activity *in vitro* and limited mammary gland repopulating activity *in vivo* (Sleeman, Kendrick et al. 2007). The cell population expressing moderate levels of CD24 ($CD24^{med/low}$)

stains mostly positive for the basal marker cytokeratin 14 (K14) but negative for K18 and contains basal epithelial cells. These can be further resolved based on the levels of β1-integrin (CD29) or α6-integrin (CD49f) in a stem cell enriched population and in a population containing mainly myoepithelial cells. The stem cell enriched population is characterized by high expression levels of CD29, high levels of CD49f, moderate levels of CD24, and the absence of Sca-1 (Shackleton, Vaillant et al. 2006; Sleeman, Kendrick et al. 2006; Stingl, Eirew et al. 2006). The $CD24^{med/low}$ cells expressing low levels of CD29/CD49f are mainly myoepithelial cells. The $CD24^{neg}$ population contains non-epithelial cells (Sleeman, Kendrick et al. 2006).

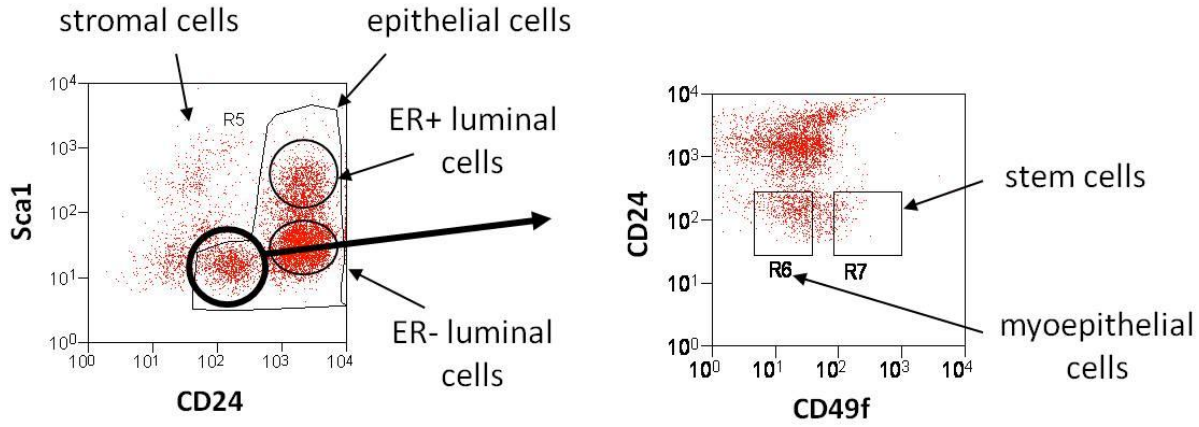

Figure 1. FACS-based separation of mammary epithelial cells into distinct subpopulations. Using the cell surface marker CD24, cells from the mammary gland can be separated into three populations: $CD24^{neg}$, $CD24^{low}$, and $CD24^{high}$. The $CD24^{neg}$ cells are stromal cells while the $CD24^{low}$ and $CD24^{high}$ cells are epithelial cells. The $CD24^{high}$ cells are luminal epithelial cells and can be further separated into a Sca-1^{+} population (enriched in ER^{+} cells) and a Sca-1^{-} population (enriched in ER^{-} cells). Based on their CD49f expression, the $CD24^{low}$ cells which are basal epithelial cells can be further separated into myoepithelial cells ($CD49f^{low}$) and a mammary stem cell enriched population ($CD49f^{high}$).

2. Breast Cancer

2.1 Breast cancer prevalence

Breast cancer is by far the most common form of cancer in women and accounts approximately for 23% of all cancers in women worldwide. In absolute numbers, in the year 2008, an

estimated 1’384’000 new breast cancer cases occurred while the disease accounted for roughly 458’000 deaths worldwide (World Health Organization).

2.2 Breast cancer classification

Breast cancer is a heterogeneous disease both histologically and molecularly. Efforts have been made in the past decades to classify breast cancers into different subtypes which would allow patient prognosis and prediction of optimal treatment. Historically, human breast cancers were grouped into approximately 18 different subtypes based on histological features (Stingl and Caldas 2007), however, the prognostic and predictive value of this classification is very limited (Sims, Howell et al. 2007). Of a better clinical value is the status of ER, progesterone receptor (PR), and the epidermal growth factor receptor 2 (HER2/ErbB2) which has direct impact on treatment strategies.

Global gene expression profiling of breast cancer has led to the identification of at least six distinct and reproducible subtypes: luminal A, luminal B, ErbB2-enriched, basal, normal-like, and claudin-low (Perou, Sorlie et al. 2000; Sorlie, Perou et al. 2001; Sorlie, Tibshirani et al. 2003; Sotiriou, Neo et al. 2003; Herschkowitz, Simin et al. 2007; Perou and Borresen-Dale 2011). Notably, patients with luminal A breast cancer have the best prognosis (Sorlie, Tibshirani et al. 2003).

The luminal subtypes are characterized by the expression of luminal cytokeratins and genes typical for luminal cells of the normal mammary gland (e.g., K8/18, K19, CD24, Mucin1, and GATA3) (Rakha, El-Sayed et al. 2007) as well as expression of the hormone receptors ER and/or PR (Rouzier, Perou et al. 2005; Hu, Fan et al. 2006; Sotiriou and Pusztai 2009). The luminal subtypes A and B can be discriminated based on tumor grade, genomic grade and patient outcome. Breast tumors of the luminal subtype A are typically of lower tumor grade, have a lower genomic grade, and correlate with improved patient survival compared to those of luminal subtype B (Sorlie, Tibshirani et al. 2003; Sotiriou, Neo et al. 2003; Loi, Haibe-Kains et

al. 2007; Sotiriou and Pusztai 2009). Further, luminal A tumors are sensitive to endocrine therapy whereas those of luminal B subtype show incomplete sensitivity to endocrine therapy (Sotiriou and Pusztai 2009).

The ErbB2-enriched molecular subtype of breast cancer is typically characterized by elevated expression of ErbB2 and accounts for ~10% of breast cancers (Perou and Borresen-Dale 2011). Another ~10% of breast cancers are clinically defined ErbB2-positive breast cancers that co-express ER and fall into the luminal subtypes (typically luminal B) (Sotiriou and Pusztai 2009; Perou and Borresen-Dale 2011). ErbB2-enriched tumors are generally of higher tumor grade than luminal tumors (Sotiriou and Pusztai 2009) and correlate with a bad prognosis (Sorlie, Perou et al. 2001; Sorlie, Tibshirani et al. 2003; Hu, Fan et al. 2006). Elevated levels of surface ErbB2 result in the formation of homodimers and heterodimers with other receptor tyrosine kinases of the human epidermal growth factor receptor (HER) family including epidermal growth factor receptor 1 (EGFR) and 3 (ErbB3) (Graus-Porta, Beerli et al. 1997; Hynes and Lane 2005). ErbB2 and ErbB3 form a potent tumorigenic heterodimer and activate key signaling cascades including the mitogen-activated protein kinase (MAPK) and phosphoinositol-3-kinase (PI3K) pathway (Holbro, Beerli et al. 2003; Hynes and Lane 2005). Some of the ErbB2 positive tumors are sensitive to trastuzumab, an antibody targeting the extracellular domain of ErbB2 which is used in combination with chemotherapy as the gold standard treatment for metastatic ErbB2 positive breast cancer (Hynes and Lane 2005; Nahta and Esteva 2006).

Breast tumors of the basal-like subtype are less frequent than those of the luminal or ErbB2 positive subtype and correlate with a very aggressive disease although they can be particularly sensitive to chemotherapy (Rouzier, Perou et al. 2005). Some basal-like tumors express high levels of basal cytokeratins like K5 and growth factor receptors including EGFR and c-Kit. However, most of the basal-like tumors lack expression of ER, PR, and ErbB2 and are therefore also called triple negative (TN) tumors (Sotiriou and Pusztai 2009). A characteristic feature of basal-like carcinomas is the dysfunction of BRCA1, a gene involved in DNA repair and chromosomal stability (Turner, Reis-Filho et al. 2007; Sotiriou and Pusztai 2009). Sporadic basal-like tumors display BRCA1 promoter methylation and/or transcriptional inactivation (Turner,

Tutt et al. 2004; Turner, Reis-Filho et al. 2007). BRCA1 germ line mutations correlate with increased breast cancer susceptibility and a link between hereditary BRCA1-associated tumors and the basal-like subtype has been described (Easton, Ford et al. 1993; Foulkes, Stefansson et al. 2003).

3. PI3K Signaling

The phosphatidylinositol 3-kinase (PI3K) pathway is often subverted during neoplastic transformation (Engelman, Luo et al. 2006) and provides cancer cells with a competitive advantage by decreasing cell death and increasing cell proliferation, migration, invasion, metabolism, angiogenesis, and resistance to chemotherapy. Mechanisms of activation of the PI3K pathway in cancer include the loss of expression or rare mutation of the PTEN phosphatase that reverses PI3K action (Rhei, Kang et al. 1997; Ueda, Nishijima et al. 1998; Perren, Weng et al. 1999; Depowski, Rosenthal et al. 2001; Perez-Tenorio, Alkhori et al. 2007), the activation downstream of oncogenic receptor tyrosine kinases, the mutation/amplification of Akt, and the mutation and/or amplification of *PIK3CA*.

3.1 PI3K classification

PI3Ks are lipid kinases that phosphorylate different phosphatidylinositols (PI) at the 3' position of the inositol ring. There are three classes of PI3K based on their substrate preferences and domain structure.

Class I PI3Ks preferentially phosphorylate PI-4,5-bisphosphate (PI-4,5-P_2 or PIP_2) to generate PI-3,4,5-trisphosphate (PI-3,4,5-P_3 or PIP_3) and are further divided into two subfamilies. Class IA PI3Ks are activated by receptor tyrosine kinases (RTKs) in contrast to class IB PI3Ks that are activated by G-protein-coupled receptors (GPCRs) (Katso, Okkenhaug et al.

2001). In response to extracellular signals class I PI3Ks regulate cell growth, survival, apoptosis, protein synthesis, and metabolism.

Class II PI3Ks preferentially generate PI-3-P but poorly phosphorylate PI-4,5-P2. Class II PI3Ks bind to clathrin and regulate clathrin-mediated membrane trafficking and receptor internalization (Gaidarov, Smith et al. 2001). Vps34 is the only member of class III PI3K and was identified in yeast as a regulator of trafficking vesicles from the Golgi apparatus to the vacuole (Odorizzi, Babst et al. 2000). However, relatively little is known about the specific functions of class II and III PI3K.

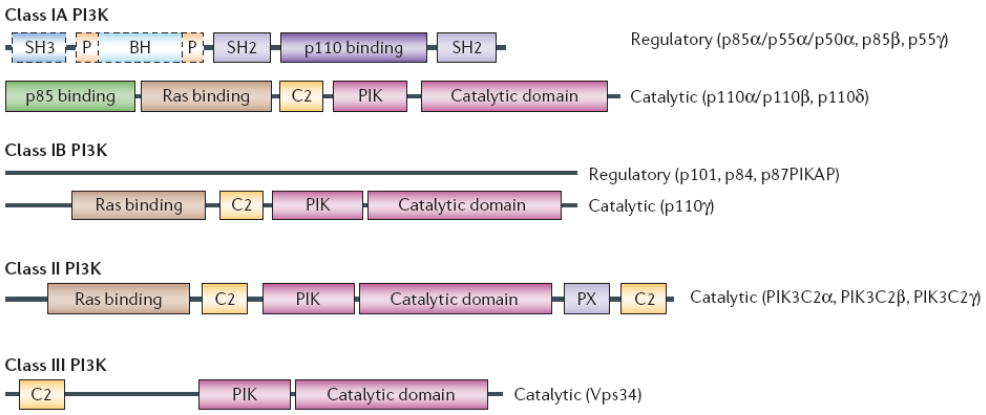

Figure 2. The classification and molecular architecture of PI3Ks. The architecture of the catalytic and adaptor subunits of class I PI3Ks and the domains of class II and III PI3Ks are shown. The dashed lines represent the extended N-terminal region that exists in the long adaptor subunits p85α and p85β but is absent in the shorter p55α/p50α and p55γ forms. The p85 binding domain (green) of class IA catalytic subunits is referred to as adaptor binding domain (ABD) in the text. BH: breakpoint cluster region homology, PIK: phosphatidylinositol kinase homology, SH2: Src-homology 2 domain, SH3: Src-homology 3 domain, Adapted from (Engelman, Luo et al. 2006).

3.2 Structure of class I PI3Ks

Class IA PI3Ks occur as heterodimers consisting of a p110 catalytic and a p85 regulatory subunit. There are three highly homologous catalytic isoforms p110α, p110β, and p110δ, which are encoded by the three genes *PIK3CA*, *PIK3CB*, and *PIK3CD*. The class IA catalytic proteins contain

an N-terminal adaptor binding domain (ABD) which interacts with the regulatory subunits, a Ras-binding domain (RBD) which enables interaction with the small GTPase Ras, a C2 domain, the helical domain, and a C-terminal kinase domain.

Class IA catalytic subunits bind to a total of five different regulatory subunits encoded by three genes. *PIK3R1* encodes p85α as well as to the two shorter proteins p55α and p50α. p85β and p55γ are encoded by *PIK3R2* and *PIK3R3*, respectively. All regulatory isoforms share a common p110-binding domain or inter-SH2 (Src-homology 2) domain flanked by two SH2 domains. The two longer isoforms p85α and p85β further contain an N-terminal Src-homology 3 (SH3) domain and a breakpoint cluster region (BCR) homology (BH) domain flanked by two proline-rich regions (Fruman, Meyers et al. 1998; Engelman, Luo et al. 2006).

3.3 The growth factor receptor/PI3K/Akt signaling axis

In its inactive state the regulatory subunit p85 keeps the kinase activity of the catalytic subunit p110 at a low activity state via an intermolecular interaction of the N-terminal SH2 domain of p85 with the helical domain of p110 (Yu, Zhang et al. 1998). As mentioned above class IA PI3Ks are activated by upstream receptor tyrosine kinases (RTK) including the insulin receptor (IR), the insulin-like growth factor 1 receptor (IGF-1R), the platelet-derived growth factor receptor (PDGFR), and members of the epidermal growth factor receptor (EGFR) family. Binding of the respective ligands induces receptor dimerization resulting in receptor autophosphorylation. Phosphorylated tyrosine residues within the cytoplasmic domain of these receptors or within adaptor molecules like the insulin receptor substrate (IRS) 1 and 2 recruit the regulatory subunit p85 via its SH2 domains. Binding of the SH2 domain of p85 to phosphotyrosine residues relieves the inhibition of p110 and mediates translocation of the catalytic subunit to the plasma membrane (Okkenhaug and Vanhaesebroeck 2001). Interaction with the GTP-bound form of the RAS protein further increases PI3K kinase activity (Rodriguez-Viciana, Warne et al. 1994; Rodriguez-Viciana, Warne et al. 1996)

Activated PI3K converts PIP_2 into PIP_3, a reaction which is reverted by the tumor suppressor phosphatase and tensin homolog deleted on chromosome ten (PTEN) (Maehama, Taylor et al. 2001; Wishart and Dixon 2002). PIP_3 recruits proteins containing a pleckstrin homology (PH) domain including the downstream molecules 3-phosphoinositide-dependent kinase 1 (PDK1) and Akt (Corvera and Czech 1998). Upon autophosphorylation, PDK1 phsophorylates the serine-threonine kinase Akt on Thr 308 (Alessi, James et al. 1997). In addition, and dependent on the physiological context, Akt is phosphorylated at the hydrophobic motif on Ser 473 by the mammalian target of rapamycin (mTOR)/rictor complex or DNA-dependent protein kinase (DNA-PK) which results in full Akt activation (Sarbassov, Guertin et al. 2005; Bozulic, Surucu et al. 2008). Akt is a key effector of PI3K-mediated signaling regulating a myriad of downstream targets and cellular responses (Figure 3).

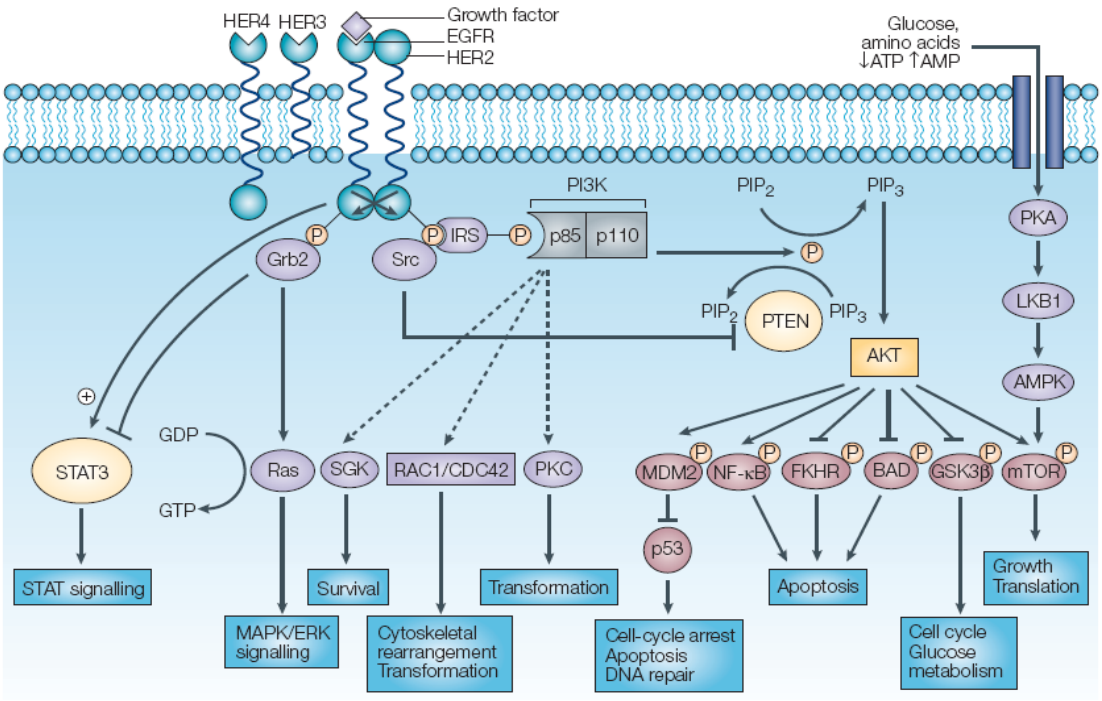

Figure 3. The PI3K/Akt signaling pathway regulates a myriad of downstream targets and cellular responses. The PI3K/Akt and related pathways are key effectors of receptor tyrosine kinases. Activation of membrane kinases including the epidermal growth factor receptor (EGFR) by external growth factors initiates receptor dimerization and activates these intracellular pathways. Akt is activated downstream of PI3K and has multiple targets including MDM2, NF , FKHR, BAD, GSK3β, and mTOR to regulate cell cycle, apoptosis, metabolism, growth, and translation. Adapted from (Hennessy, Smith et al. 2005).

3.4 PI3K signaling mediates cell survival and cell cycle progression

Akt promotes cell cycle progression by blocking forkhead box (FOXO) transcription factors. Akt phosphorylates discrete sites on FOXO proteins resulting in their exclusion from the cell nucleus and targeting to proteasomal degradation (Biggs, Meisenhelder et al. 1999; Brunet, Bonni et al. 1999; Kops, de Ruiter et al. 1999; Takaishi, Konishi et al. 1999; Tang, Nunez et al. 1999; Matsuzaki, Daitoku et al. 2003; Plas and Thompson 2003). Inhibition of FOXO results in decreased expression of cyclin dependent kinase inhibitors $p27^{kip1}$ and $p21^{cip1}$, increased levels of cyclin D1 and D2 and a decline in proapoptotic proteins including BIM and FasL (Medema, Kops et al. 2000; Dijkers, Birkenkamp et al. 2002; Ramaswamy, Nakamura et al. 2002; Schmidt, Fernandez de Mattos et al. 2002; Seoane, Le et al. 2004). Akt negatively regulates levels of the tumor suppressor p53 via phosphorylation of MDM2, an E3 ubiquitin ligase, which causes degradation of p53 (Zhou, Liao et al. 2001). In contrast to FOXO and p53, PI3K activity results in activation of the transcription factor NFκB mediating cell survival and cell proliferation (Bader, Kang et al. 2005). Akt can also regulate survival and cell cycle progression by directly phosphorylating and inhibiting the proapoptotic protein BAD (Datta, Dudek et al. 1997; del Peso, Gonzalez-Garcia et al. 1997) and the cell cycle inhibitor $p27^{kip1}$ (Liang, Zubovitz et al. 2002; Shin, Yakes et al. 2002; Viglietto, Motti et al. 2002).

3.5 PI3K signaling regulates protein synthesis

Akt phosphorylates the protein tuburin, a member of the tuberous sclerosis complex 2 (TSC2) (Inoki, Li et al. 2002; Potter, Pedraza et al. 2002). This event inhibits the GAP (GTPase activating protein) activity of the TSC1-TSC2 complex resulting in an increase in the active GTP-bound form of its substrate Rheb (small G protein Ras homologue enriched in brain) which in turn phosphorylates and activates the mTOR complex 1 (mTOR-raptor complex or mTORC1) (Garami, Zwartkruis et al. 2003; Inoki, Li et al. 2003; Zhang, Gao et al. 2003). The mTORC1 in

turn phosphorylates the eukaryotic translation initiation factor 4E-binding protein (4E-BP1) and $p70^{S6Kinase}$. On the one hand hyperphosphorylated 4E-BP1 dissociates from the eukaryotic translation initiation factor 4E (eIF4E) allowing it to form an active translation initiation complex at the 5' end of mRNA (Ruggero and Sonenberg 2005). On the other hand $p70^{S6Kinase}$ phosphorylates the ribosomal protein S6 resulting in increased protein synthesis (Hay and Sonenberg 2004; Engelman, Luo et al. 2006).

3.6 PI3K signaling controls metabolism

Upon growth factor binding, PI3K regulates several processes important for nutrient uptake and cell metabolism via its downstream mediator Akt. In insulin-responsive tissues like fat and striated muscle, Akt2 is the predominant Akt isoform and activation of Akt2 promotes the translocation of the glucose transporter 4 (GLUT4) to the plasma membrane (Engelman, Luo et al. 2006; Manning and Cantley 2007). Once glucose is within the cell it can be converted into glycogen for storage or enter glycolysis for energy production, two processes in which Akt is involved. Akt phosphorylates and inhibits glycogen synthase kinase 3 (GSK3) which prevents it from blocking glycogen synthase and thus stimulates glycogen synthesis (Manning and Cantley 2007). At the same time, in liver, Akt can inhibit gluconeogenesis and fatty acid oxidation through direct control of peroxisome proliferator-activated receptor-coactivator 1α (PGC-1α) (Li, Monks et al. 2007).

4. The PI3K pathway in normal mammary gland physiology

4.1 The roles of Akt isoforms in normal mammary gland physiology

The expression levels of the different isoforms of Akt in the mammary gland differ significantly during a reproductive cycle. By the end of pregnancy and throughout lactation, Akt1 is the predominant isoform being expressed. With the onset of mammary gland involution Akt1 levels drop dramatically. In contrast, Akt2 levels drop by the end of pregnancy and remain low during

lactation and early involution. Expression of both isoforms goes back to pre-pregnancy levels by the end of involution (day7) (Boxer, Stairs et al. 2006; Maroulakou, Oemler et al. 2008). Unlike for Akt1 and Akt2, expression levels of Akt3 do not change much during the reproductive cycle of mice (Boxer, Stairs et al. 2006; Maroulakou, Oemler et al. 2008).

Expression of a constitutively active form of human Akt1 in mice under the control of the mouse mammary tumor virus long terminal repeat (MMTV-LTR) caused a dramatic delay in mammary gland involution by attenuating cell death (Hutchinson, Jin et al. 2001). Elevated and prolonged expression of tissue inhibitor of metalloproteinase-1 (TIMP1) was detected in transgenic animals throughout involution. This may contribute to the delay in involution by inhibiting matrix metalloproteinases (MMP) such as MMP-3 (Schwertfeger, Richert et al. 2001). In addition to delayed involution, a precocious accumulation of lipids during pregnancy and an overall increase in the size and number of lipid droplets as well as milk stasis was found in these animals. Moreover, the milk fat content was increased in transgenic mice expressing activated Akt1 which might be a cause for the lactation defect observed in these animals (Schwertfeger, McManaman et al. 2003). Overexpression of wild-type Akt1 under the control of the MMTV promoter resulted in a similar delay in involution, however, unlike for activated forms of Akt, overexpression of wildtype Akt1 did not evoke neoplasias (Ackler, Ahmad et al. 2002).

Mice with mammary epithelial cell specific deletion of Akt1 but not Akt2 fail to produce sufficient milk. Although the lobuloalveolar development in Akt1 deficient mice appeared normal, epithelial cells secreted less milk than in wild-type (Boxer, Stairs et al. 2006) and the alveolar structures found in glands of mice with ablated Akt1 were significantly smaller and were completely devoid of lipid droplets. Expression of milk proteins such as the whey acidic protein (WAP) and β-casein was delayed which correlated with decreased phosphorylation of signal transducer and activator of transcription 5a (Stat5a), an important mediator of prolactin-induced signaling.

In contrast to *AKT1* deletion, *AKT2* ablation resulted in enhanced formation of lobuloalveolar structures and precocious luminal cell differentiation. Interestingly, the

accelerated mammary epithelial differentiation observed in *AKT2*-null mice is non-cell-autonomous as transplantation of *AKT2*-null mammary epithelial cells into wild-type recipient mice resulted in normal formation of lobuloalveolar structures and differentiation. This observation can be explained by the fact that Akt2 is mainly expressed in stromal cells of the mammary gland (Maroulakou, Oemler et al. 2007). Further, the lack of Akt1 caused accelerated involution whereas the ablation of *AKT2* resulted in a delay in involution. Deletion of *AKT3* does not have an overt effect on lobuloalveolar differentiation and involution (Maroulakou, Oemler et al. 2008).

4.2 The roles of PTEN in normal mammary gland physiology

MMTV-targeted overexpression of PTEN results in a lactation defect due to a reduced number of alveolar epithelial cells, a consequence of reduced proliferation and increased apoptosis during pregnancy (Dupont, Renou et al. 2002). Conversely, mammary-specific deletion of both *PTEN* alleles resulted in precocious mammary gland development including increased proliferation, excessive side branching, and expression of milk proteins at the virgin state. On the other hand, involution was delayed due to an Akt-mediated reduction in apoptotic cells (Li, Robinson et al. 2002).

4.3 The effects of p110α on normal mammary gland physiology

MMTV-mediated expression of myristoylated p110α, which is directed to the plasma membrane, resulted in constitutive activation of the PI3K pathway and delayed mammary gland involution (Renner, Blanco-Aparicio et al. 2008). In the present work, I found that expression of the gain-of-function mutant p110α H1047R (see section 6.1) delayed mammary gland involution which is in line with the above mentioned study (Renner, Blanco-Aparicio et al. 2008).

5. PI3K pathway in mammary gland tumorigenesis

5.1 Akt isoforms in mammary gland tumorigenesis

Akt1 and Akt2 have different effects on tumorigenesis. In mice that develop tumors due to mammary gland specific expression of the viral oncogene polyoma middle T (PymT) uncoupled from the PI3K pathway (MTY315/322F), coexpression of active Akt1 severely accelerated tumor formation by reducing cell death, but did not affect metastasis (Hutchinson, Jin et al. 2001). In mice expressing activated ErbB2 (NDL), constitutively active Akt1 reduced tumor latency, led to a more differentiated tumor phenotype, and significantly decreased the number of lung metastases (Hutchinson, Jin et al. 2004). Conversely, ablation of *AKT1* dramatically delayed tumor onset in PymT and ErbB2 transgenic mice (Maroulakou, Oemler et al. 2007).

In contrast to Akt1, expression of active Akt2 did not affect tumor latency in either PymT or in ErbB2 transgenic mice, however, it increased the number of lung metastases (Dillon, Marcotte et al. 2009). Conversely, deletion of *AKT2* accelerated tumor formation in either mouse model (Maroulakou, Oemler et al. 2007).

Deletion of Akt3 had no overt effect on tumorigenesis in either PymT or ErbB2 transgenic mice (Maroulakou, Oemler et al. 2007).

5.2 PTEN in mammary gland tumorigenesis

Mammary-specific deletion of *PTEN* resulted in mammary epithelial hyperplasia and tumor formation eventually (Li, Robinson et al. 2002). Heterozygous deletion of *PTEN* in mice conditionally expressing the oncogene Wnt-1 significantly decreased tumor latency. Notably, in the majority of the resulting tumors expression of the remaining wild-type allele was lost. This suggests that tumor cells with loss of heterozygosity (LOH) have a growth advantage over cells retaining one *PTEN* allele (Li, Podsypanina et al. 2001). Interestingly, even subtle changes in PTEN expression can affect suscebtibility to cancer. Mice bearing a hypomorphic allele of *PTEN* expressed ~20% less PTEN mRNA than wild-type mice, a reduction that was sufficient to induce mammary tumors in the majority of animals (Alimonti, Carracedo et al. 2010). In contrast to

PTEN deletion, overexpression of PTEN increased tumor latency and decreased tumor growth rate in mice expressing oncogenic Wnt-1 (Zhao, Cui et al. 2005).

Notably, a non cell-autonomous role was demonstrated for PTEN in the formation of breast carcinomas. In a recent study, ablation of *PTEN* in fibroblasts of the mammary gland accelerated tumorigenesis. The lack of *PTEN* caused elevated levels of the transcription factor Ets2 and induced genes involved in matrix remodeling and macrophage recruitment (MMP9, CCL3) (Trimboli, Cantemir-Stone et al. 2009).

5.3 p110α in mammary gland tumorigenesis

Expression of myristoylated p110α in mice under the control of the MMTV promoter caused morphological changes in mammary ducts of young virgin animals and induced mammary carcinomas in ~30% of multiparous females (Renner, Blanco-Aparicio et al. 2008). This demonstrates that constitutive activation of p110α results in phenotypes resembling those of *PTEN* loss *in vivo* (see above). However, this system is artificial and myristoylated p110α does not occur in human disease. More recently, we and others (Adams, Xu et al.) generated mice conditionally expressing mutant p110α (see section 6.1). These animals form a diverse spectrum of mammary carcinomas with 100% penetrance (see section “Results” in this work).

6. PI3K in breast cancer

6.1 PIK3CA mutations are oncogenic

Mutations in the gene *PIK3CA* which encodes for the alpha catalytic subunit of PI3K occur with high frequency in several solid carcinomas including those of the colon, breast, brain, and stomach (Bachman, Argani et al. 2004; Broderick, Di et al. 2004; Campbell, Russell et al. 2004; Samuels, Wang et al. 2004; Lee, Soung et al. 2005; Levine, Bogomolniy et al. 2005). Interestingly, the vast majority of mutations in *PIK3CA* occur at two “hotspots” within the coding sequence. Two missense mutations result in the amino acid substitutions E542K and

E545K in the helical domain of the protein and another missense mutation leads to the substitution H1047R within the kinase domain.

Expression of the mutant p110α proteins in chicken embryonic fibroblasts (CEFs) was transforming and all three mutations increased the lipid kinase activity of the enzyme and caused constitutive activity of the PI3K pathway (Kang, Bader et al. 2005). Injection of these mutant p110α transformed CEFs into newly hatched chickens induced tumors that showed a high degree of vascularization (Bader, Kang et al. 2006). Interestingly the kinase domain mutation (H1047R) induced tumors more potently than the helical domain mutations (E542K/E545K). Administration of the mTOR inhibitor RAD001 inhibited tumor growth suggesting that activation of mTOR signaling is important in mutant p110α-mediated tumorigenesis (Bader, Kang et al. 2006). Expression of E545K and H1047R mutant p110α in the immortalized but non-transformed mammary epithelial cell line MCF10A increased the PI3K kinase activity, allowed epidermal growth factor (EGF)-independent cell growth, anchorage-independent growth, and disrupted the normal architecture of these cells when grown in 3-dimensional culture, a phenotype that was mTOR-dependent (Isakoff, Engelman et al. 2005). In a cultured human mammary epithelial cell line expressing inactivated p53, hTERT, and high levels of c-myc, mutant p110α (E545K, H1047R, myr-*PIK3CA*) could substitute for the need of SV40 largeT antigen for cell transformation (Zhao, Liu et al. 2005).

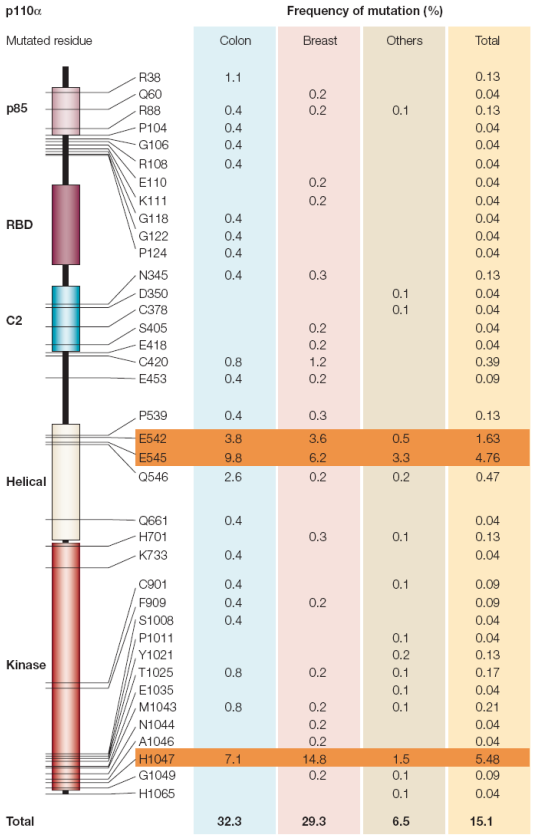

Figure 4. Point mutations in *PIK3CA* observed in human tumors. Sequencing of the *PIK3CA* gene in human tumor samples revealed somatic point mutations in 38 residues. The mutations localize to various domains of the p110α primary structure as indicated. 'Hot-spot' mutations are observed at residues E542, E545 and H1047 and are highlighted in orange. The figure indicates frequencies of mutation for cancers of the colon, breast, and others, which include liver, brain, stomach, lung, and ovary. Adapted from (Bader, Kang et al. 2005).

In contrast to p110δ and p110γ wild-type isoforms, wild type p110α is unable to transform CEFs by itself (Kang, Denley et al. 2006). The activation loop of PI3K was shown to determine phosphoinositide substrate specificity (Bondeva, Pirola et al. 1998), however substitution of the p110α activation loop with that of p110γ and p110δ respectively was not sufficient to render p110α oncogenic showing that the activation loop does not determine oncogenicity (Denley, Gymnopoulos et al. 2009) among class I PI3Ks.

Apart from their lipid kinase activity all class I p110 isoforms possess protein serine kinase activity (Dhand, Hiles et al. 1994; Lam, Carpenter et al. 1994). However, it was demonstrated that it is the lipid kinase activity as well as the lipid product PIP_3 that are

essential for mutant p110α-mediated transformation (Kang, Denley et al. 2006; Denley, Gymnopoulos et al. 2009).

Rare mutations in p110α also possess the potential to transform cells and to activate downstream signaling albeit to a smaller extent than the 3 most common mutations (E542K, E545K, H1047R) (Gymnopoulos, Elsliger et al. 2007).

6.2 Different mechanisms lead to hyperactivity of p110α hotspot mutants

Recent genetic and biochemical studies suggest different mechanisms of activation for p110α helical and kinase domain mutants. The kinase domain mutant H1047R is thought to trigger a conformational shift mimicking the one induced by Ras binding. This model is supported by an earlier study demonstrating that Ras binding to p110 induces a conformational change of the substrate-binding site (Pacold, Suire et al. 2000) and by mutagenesis experiments in which either the p85 binding domain (ABD) or the Ras binding domain (RBD) were deleted. While deletion of the ABD completely abolishes the transforming potential of the H1047R kinase domain mutant, mutagenesis in the RBD leaves the oncogenic potential of H1047R unaffected (Zhao and Vogt 2008). In addition, computational and structural analysis of the H1047R protein suggests that the mutation could allow enhanced substrate-to-product turnover (Mankoo, Sukumar et al. 2009). Interestingly, although H1047R depends on binding to p85 for transforming cells, activation of Akt occurred also in the absence of p85 interaction highlighting the importance of additional mechanisms than Akt activation for cellular transformation by mutant p110α (Zhao and Vogt 2008).

In contrast to H1047R, the amino acid substitutions E542K and E545K mimic relief of inhibition of p110α upon binding of p85 to growth factor receptors. This model is supported by structural data gained from p110α bound to p85 which demonstrates that the charge reversal caused by the mutations E542K and E545K disrupts the inhibitory interaction between p85 and the helical domain of p110α (Miled, Yan et al. 2007). Further studies showed that mutagenesis of the RBD disrupts the oncogenic activity of the helical domain mutants whereas deletion of

the ABD has no effects on the transforming potential of E542K/E545K demonstrating that kinase and helical domain mutants have opposing requirements of either p85 or Ras for their oncogenic capacity (Zhao and Vogt 2008). Of note, the kinase activity of H1047R mutated p110α could be increased by binding to phosphorylated IRS-1 as a consequence of growth factor stimulation similar to the wild type enzyme. In contrast, the activity of E542K and E545K mutated molecules was independent of growth factor signaling (Carson, Van Aller et al. 2008).

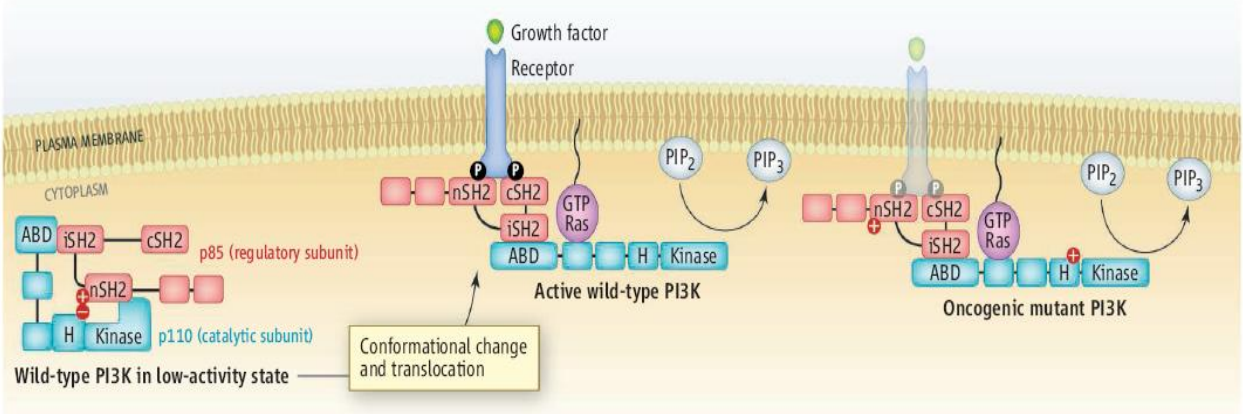

Figure 5. Mechanism of activation of *PIK3CA* mutants E542K/E545K. In the wild-type PI3K enzyme, the catalytic subunit p110α is kept in a low-activity state via an intramolecular interaction with the regulatory subunit p85 (left). Upon binding of the SH2 domains of p85 to phosphorylated tyrosine residues on growth factor receptors, p110α is relieved from the inhibitory interaction with p85 and becomes active (center). The glutamate to lysine substitution in the helical domain mutants causes a charge reversal which interferes with this inhibitory interaction resulting in constitutive active p110α independent of activated growth factor receptors (right). Adapted from (Lee, Engelman et al. 2007).

6.3 PIK3CA mutations in human breast cancer

PIK3CA is mutated in ~30% of human breast cancers (Bachman, Argani et al. 2004; Campbell, Russell et al. 2004; Samuels, Wang et al. 2004; Lee, Soung et al. 2005; Levine, Bogomolniy et al. 2005; Saal, Holm et al. 2005; Buttitta, Felicioni et al. 2006; Li, Rong et al. 2006; Maruyama, Miyoshi et al. 2007; Gonzalez-Angulo, Stemke-Hale et al. 2009; Kalinsky, Jacks et al. 2009; Michelucci, Di Cristofano et al. 2009). Interestingly, the kinase domain mutations are more common in breast cancer (~15% of breast cancers) than the helical domain mutations (~10%)

(Bachman, Argani et al. 2004; Saal, Holm et al. 2005; Li, Rong et al. 2006; Maruyama, Miyoshi et al. 2007; Perez-Tenorio, Alkhori et al. 2007; Lai, Mau et al. 2008; Gonzalez-Angulo, Stemke-Hale et al. 2009; Kalinsky, Jacks et al. 2009; Michelucci, Di Cristofano et al. 2009) although some studies found similar frequencies of exon 9 and exon 20 mutations (Buttitta, Felicioni et al. 2006; Barbareschi, Buttitta et al. 2007). This is in contrast to *PIK3CA* mutation in colorectal cancer where the helical domain mutations are predominant (Samuels, Wang et al. 2004). Helical domain and kinase domain mutations appear to be mutually exclusive although in rare cases tumor samples with double mutants were reported (Saal, Holm et al. 2005). However, it could be possible that these rare cases are multiclonal tumors with areas harboring one mutation and different areas expressing the other mutation type. *PIK3CA* mutations and loss of PTEN do not seem to be mutually exclusive events although in one report only little overlap between mutant *PIK3CA* and loss of expression of PTEN was found (Saal, Holm et al. 2005; Perez-Tenorio, Alkhori et al. 2007; Stemke-Hale, Gonzalez-Angulo et al. 2008; Li, Zhu et al. 2010).

6.4 Association of PIK3CA mutations with clinicopathological markers

The association of *PIK3CA* mutations with clinicopathological parameters is still under debate. *PIK3CA* mutations associate significantly with ER- and PR-positive tumors (Saal, Holm et al. 2005; Li, Rong et al. 2006; Maruyama, Miyoshi et al. 2007; Kalinsky, Jacks et al. 2009; Li, Zhu et al. 2010) although some studies failed to find significant association of *PIK3CA* mutations and ER (Buttitta, Felicioni et al. 2006; Barbareschi, Buttitta et al. 2007; Michelucci, Di Cristofano et al. 2009). In some studies an association of mutant *PIK3CA* with overexpression of the growth factor receptor ErbB2 (Saal, Holm et al. 2005) was observed whereas in other studies no such correlation could be detected (Li, Rong et al. 2006; Maruyama, Miyoshi et al. 2007; Li, Zhu et al. 2010) or even an inverse correlation was observed (Buttitta, Felicioni et al. 2006; Perez-Tenorio, Alkhori et al. 2007; Kalinsky, Jacks et al. 2009). Further, mutations in *PIK3CA* correlated with the occurrence of lymph node metastases (Saal, Holm et al. 2005) whereas other studies failed to

detect a positive association with lymph node metastases (Buttitta, Felicioni et al. 2006; Maruyama, Miyoshi et al. 2007) or found H1047R mutations to anti-correlate with lymph node involvement (Kalinsky, Jacks et al. 2009). No association of mutant *PIK3CA* with mutation in the tumor suppressor gene TP53 was observed (Buttitta, Felicioni et al. 2006; Li, Rong et al. 2006; Maruyama, Miyoshi et al. 2007). Furthermore, no association with several clinicopathological markers was apparent when the helical and kinase domain mutation were analysed separately (Barbareschi, Buttitta et al. 2007).

In one report, the presence of *PIK3CA* mutations correlated with tumor diameter and with well differentiated histology (Li, Rong et al. 2006), while in other reports no association of *PIK3CA* mutations with tumor size and histological grade was observed (Buttitta, Felicioni et al. 2006; Maruyama, Miyoshi et al. 2007). In one study, even an association of *PIK3CA* mutations with small tumor size was reported (Perez-Tenorio, Alkhori et al. 2007).

In terms of tumor histology, *PIK3CA* mutations were observed more frequently in invasive lobular carcinomas (ILC) (45% with *PIK3CA* mutations) than in invasive ductal carcinomas (IDC) (25%) (Buttitta, Felicioni et al. 2006; Maruyama, Miyoshi et al. 2007). Interestingly, a particular correlation of helical domain mutations with lobular carcinomas could be detected while no difference in the distribution of kinase domain mutations was found (Buttitta, Felicioni et al. 2006; Barbareschi, Buttitta et al. 2007).

Similar frequencies of *PIK3CA* sequence alterations were observed in carcinomas *in situ* and adjacent invasive carcinomas suggesting that genetic mutations in *PIK3CA* occur relatively early in breast tumorigenesis (Dunlap, Le et al. 2010; Li, Zhu et al. 2010; Miron, Varadi et al. 2010). This finding is consistent with a report that *PIK3CA* mutations were observed in breast tumor samples from various stages (I-IV) (Saal, Holm et al. 2005). Since *PIK3CA* mutations were rarely detected in ductal intraepithelial neoplasias (IDN) *PIK3CA* events mostly seem to occur during progression from IDN to the carcinomas *in situ* (Li, Zhu et al. 2010).

6.5 PIK3CA mutations and patient outcome

Studies of *PIK3CA* mutants with respect to metastases-free survival and overall patient survival are contradictory. While some studies did not find a correlation of *PIK3CA* mutations with patient prognosis (Saal, Holm et al. 2005; Stemke-Hale, Gonzalez-Angulo et al. 2008; Michelucci, Di Cristofano et al. 2009) other studies associated *PIK3CA* mutations with worse outcome (Li, Rong et al. 2006) while in yet other reports a favorable outcome was associated with *PIK3CA* mutations (Maruyama, Miyoshi et al. 2007; Kalinsky, Jacks et al. 2009). The association of *PIK3CA* mutations with favorable patient outcome appears to be paradoxical given the potent transformation potential of *PIK3CA* mutation *in vitro* (Meyer and Bentires-Alj 2010). One possible explanation for this "*PIK3CA* paradox" is that most experimental models assess effects on primary tumor growth and not metastases and long-term survival. Alternatively, *PIK3CA* mutations might only moderately activate the pathway and/or constitutive activity of mutant *PIK3CA* may induce negative feedback loops that preclude a more pronounced activation of the pathway (Li, DeFea et al. 1999).

Interestingly, there was a significant difference between E542K/E545K and H1047R mutations in terms of patient outcome. While H1047R mutations were associated with improved survival (Barbareschi, Buttitta et al. 2007; Kalinsky, Jacks et al. 2009), E542K/E545K mutations predict poor prognosis for disease-free survival (Barbareschi, Buttitta et al. 2007). Of note, in the latter study no association with survival was found when both classes of *PIK3CA* mutation were combined (Barbareschi, Buttitta et al. 2007). Another group associated particularly H1047R mutations with a worse patient outcome, however, in these studies either only IDCs were used excluding for example ILCs in which helical domain mutations were shown to be enriched (Lai, Mau et al. 2008) or only aggressive ErbB2-positive and triple negative cancers, in which *PIK3CA* mutation are very rare, were analyzed (Lerma, Catasus et al. 2008; Michelucci, Di Cristofano et al. 2009).

Rationale and Aims of the Work

Breast cancer is the most common form of cancer in women and accounts for more than 450'000 deaths worldwide annually. Breast cancer treatment includes surgery, radio-, and chemotherapy, as well as targeted therapy for ER-positive and ErbB2-positive tumors. Many breast cancer patients show either *de novo* or acquired resistance to those therapies highlighting the urgent need for new therapeutic targets and preclinical models in which the molecular mechanisms of treatments and resistance can be studied.

PIK3CA, which encodes the alpha catalytic subunit of PI3K, was found to be mutated at a high frequency in various types of cancer including breast cancer. These mutations result in constitutive activation of the enzyme and were demonstrated to be transforming *in vitro* and *in vivo*, however, whether mutant *PIK3CA* can initiate mammary carcinomas in mice was unknown.

Mouse models of breast cancer including various transgenic mice overexpressing activated ErbB2 have made significant contributions to the understanding of the biology of breast cancer. Given the high frequency of *PIK3CA* mutations in breast cancer, we decided to generate and characterize mouse models expressing the two most common activating mutations (E545K and H1047R). Our aims were:

1) to investigate whether *PIK3CA* mutations induce carcinomas in the mouse and to characterize such tumors both, histologically and molecularly
2) to identify molecular differences between E545K- and H1047R-evoked tumors
3) to identify the cell(s)-of-origin for mutant *PIK3CA*-driven mammary tumors

Part I: *PIK3CA* H1047R Induces Heterogeneous Mammary Carcinomas

Results and discussion of the published manuscript "Luminal Expression of *PIK3CA* Mutant H1047R in the Mammary Gland Induces Heterogeneous Tumors"

Expression of PIK3CA H1047R in luminal mammary epithelial cells induces carcinomas

To test whether *PIK3CA* H1047R evokes mammary carcinoma, we generated transgenic mice that conditionally expressed this mutation in the mammary epithelium. The correct integration of the construct in ES cells conditionally expressing *PIK3CA* H1047R (Figure 1A) was tested by Southern blotting and PCR (Figure 1B and data not shown). The ES cells were used to generate the H1047R line and the mutation was confirmed by DNA sequencing (Figure 1B right). Next, H1047R animals were crossed to WAPiCre mice in which expression of recombinase Cre was driven by the whey acidic protein (WAP) promoter that is active in alveolar progenitor cells and differentiated secretory luminal cells (Wintermantel, Mayer et al. 2002; Boulanger, Wagner et al. 2005; Booth, Boulanger et al. 2007; Bruno and Smith 2010). We also crossed H1047R animals to mice expressing Cre under the control of the mouse mammary tumor virus long terminal repeat (MMTV-Cre), which results in expression within luminal mammary epithelial cells (Andrechek, White et al. 2005).

Female bi-transgenic WAPiCre H1047R mice and littermate controls (WAPiCre) were generated. Mammary glands from WAPiCre H1047R virgin mice had GFP-positive areas indicating expression of the oncogene (Figure 1C left). This is consistent with previous studies that reported activity of the WAP promoter in a fraction of mammary epithelial cells in virgin mice (Booth, Boulanger et al. 2007; Bruno and Smith 2010). Examination of whole-mounts and hematoxylin and eosin (H&E)-stained sections revealed on average 5.7 (±2.2) neoplastic lesions in glands from 21- to 24–week-old virgin WAPiCre H1047R mice but not from up to 18–week-old WAPiCre H1047R virgin or age matched littermate controls (Figure 1C right).

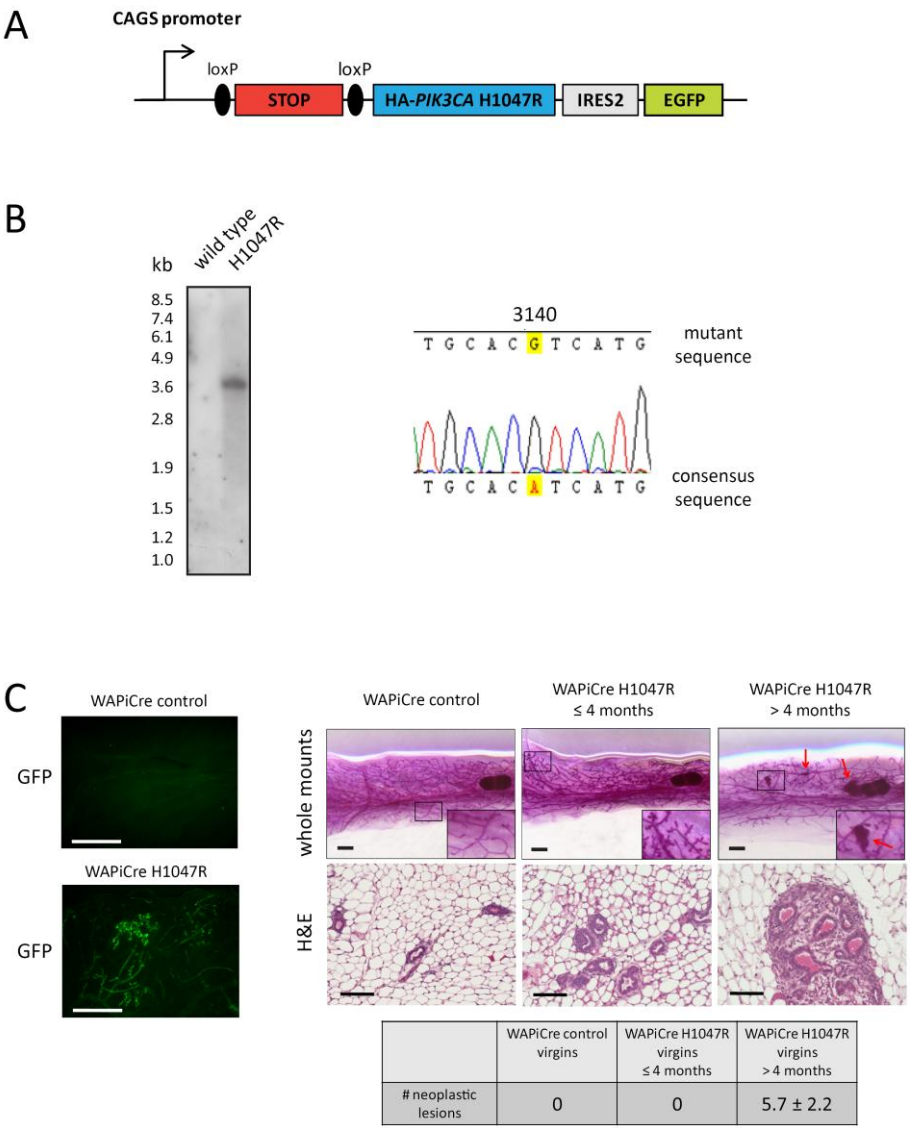

Figure 1. Targeted expression of mutant p110α in luminal mammary epithelial cells. (A) Schematic of the construct used for generating transgenic mice conditionally expressing *PIK3CA* H1047R. The *PIK3CA* cDNA is flanked by a floxed STOP cassette upstream and an IRES2-EGFP reporter element downstream. Expression of *PIK3CA* H1047R is driven by a chicken β-actin (CAGS) promoter. (B) Southern blotting of genomic DNA from wild-type and *PIK3CA* H1047R mice (*left*) and sequencing of genomic DNA from H1047R transgenic mice harboring a A to G mutation at nucleotide 3140 (*right*). (C) Left panel: Fluorescence images of glands from virgin WAPiCre control and virgin WAPiCre H1047R mice showing GFP expression. Right panel: Representative images of mammary glands from WAPiCre control mice (*left*), WAPiCre H1047R virgin mice between 12 and 18 weeks old (*center*), and WAPiCre H1047R virgin mice between 21 and 24 weeks old (*right*). Images show whole-mount preparations (*top*) and H&E-stained sections (*bottom*). The red arrows indicate neoplastic lesions. Inserts show the indicated areas at higher magnification. Table shows quantification of neoplastic lesions. Scale bars = 1 mm (*whole mounts, fluorescence images*) and 100 µm (*H&E images*).

The WAPiCre H1047R and control mice were impregnated to achieve maximal Cre-mediated recombination and the pubs were removed the day after delivery. Whereas parous WAPiCre mice did not form tumors, WAPiCre H1047R mice developed mammary tumors on average 36.8 (±4.9) days after delivery of the pups, corresponding to an age of 140.3 (± 6.9) days (Figure 2A). Bi-transgenic MMTV-Cre H1047R mice and littermate controls (MMTV-Cre) were generated and left as virgins. Surprisingly, ~75% of the MMTV-Cre H1047R animals died before the age of 4 months. Although we did not identify the cause of death, we consider that leakiness of the MMTV promoter causing deleterious H1047R expression in tissues other than the mammary gland was a likely cause (D.S.M. and M.B-A., unpublished observations). However, ~25% of the MMTV-Cre H1047R mice were viable and formed mammary carcinomas on average after 214 (±22.6) days, whereas no tumors were detected in MMTV-Cre control mice (Figure 2B).

Since the average age of tumor onset between parous WAPiCre H1047R and virgin MMTV-Cre H1047R mice differs by ~75 days (140.3 vs. 214 days), we sought to investigate whether pregnancy accelerates *PIK3CA* H1047R-driven tumorigenesis. To address this question we compared tumor onset in nulliparous and parous WAPiCre H1047R mice and found tumor onset to occur significantly earlier in parous mice than in nulliparous mice (Figure 2C). These data show that pregnancy accelerates tumor onset in WAPiCre H1047R mice.

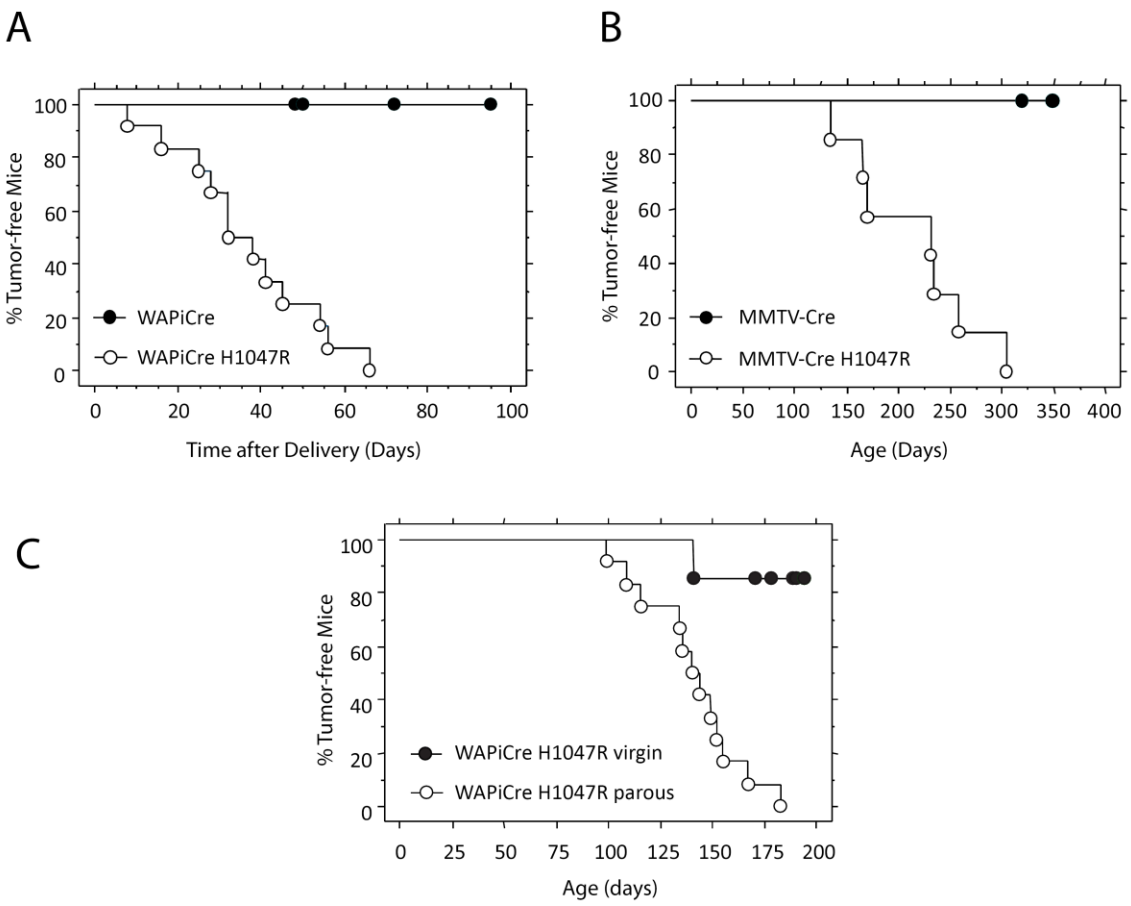

Figure 2. WAPiCre H1047R and MMTV-Cre H1047R mice develop mammary tumors. (A) Kaplan-Meier curves showing tumor onset in bi-transgenic WAPiCre H1047R mice (*n*=12) and WAPiCre littermate controls (*n*=7). The mice were impregnated and the pups removed from the mothers the day after delivery. Bi-transgenic animals developed palpable tumors on average 36.8 (±4.9) days after delivery, corresponding to age 140.3 (±6.9) days. (B) Kaplan-Meier curves showing tumor onset in double transgenic MMTV-Cre H1047R mice (*n*=7) and MMTV-Cre littermate controls (*n*=8). MMTV-Cre H1047R mice developed palpable tumors on average within 214 (±22.6) days. (C) Kaplan-Meier curves showing tumor onset in virgin WAPiCre H1047R (*n*=7) and parous WAPiCre H1047R mice (*n*=12). Parous animals developed palpable tumors on average at 140.3 (±6.9) days and all animals had at least one tumor within 183 days of age. In contrast, by 170 days, only one out of seven virgin WAPiCre H1047R mice developed a tumor (at 141 days). The difference in tumor latency between parous and virgin animals is significant ($P = 0.0006$).

We then assessed the mechanisms underlying the accelerated tumor onset seen in parous vs. nulliparous WAPiCre H1047R mice. Fluorescence images and Western Blot analysis showed enhanced GFP expression in glands from parous mice indicating an increase in the number of cells that underwent Cre-mediated recombination and thus expressed H1047R

(Figure 3). In addition, whole mounts of the involuting glands revealed a dramatic delay in involution in mice expressing *PIK3CA* H1047R compared with control animals (Figure 4A), which is in line with previous reports of a delayed involution when the PI3K pathway is hyperactivated (Schwertfeger, Richert et al. 2001; Li, Robinson et al. 2002). Immunostaining for cleaved caspase-3 revealed a decrease in the number of apoptotic cells in involuting glands from WAPiCre H1047R mice compared with control mice, suggesting that reduced cell death is the cause of the delayed involution (Figure 4B,C). Our results suggest, therefore, that the acceleration of tumor onset is most likely due to an increase in the number of cells expressing *PIK3CA* H1047R in parous glands and to impaired cell death in involuting glands with the H1047R mutation. Indeed, pregnancy-induced proliferation could facilitate the acquirement of further genomic alterations and therefore accelerates tumorigenesis.

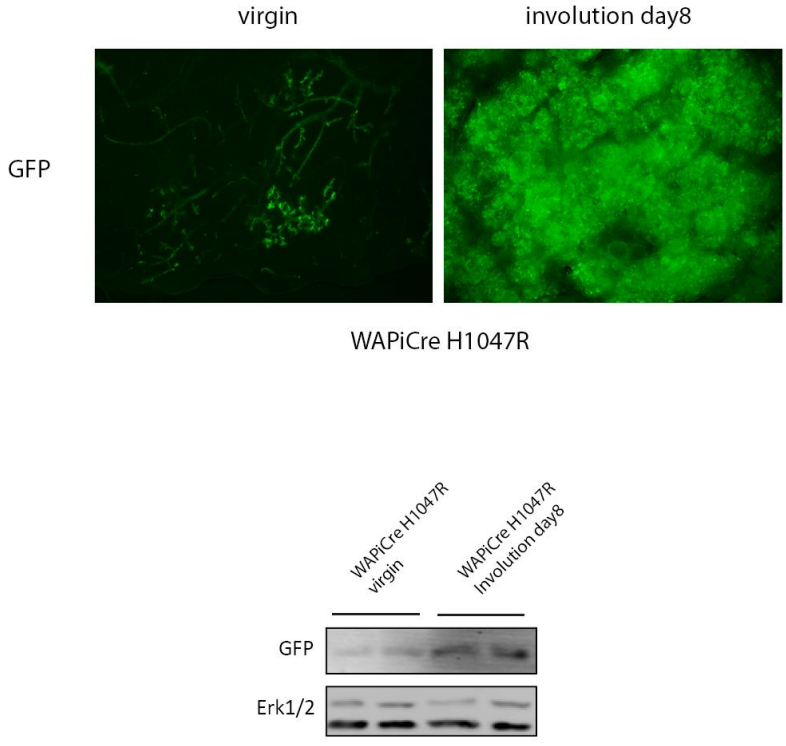

Figure 3. GFP expression in glands from virgin and parous WAPiCre H1047R mice. Fluorescence images of a gland from WAPiCre H1047R virgin mouse (*left*) and of a day 8-involuting gland (*right*) showing GFP expression (*upper panel*). Immunoblotting of mammary gland lysates from virgin and parous WAPiCre H1047R mice as indicated (*lower panel*). Scale bars = 1 mm.

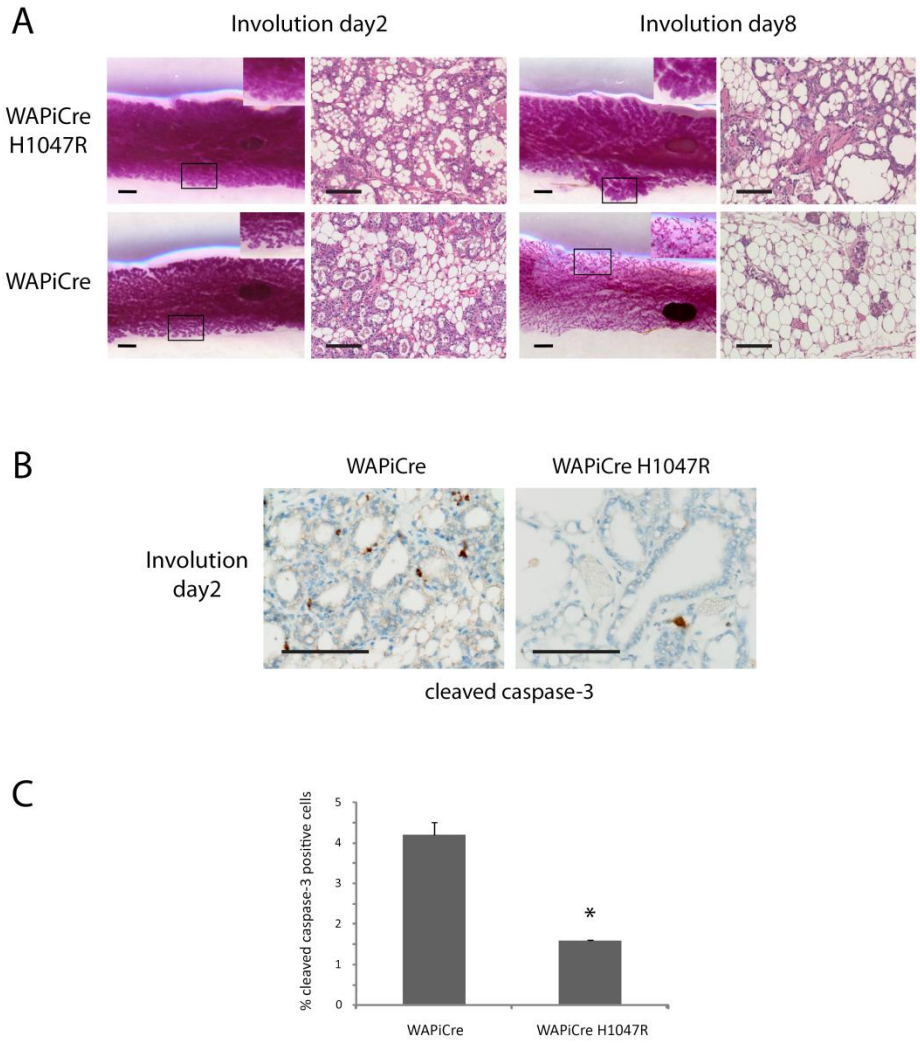

Figure 4. Expression of *PIK3CA* H1047R delays mammary gland involution. (A) Representative images of involuting glands. The pups were removed from the mothers the day after delivery and the glands isolated 2 days (*left panel*) and 8 days (*right panel*) later. Whole mounts (*left*) and H&E-stained sections (*right*) are shown. (B) Cleaved caspase-3 immunostainings for glands at involution day 2 for both the WAPiCre control (*left*) and WAPiCre H1047R mice (*right*). (C) Relative proportion of cleaved caspase-3-positive cells in day 2-involuting glands from WAPiCre control (*left*) and WAPiCre H1047R mice (*right*). * $P < 0.001$. Scale bars = 1 mm (*whole mounts*) and 100 µm (*H&E images*).

Analysis of RNA and proteins from WAPiCre H1047R and MMTV-Cre H1047R-induced tumors confirmed that mutant *PIK3CA* was expressed in the bi-transgenic mice (Figure 5A, B). In addition, tumors from both WAPiCre H1047R and MMTV-Cre H1047R mice showed threefold higher phospho-Akt levels than mammary tumors from the MMTV-NeuNT model. In contrast, activation of the Erk1/2 pathway in *PIK3CA* H1047R tumors tended to be weaker than in tumors from MMTV-NeuNT mice (Figure 5C).

Our results show that luminal expression of *PIK3CA* H1047R induces mammary tumor formation. This is consistent with the observation that conditional expression of mutant *PIK3CA* H1047R in type II lung alveolar epithelial cells causes lung adenocarcinomas in transgenic mice (Engelman, Chen et al. 2008) and suggests that this mutation plays a causal role in epithelial cancers.

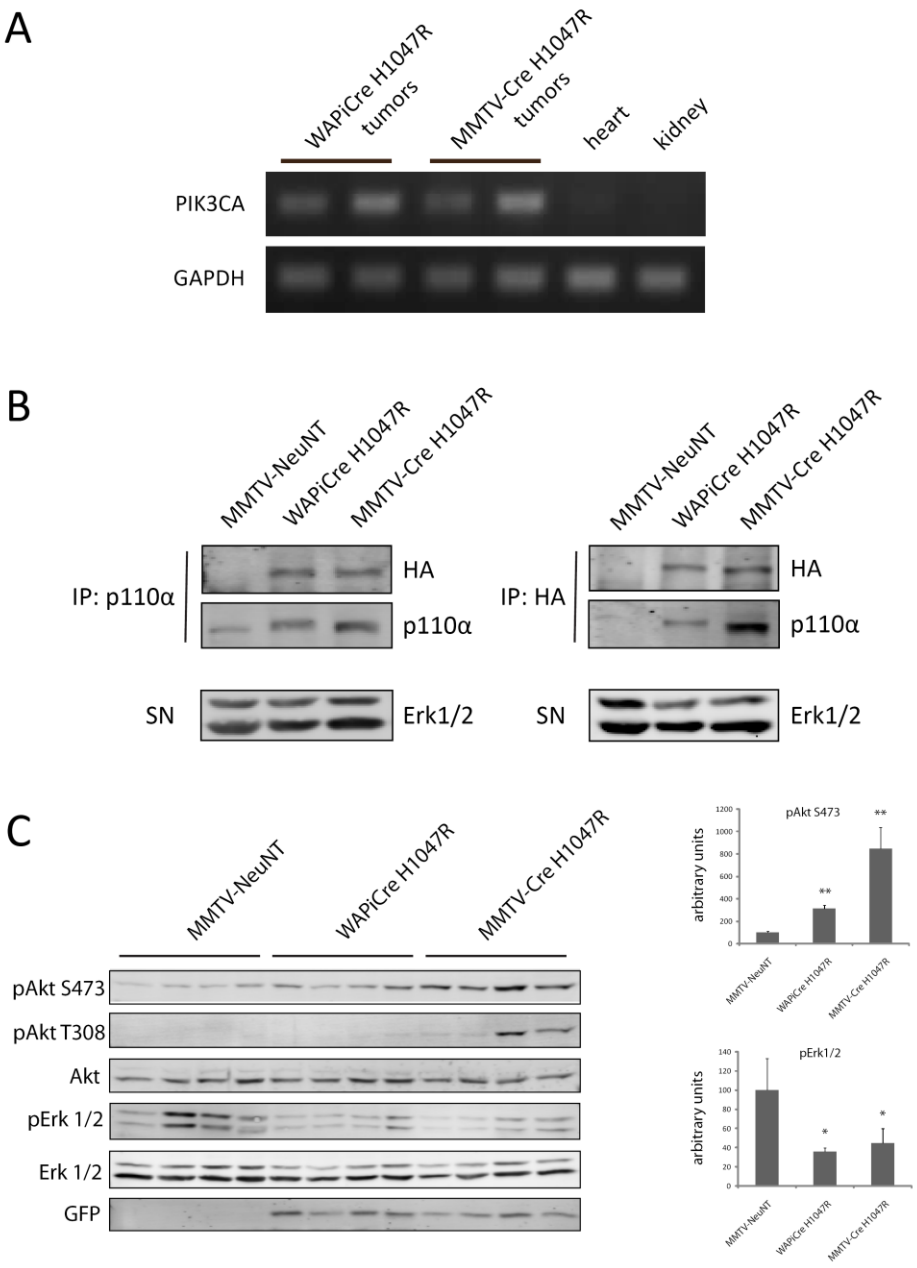

Figure 5. Tumors from WAPiCre H1047R and MMTV-Cre H1047R mice express mutant *PIK3CA*. (A) RT-PCR showing expression of *PIK3CA* H1047R in WAPiCre H1047R and MMTV-Cre H1047R mammary tumors but not in heart or kidney of a WAPiCre H1047R animal. (B) Expression of exogenous p110α as indicated by P110α-immunoprecipitation (IP) from MMTV-NeuNT, WAPiCre H1047R, and MMTV-Cre H1047R tumor lysates using anti-p110α (*left*) or anti-HA antibodies (*right*). (C) Immunoblotting of mammary tumor lysates from the indicated genotypes using the specified antibodies (*left*) and quantification of pErk1/2 and pAkt S473 signals (*right*). * not significant; ***P* <0.01; *SN*: supernatant.

WAPiCre H1047R and MMTV-Cre H1047R-evoked mammary tumors are heterogeneous

To gain insight into significant patho-physiological features, 22 WAPiCre H1047R and 21 MMTV-Cre H1047R-induced mammary tumors were characterized histologically. MMTV-Cre H1047R-caused tumors showed multiple adenomyoepitheliomas, with clusters of well-delineated polypoid tumors composed of a mixture of glandular epithelium and interstitial fusiform cells with abundant polar cytoplasm (Figure 6 top row left). Similar tumors have been reported in MMTV-Cre/Pten$^{fl/fl}$/ErbB2^{KI} mice, suggesting that an activated PI3K pathway mediates this histotype (Schade, Rao et al. 2009).

In contrast, the WAPiCre H1047R mice formed a more diverse spectrum of tumors with five distinct histotypes. The most prevalent tumor phenotypes found are adenosquamous carcinomas (54.6%) and adenomyoepitheliomas (22.7%). Adenocarcinomas with squamous metaplasia (13.6%) and adenocarcinomas (9.1%) were also observed albeit at lower frequencies (Figure 6 top row and Figure 7A). All the glands surrounding the tumors displayed diffuse adenocarcinomatosis with invasive periductal cords of neoplastic epithelial cells in dense connective tissue (Figure 6 top row right).

To further characterize H1047R-induced carcinomas, tumors were stained for luminal cytokeratin 18 (K18), basal/myoepithelial cytokeratin 14 (K14), and myoepithelial α-smooth muscle actin (α-SMA) markers, as well as for ER and the progesterone receptor (PR). Notably, ~18 to ~26% of the tumor cells of the adenomyopitheliomas from both transgenic mice expressed ER and ~16% expressed PR in the luminal cells (Figure 6 and Figure 7B). Other tumor histotypes also contained ER-positive cells but at lower frequencies (<5%) (Figure 6 and Figure 7B). WAPiCre- and MMTV-Cre H1047R tumors were positive for both luminal K18 and basal K14. The relative tumor area positive for K14 was ~15% in adenomyoepitheliomas and adenocarcinomatosis, whereas in the other phenotypes it ranged between 26% and 43%. The percentage of K18-positive tumor area was 25% in adenocarcinomatosis and ranged between 36 to 45% in the other tumor histotypes (Figure 6 and Figure 7B). Although the majority of

tumor cells expressed either K18 or K14, some cells were positive for both K14 and K18 (Figure 8A). As expected, the K14-positive cells within WAPiCre- and MMTV-Cre H1047R adenomyoepitheliomas were also α-SMA-positive (Figure 6). In contrast, the K14-positive cells within adenosquamous carcinomas observed in WAPiCre H1047R mice were largely negative for α-SMA, a characteristic of human metaplastic breast cancer in which *PIK3CA* is mutated in ~50% of cases (Hennessy, Gonzalez-Angulo et al. 2009). Interestingly, all tumors showed very low rates of apoptosis (0.2-1.4%) (Figure 6 and Figure 7B), most likely due to the anti-apoptotic effect of an activated PI3K pathway. We also found the percentage of Ki-67-positive cells to be lower in adenomyoepitheliomas and adenocarcinomatosis than in all other tumor phenotypes (Figure 6 and Figure 7B).

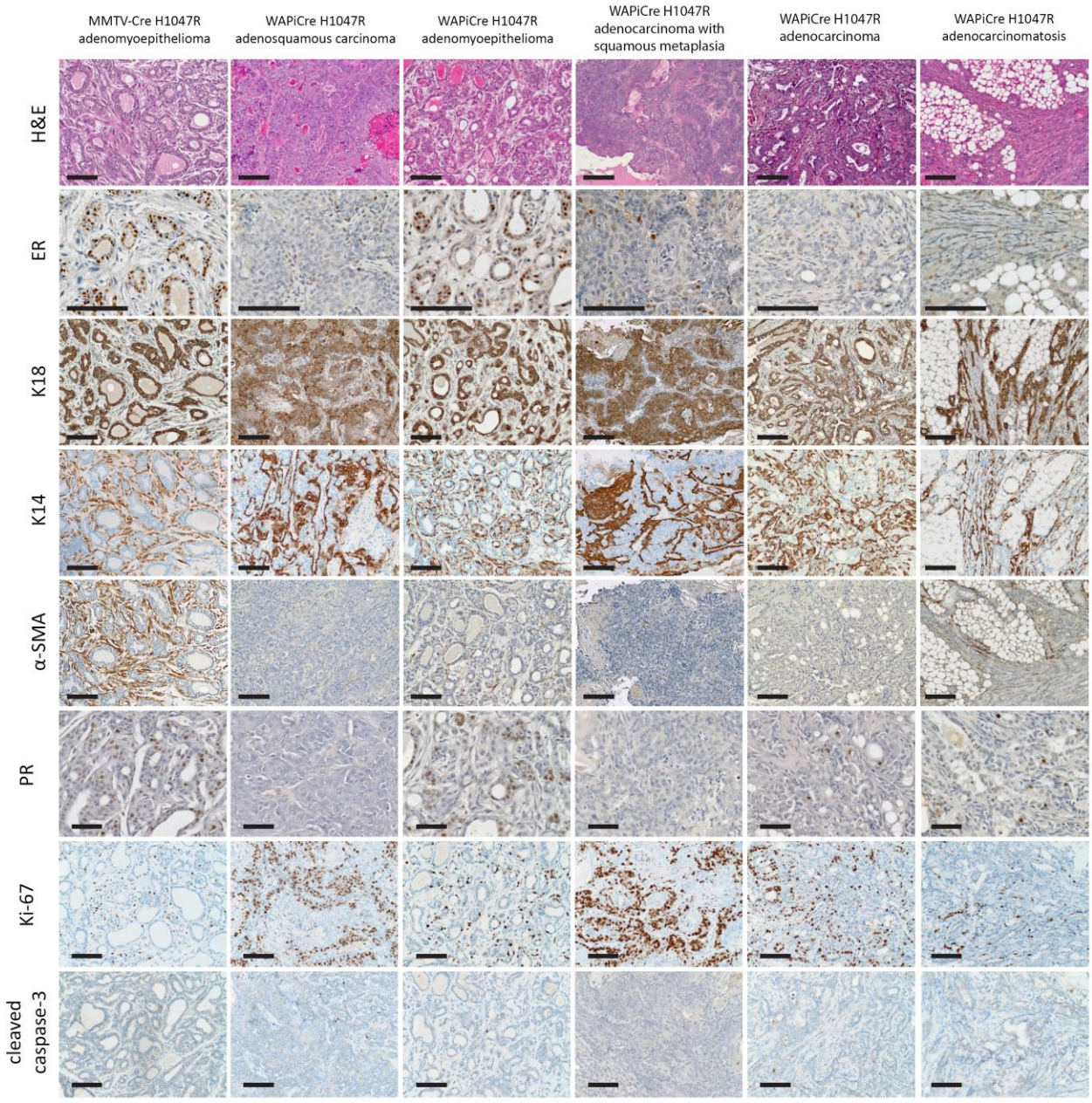

Figure 6. WAPiCre H1047R and MMTV-Cre H1047R-evoked tumors express basal markers. (A) H&E-stained sections and immunostainings for ER, K18, K14, and α-SMA from MMTV-Cre H1047R adenomyoepithelioma and different WAPiCre H1047R tumor histotypes as indicated.

A

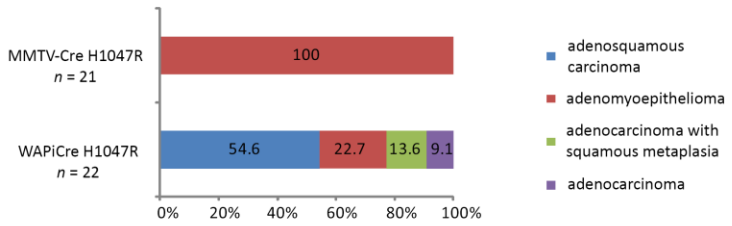

B

		% of tumor area			% of tumor cells			
Model	**Phenotype**	**K18**	**K14**	**α-SMA**	**ER**	**PR**	**Ki-67**	**cleaved caspase-3**
WAPiCre H1047R	adenosquamous carcinoma (*n*=8)	45	43	0.3	4.7	0.1	32	1.4
	adenomyoepithelioma (*n*=5)	36	14	6.5	18.4	17.5	17	0.4
	adenocarcinoma with squamous metaplasia (*n*=3)	43	26	0.1	4.5	0.0	54	0.8
	adenocarcinoma (*n*=2)	45	28	0.1	4.5	1.4	24	1.2
	adenocarcinomatosis (*n*=3)	25	15	1.0	4.0	3.0	12	1.4
MMTV-Cre H1047R	adenomyoepithelioma (*n*=4)	42	14	9.7	26.1	15.6	14	0.2

Figure 7. Quantification of H1047R-evoked tumors. (A) Relative prevalence of adenosquamous carcinoma (blue), adenomyoepithelioma (red), adenocarcinoma with squamous metaplasia (green), and adenocarcinoma (purple) among MMTV-Cre H1047R and WAPiCre H1047R-evoked tumors. (B) The table summarizes histological analysis for the markers ER, PR, K18, K14, α-SMA, Ki-67, and cleaved caspase-3 in 25 different tumors consisting of five distinct tumor histotypes from both WAPiCre H1047R and MMTV-Cre H1047R mice. Indicated is the proportion of positive tumor cells (ER, PR, Ki-67, cleaved caspase-3) or the positive tumor area (K18, K14, α-SMA).

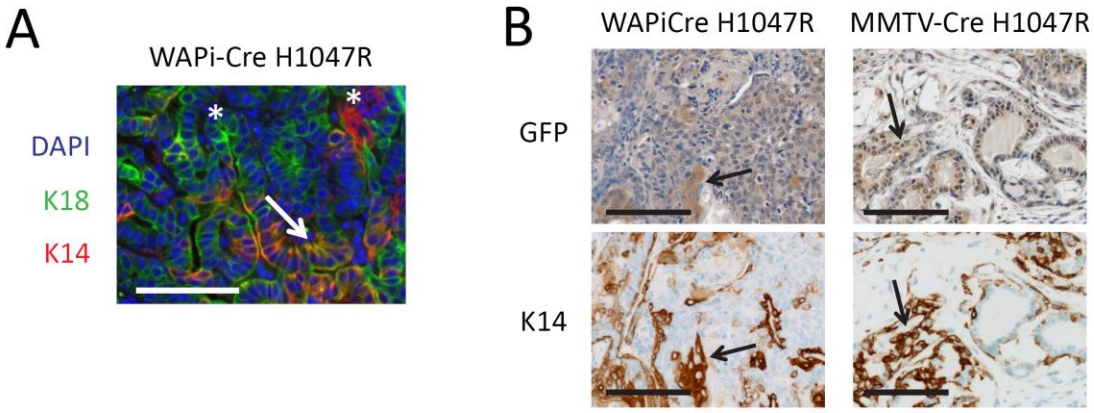

Figure 8. (C) Fluorescent image of DAPI staining (*blue*) and immunostaining of K18 (*green*) and K14 (*red*) in a WAPiCre H1047R tumor section. The arrow indicates K14/K18 double-positive cells. Asterisks indicate K14 and K18 single-positive cells. (D) Images of immunostaining for GFP and K14 in WAPiCre H1047R (*top*) and MMTV-Cre H1047R tumor sections (*bottom*). Arrows indicate areas of K14/GFP double-positive cells. Scale bars = 100 µm.

These data show that luminal expression of *PIK3CA* H1047R can induce mammary tumors expressing the basal marker K14. To exclude the possibility that luminal *PIK3CA* H1047R induces expression of paracrine factors that transform basal cells, we analyzed K14-positive cancer cells for GFP expression by immunostaining and FACS. There was a significant overlap between K14 and GFP expression (Figure 8B), suggesting that some K14-positive cancer cells within the WAPiCre H1047R and MMTV-Cre H1047R tumors resulted from expression of the oncogene in luminal cells. This supports the emerging notion that some tumors with basal characteristics arise from luminal cells (Lim, Vaillant et al. 2009; Molyneux, Geyer et al. 2010).

Taken together, our results show that luminal expression of *PIK3CA* H1047R evokes mammary tumors, recapitulating the heterogeneity of human breast cancer. These results lead to major conclusions. The finding that *PIK3CA* H1047R causes ER- and PR-positive tumors suggests that PI3K activity expands ER-positive mammary cells, consistent with the presence of *PIK3CA* H1047R mutations in human ER-positive tumors (Saal, Holm et al. 2005).

The presence of cancer cells expressing luminal and basal markers in WAPiCre- and MMTV-Cre H1047R-evoked tumors suggests in both models that multipotent progenitor cells are the targets of H1047R-mediated transformation. The WAP promoter is active in a multipotent progenitor population, the parity-identified mammary epithelial cells (PI-MECs), which are present in nulliparous mice and are expanded after pregnancy (Booth, Boulanger et al. 2007; Bruno and Smith 2010). Tumors that developed in WAPiCre H1047R nulliparous mice most likely derived from PI-MECs because this is the cell population that expresses WAP-driven Cre in glands from nulliparous mice (Bruno and Smith 2010). PI-MECs were shown recently to be the target of MMTV-NeuNT-driven carcinogenesis (Bruno and Smith 2010; Jeselsohn, Brown et al. 2010). Therefore, it is plausible that PI-MECs are the cells-of-origin of cancer in both WAPiCre- and MMTV-Cre H1047R-evoked tumors but at this stage we cannot completely exclude that expression of *PIK3CA* H1047R in more differentiated cells also contributes to tumor formation in these models.

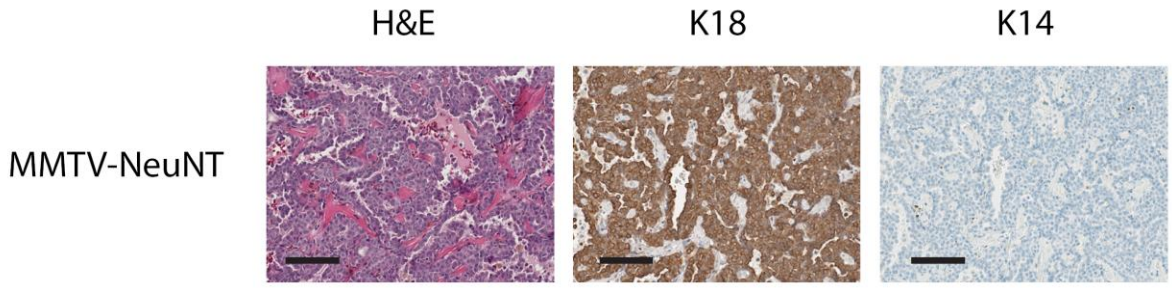

Figure 9. H&E-stained sections and immunostainings for K18 and K14 from MMTV-NeuNT-evoked tumors. Scale bars = 100 µm.

The observation of different histotypes between WAPiCre H1047R- and MMTV-Cre H1047R-derived tumors has several possible explanations. First, WAPiCre H1047R mice but not MMTV-Cre H1047R mice went through pregnancy. Second, it is possible that the cellular targets of MMTV- and WAP- are overlapping but not congruent.

The fact that tumors from MMTV-Cre H1047R but not MMTV-NeuNT mice express K14 (Figure 6 and Figure 9) suggests a model in which *PIK3CA* H1047R transforms multipotent progenitors, allowing differentiation along the luminal and basal lineages. In contrast, the NeuNT oncogene favors luminal differentiation resulting in K18-positive but not K14-positive tumors. An alternative and more interesting explanation is that the MMTV promoter is active in differentiated luminal cells and H1047R causes their dedifferentiation to multipotent progenitor cells, which then give rise to K14- and/or K18-positive cancer cells. This would suggest a role for *PIK3CA* H1047R in cancer cell plasticity, a hypothesis that merits testing.

Part II: *PIK3CA* E545K and H1047R Induce Mammary Carcinomas with Different Latencies

Results

WAPiCre E545K but not PIK3CA wild-type mice form mammary tumors

In order to test whether expression of wild-type *PIK3CA* (*PIK3CA*^{wt}) or the helical domain mutation E545K induces mammary tumors we generated transgenic mice that carry a conditional allele of human *PIK3CA*^{wt} or the E545K mutant cDNA analogous to the H1047R mice described before (see Figure 1 in section "Part I: Characterization of the WAPiCre H1047R Mouse Model"). We then crossed these mice to WAPiCre mice to obtain mammary gland specific expression of the transgenes. The resulting WAPiCre *PIK3CA*^{wt} and WAPiCre E545K females were impregnated to induce maximal WAP activity and Cre-mediated excision of the STOP cassette and subsequently monitored for tumor formation. While WAPiCre *PIK3CA*^{wt} mice did not develop mammary carcinomas after 230 days, WAPiCre E545K females had palpable tumors after an average of 80.8 (± 8.0) days (Figure 1).

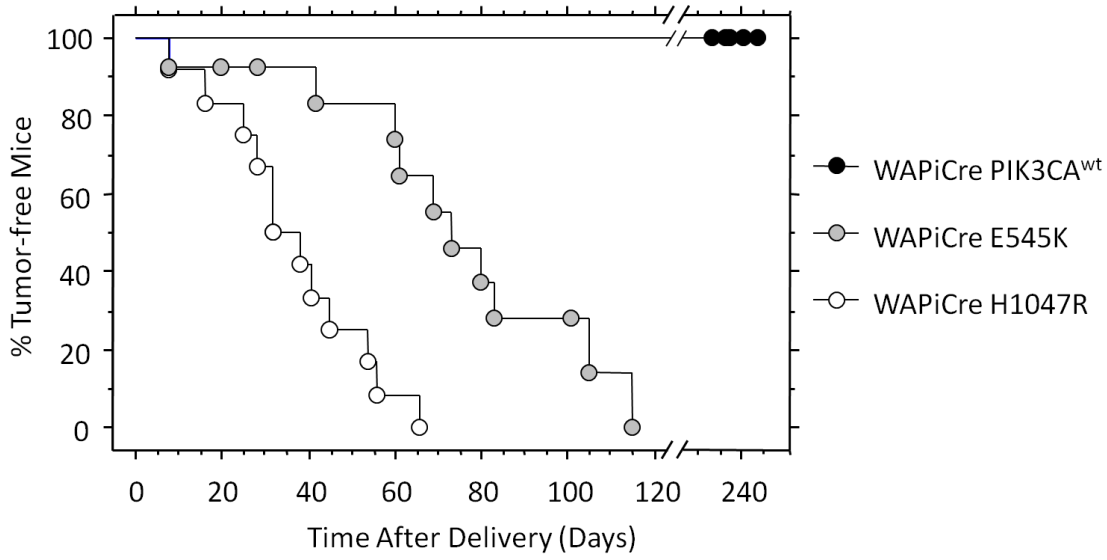

Figure 1. WAPiCre E545K mice develop mammary tumors with longer latency than WAPiCre H1047R mice. (A) Kaplan-Meier curves showing tumor onset in bi-transgenic WAPiCre H1047R mice (*n*=12), WAPiCre E545K mice (n=10) and WAPiCre *PIK3CA*^{wt} females (n=7). The mice were impregnated and the pups removed from the mothers the day after delivery. Bi-transgenic H1047R animals developed palpable tumors on average 36.8 (±4.9) days after delivery, WAPiCre E545K mice formed tumors on average 80.8 (±8.0) days after delivery, whereas WAPiCre *PIK3CA*^{wt} mice did not form palpable tumors after 230 days.

PIK3CA E545K is a weaker inducer of mammary carcinomas than H1047R

Expression of both the helical domain and the kinase domain mutation caused tumor formation *in vivo*, however, the average latency to tumor onset was different (80 days for WAPiCre E545K vs. 37 days for WAPiCre H1047R). To gain insight into possible differences in molecular signaling pathways activated by the two different p110α mutants we performed immunoblotting for various signaling molecules including downstream effectors of PI3K such as Akt and mTOR (Figure 2). Surprisingly, lysates from WAPiCre E545K evoked tumors contained comparable phospho-levels for Akt, Erk1/2, mTOR and the ribosomal protein S6 which is a downstream target of mTOR. This finding suggests that in tumors, both activating mutations of *PIK3CA* activate the investigated downstream signaling to a similar extent.

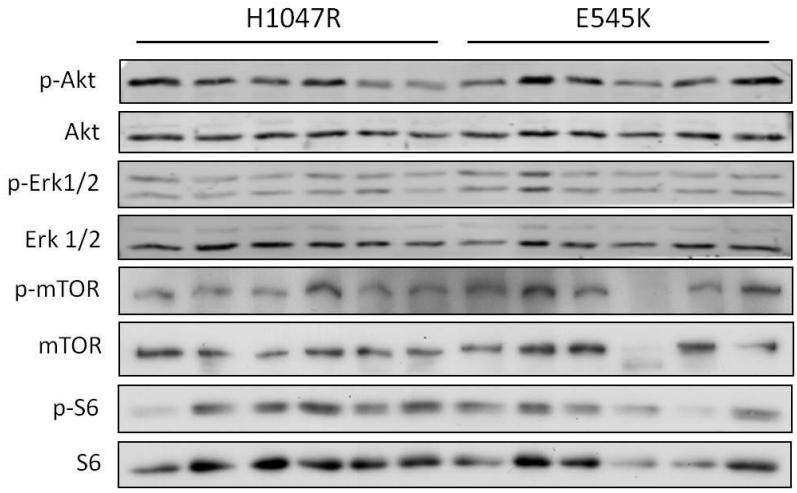

Figure 2. Tumors from WAPiCre H1047R and WAPiCre E545K mice express comparable levels of p-Akt, p-Erk1/2, p-mTOR, and p-S6. Immunoblotting of mammary tumor lysates from the indicated genotypes using the specified antibodies.

Discussion and Outlook

Parous WAPiCre *PIK3CA*^{wt} mice do not form tumors after 230 days while mice expressing either E545K or H1047R mutant p110α develop mammary carcinomas after an average of 80.8 and 36.8 days after delivery, respectively. This suggests that the tumorigenic effect caused by mutant *PIK3CA* is mostly due to the mutation rather than overexpression of the gene (Figure 1).

Furthermore, the shorter tumor latency observed in WAPiCre H1047R mice as compared to WAPiCre E545K animals suggests that p110α H1047R is a more potent oncogene than the helical domain mutation E545K which is in concordance with a previous study performed on chicken embryonic fibroblasts (Bader, Kang et al. 2006). The lipid product PIP_3 was demonstrated to be essential for p110α-mediated transformation and therefore a simple explanation for the difference in tumor latency would be that p110α E545K produces less PIP_3 than H1047R resulting in less activation of the effector Akt and its downstream targets. However, levels of S473 phosphorylated Akt and S6, both indicating active PI3K signaling, are comparable in E545K- and H1047R-evoked tumors suggesting that the signaling amplitude induced by either mutant p110α E545K or H1047R is similar. Based on this finding and the fact that the helical and kinase domain mutants have different requirements for Ras and p85 (Zhao and Vogt 2008), it is tempting to speculate that these mutations might activate a distinct set of downstream pathways.

In order to test this hypothesis we isolated RNA from a set of WAPiCre E545K and H1047R tumors and performed whole genome expression profiles.

In the future we will:

1) Test whether WAPiCre E545K mice produce a comparable set of tumor histotypes as WAPiCre H1047R mice. For this purpose we harvested tumors from WAPiCre E545K mice and we are currently analyzing their histology similar to that of WAPiCre H1047R-evoked tumors.
2) Analyze whole gene expression profiles that we gained from WAPiCre E545K- and H1047R-evoked mammary tumors.
3) Investigate whether involution in WAPiCre E545K mice is delayed as in WAPiCre H1047R mice.

Part III: Total Body Expression of Mutant *PIK3CA* Results in Premature Death and Alters Mammary Epithelial Cell Properties

Results

Whole body expression of mutant PIK3CA is lethal

In order to investigate how whole body expression of mutants of p110α affects the physiology of mice and whether they induce mammary tumors we crossed mice carrying a conditional allele of either wild-type, E545K or H1047R mutant *PIK3CA* to animals expressing a tamoxifen-inducible CreERT2 fusion protein under the control of a chicken β-actin promoter (CAGS-CreERT2 mice). CAGS-CreERT2 mice expressing conditional *PIK3CA* alleles were treated with tamoxifen on five consecutive days before two days without injection followed by another tamoxifen treatment for five consecutive days (Figure 1).

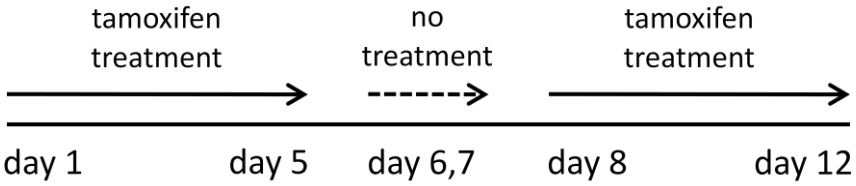

Figure 1. Tamoxifen induction scheme. Control and CAGS-CreERT2 *PIK3CA* transgenic mice were injected on 5 consecutive days with 1 mg tamoxifen. On days 6 and 7, the mice were left untreated before receiving tamoxifen injections for an additional 5 consecutive days. Note that in contrast to CAGS-CreERT2 *PIK3CA*^{wt} or E545K mice, CAGS-CreERT2 H1047R mice were never injected with more than 5 doses of tamoxifen because they died within the first week of treatment.

To test whether wild-type and mutant *PIK3CA* is expressed in the bi-transgenic mice and in the mammary gland in particular, we isolated mammary epithelial cells from mice of all genotypes. After growing them as spheroids in suspension culture for one week to increase the number of cells, we isolated RNA and performed reverse transcription-PCR (RT-PCR). Using primers specifically binding to the human *PIK3CA* gene and the HA-tag we detected a PCR product in all the transgenic mice but not in the control mice demonstrating expression of the transgene (Figure 2).

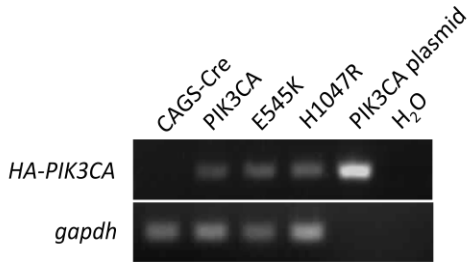

Figure 2. Wild-type and mutant *PIK3CA* are expressed in CAGS-CreERT2 *PIK3CA* mice. RT-PCR amplification of transgenic *HA-PIK3CA* was performed on cDNA from mammary cells isolated from mice with the indicated genotypes. cDNA from CAGS-CreERT2 mice and water served as negative controls (columns 1 and 6) and plasmid containing *PIK3CA* DNA was used as positive control (column 5). Cells isolated from CAGS-CreERT2 *PIK3CA*^{wt}, E545K, and H1047R mice express the transgene (columns 2-4). RT-PCR amplification of *gapdh* was performed for equal loading (bottom row).

While tamoxifen-induction in CAGS-CreERT2 mice expressing *PIK3CA* wild-type (CAGS-CreERT2 *PIK3CA*^{wt}) caused no obvious phenotype, tamoxifen-treated CAGS-CreERT2 expressing mutant *PIK3CA* E545K or H1047R developed a severe phenotype. CAGS-CreERT2 H1047R animals died within one week and CAGS-CreERT2 E545K mice within three weeks. Interestingly, even without any tamoxifen administration, both CAGS-CreERT2 H1047R and E545K mice died within 2 months and 4 months, respectively, which is most likely due to leakiness of the CreERT2 system. Although macroscopic analysis of organs including heart, liver, spleens, and colon revealed no obvious phenotype, hematomas on ears, tail and pads were observed (Figure 3).

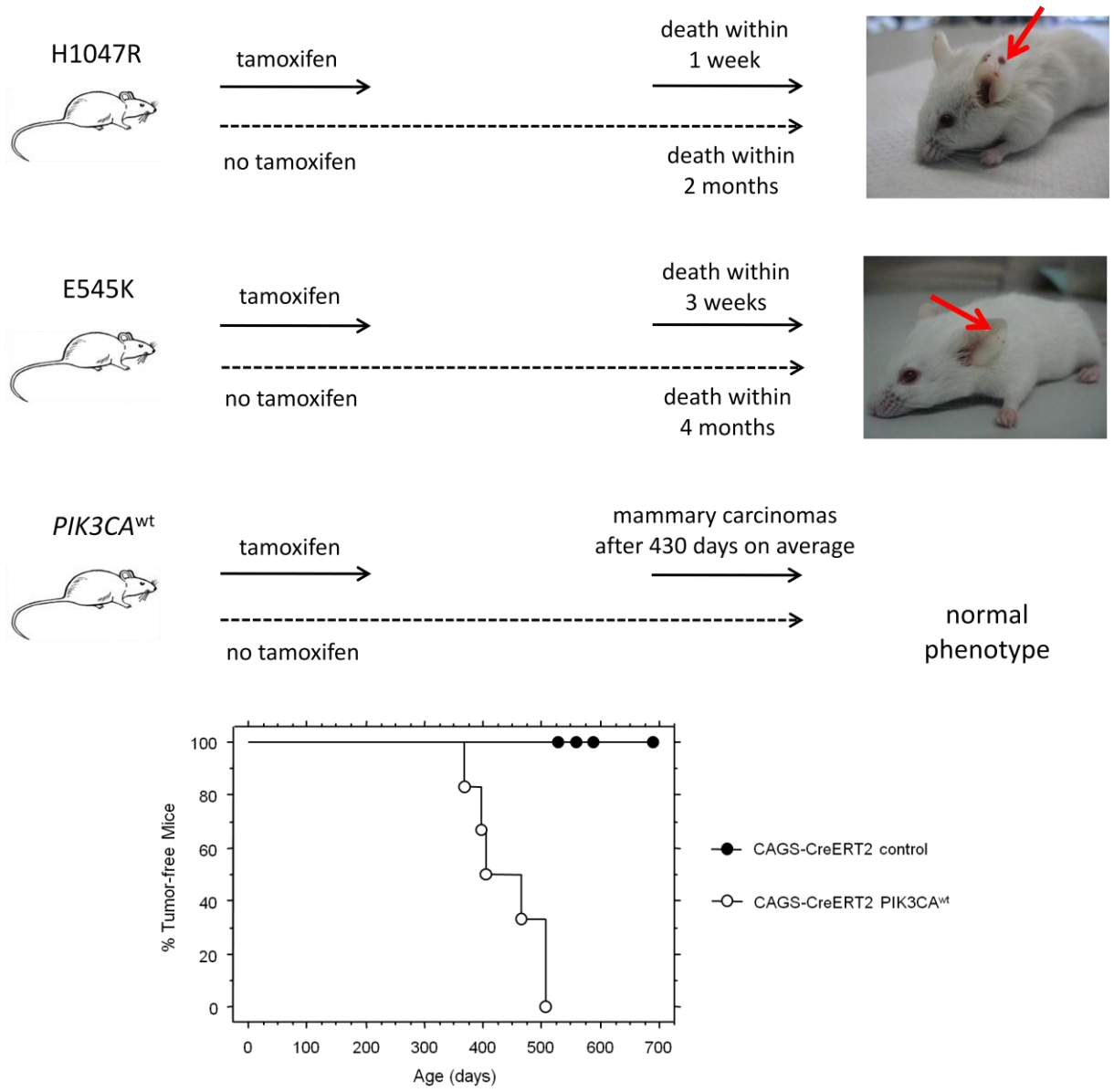

Figure 3. Whole body expression of mutant *PIK3CA* is lethal whereas expression of wild-type *PIK3CA* induces mammary carcinomas with a long latency. In the absence of tamoxifen, mice carrying a conditional allele of mutant H1047R or E545K develop hematomas on the ears, tail, and pads starting at the age of around 3 weeks. Eventually both, CAGS-CreERT2 H1047R and E545K mice, die prematurely within 2 and 4 months, respectively (top two panels). Tamoxifen induction in these mice accelerates the phenotype and leads to death within 1 (CAGS-CreERT2 H1047R) and 3 weeks (CAGS-CreERT2 E545K). Untreated CAGS-CreERT2 *PIK3CA*^{wt} mice are of normal phenotype and do not die prematurely. Treatment of these mice with tamoxifen does not result in an abnormal phenotype at young age, however, at an average age of 429 (±25) days CAGS-CreERT2 *PIK3CA*^{wt} mice develop mammary carcinomas with 100% penetrance as shown by the Kaplan-Meier curves. Red arrows point on hematomas observed on untreated CAGS-CreERT2 H1047R and E545K mice (bottom two panels).

To check what might cause the rapid death in CAGS-CreERT2 H1047R mice after tamoxifen induction, we administrated tamoxifen to CAGS-CreERT2 H1047R and CAGS-CreERT2 control mice on 3 consecutive days and sent the animals to the company "Frimorfo" (Marly, Switzerland) for in-depth analysis. Since the only overt phenotype observed in CAGS-CreERT2 H1047R mice were hematomas, the analysis carried out by Frimorfo was centered on blood coagulation, blood parameters, and metabolic parameters.

The platelet counts were similar in control and CAGS-CreERT2 H1047R mice and the bleeding time and bone marrow histology were normal in the mutant mice. Based on these findings, a platelet defect in CAGS-CreERT2 H1047R animals can be excluded. Further, the coagulation cascade does not seem to be involved since both, Quick-time and TPP assays, produced similar results in control and CAGS-CreERT2 H1047R mice. Histological examination did not reveal major abnormalities in the vessel wall, however, in one CAGS-CreERT2 H1047R mouse, neovascularization of thrombotic vessels was taking place. In certain mutant animals vascular dilation occured, however, the cause for this observation could not be identified. Weakness of the vessel wall or a failure of the right heart might be the reason for this phenotype.

Analysis of blood plasma revealed pathological values for some liver and pancreas enzymes. The levels of the enzymes glutamic pyruvic transaminase (GPT) and glutamic oxaloacetic transaminase were increased ~2 fold and the pancreatic enzyme amylase was elevated ~50% in CAGS-CreERT2 H1047R mice compared to control animals. Major differences were also detected for plasma metabolites. The plasma levels of glucose in CAGS-CreERT2 H1047R mice were ~50% and the levels of triglycerides only ~20% of the levels in control animals. The detailed Frimorfo report is in the Appendix on page 93.

Interestingly, induction of CAGS-CreERT2 *PIK3CA*^{wt} mice with tamoxifen did not cause any phenotype comparable to that of *PIK3CA* mutant mice and the animals were healthy as were control mice. However, after a long latency of ~430 days, these mice started to develop mammary carcinomas with 100% penetrance.

CAGS-CreERT2 H1047R-derived mammary epithelial cells exhibit increased sphere-forming capacity

To investigate whether the MECs from mice expressing wild-type or mutant *PIK3CA* have altered properties regarding self-renewal and proliferation, we isolated cells from the mammary glands of transgenic animals and cultured them in suspension as mammospheres. Mammospheres were first described by Dontu and co-workers (Dontu, Abdallah et al. 2003) as a surrogate assay for stemness/progenitor properties of epithelial cells. A stable number of mammospheres simplistically means that every mammosphere contains one mammosphere-forming cell. If the number of spheres increases with passaging one mammosphere must contain more than one sphere-forming cell arguing for enhanced self-renewing to occur. The size of the spheres allows conclusions on the proliferative capacity of the sphere-forming epithelial cells.

5'000 freshly isolated mammary cells were seeded as single cells and cultured for one week. Interestingly, cells isolated from mammary glands of CAGS-CreERT2 E545K or H1047R formed significantly more mammospheres than CAGS-CreERT2 control mice or mice expressing wild type *PIK3C*A (Figure 4A). Moreover, spheres expressing mutant p110α formed larger mammospheres (Figure 4B). For the subsequent passage (M1), mammospheres were enzymatically digested and 5'000 cells were seeded again as single cells. For the M1 passage only CAGS-CreERT2 control- and CAGS-CreERT2 H1047R-derived MECs were seeded. The number of mammospheres formed was similar to that in passage M0 (Figure 4A).

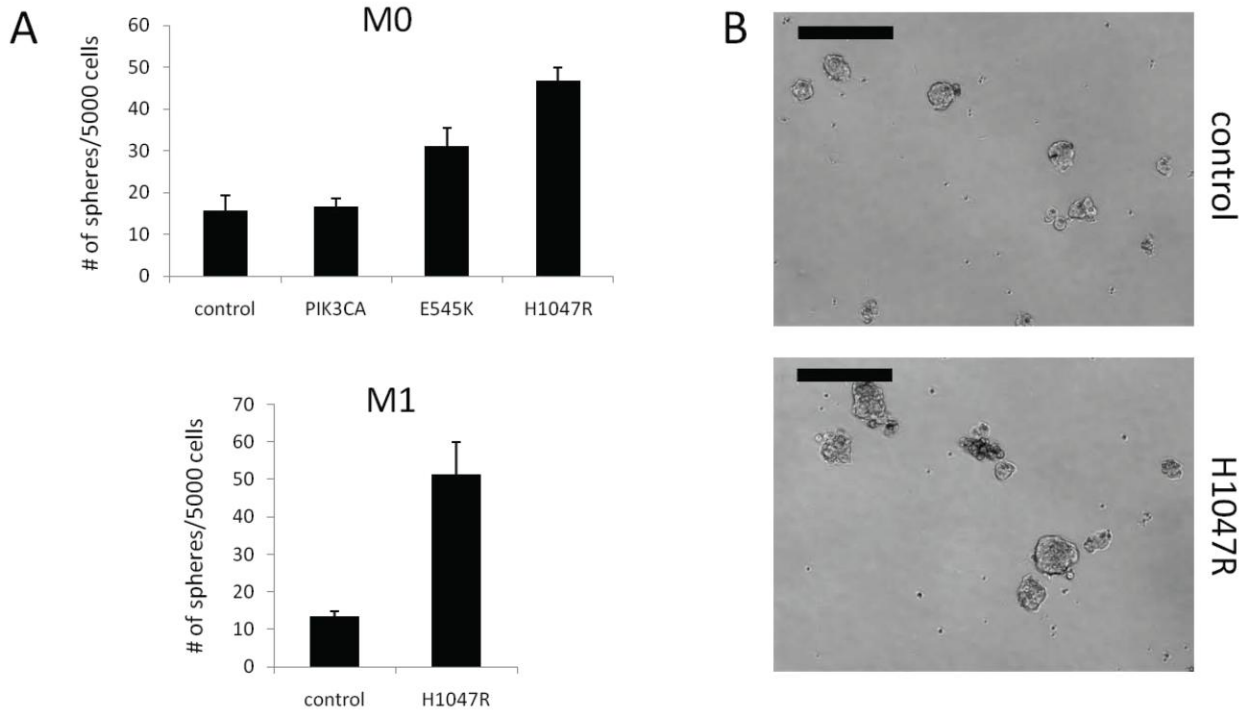

Figure 4. Mammary cells expressing *PIK3CA* mutants have enhanced sphere-forming capacity. (A) 5000 freshly isolated mammary cells from mice of the indicated genotypes were seeded in triplicates on a 24-well ultra-low attachment dish. Cells were grown in suspension for 7 days and the number of mammospheres (>50µm diameter) formed in each well was counted. For CAGS-CreERT2 control 15.7 (±3.7), for CAGS-CreERT2 *PIK3CA* 16.7 (±2.0), for CAGS-CreERT2 E545K 31.0 (±4.5), and for CAGS-CreERT2 H1047R 46.7 (±3.2) mammospheres were formed on average (M0, top). Mammospheres were enzymatically digested into single cells which were seeded again (M1, bottom). (B) Examples of typical M0 mammospheres from CAGS-CreERT2 control (top) and CAGS-CreERT2 H1047R cells are shown (bottom). Scale bar represents 200 µm.

Expression of H1047R results in an accumulation of a mammary epithelial cell population enriched in ER-negative cells

We next assessed whether expression of H1047R altered the mammary epithelial cell hierarchy. We isolated MECs from untreated seven-week old CAGS-CreERT2 control and H1047R mice and excluded lymphocytes via CD45 negative selection. Using the cell surface markers Sca-1 and CD24, we separated the epithelial cells into three subpopulations: Sca-1^{neg} CD24^{med} (enriched in stem cells and myoepithelial cells), Sca-1^{neg} CD24^{high} (enriched in ER^{-} luminal epithelial cells),

and Sca-1^{pos} CD24^{high} (enriched in ER^{+} luminal epithelial cells). Analysis of MECs from glands expressing H1047R revealed a much less clear resolution into the subpopulations showing only two major populations (Figure 5A). Since the mice used for the FACS analysis were not induced with tamoxifen, only 25-35% of the epithelial cells were GFP-positive and therefore the density plot in Figure 5A represents the overlap of H1047R-expressing and –non-expressing cells. When we restricted the analysis on the H1047R cells expressing GFP, resolution into the three subpopulations was possible, however, a dramatic accumulation of Sca-1^{neg} CD24^{high} cells was manifested (Figure 5B). While in the normal gland ~30% of the epithelial cells are Sca-1^{neg} CD24^{high} this population accounts for ~85% of mutant epithelial cells (Figure 5B). These data suggest that H1047R expression results in an accumulation of the Sca-1^{neg} CD24^{high} cell population.

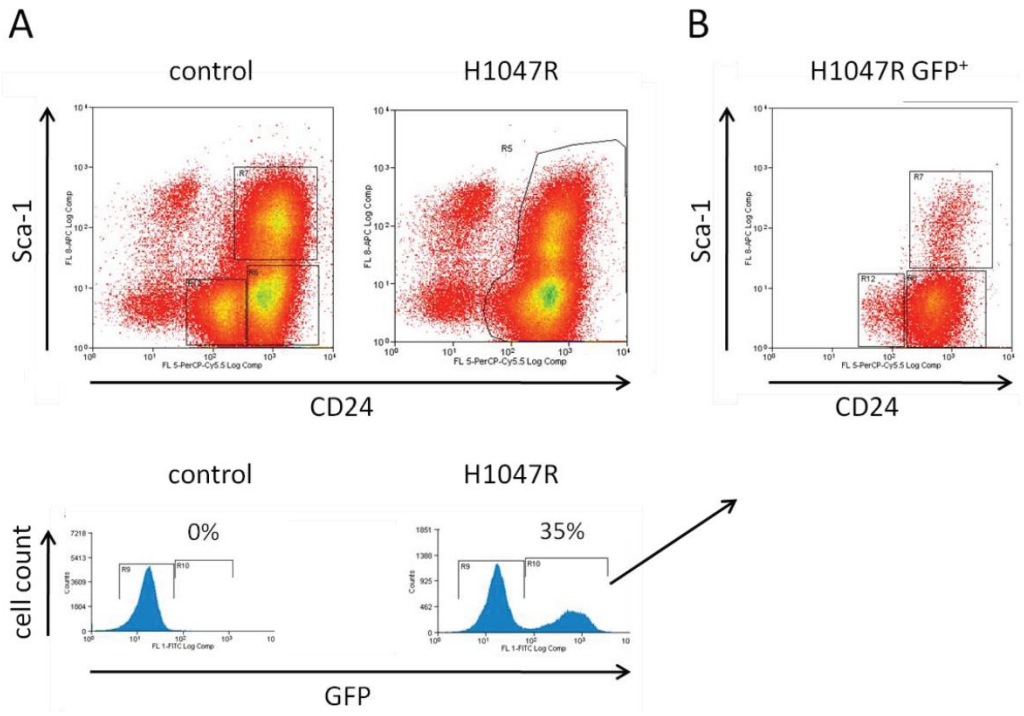

Figure 5. FACS analysis of cells from CAGS-CreERT2 H1047R mammary glands reveals a dramatic accumulation of Sca-1^{neg} CD24^{high} cells. (A, top) Mammary gland cells were isolated from at least 7 mice and digested to single cells which were stained for CD45, CD24 and Sca-1. The CD45^{-} epithelial cells from both control (left) and CAGS-CreERT2 H1047R mutant mice (right), were separated based on their expression levels of CD24 (x-axis) and Sca-1 (y-axis). (A, bottom). Histograms show expression levels of GFP (x-axis) in mammary epithelial cells from above. (B) Distribution of only GFP^{+} mammary epithelial cells from CAGS-CreERT2 H1047R mice based on their expression levels of CD24 (x-axis) and Sca-1 (y-axis).

CAGS-CreERT2 H1047R mutant MECs produce aberrant outgrowths and mammary tumors eventually

The major aim of generating mice expressing mutant *PIK3CA* H1047R in all cells (CAGS-CreERT2 H1047R) was to investigate whether such mice would develop mammary carcinomas and, if so, whether these tumors are different from tumors formed in mice specifically expressing mutant H1047R in luminal mammary epithelial cells (WAPiCre H1047R). Since CAGS-CreERT2 H1047R mice die before overt tumor onset, we transplanted the mammary epithelium of CAGS-CreERT2 H1047R and CAGS-CreERT2 control mice into wild-type Balb/c recipient mice. We isolated the mammary glands of the donor mice, chopped them into pieces, and digested them enzymatically. The resulting organoids were incubated as suspension culture over night and injected the next day into cleared fat pads of three-week old recipient mice. The outgrowth was scored six to twelve weeks after the transplantation. Whole mount preparations revealed that transplanted control epithelium repopulated the whole fat pad while H1047R mutant epithelium was hyperplastic and repopulated the fat pad only partially (Figure 6A). H&E stainings prepared from glands isolated six weeks after transplantation confirmed the hyperplastic phenotype of H1047R mutant epithelium (Figure 6B).

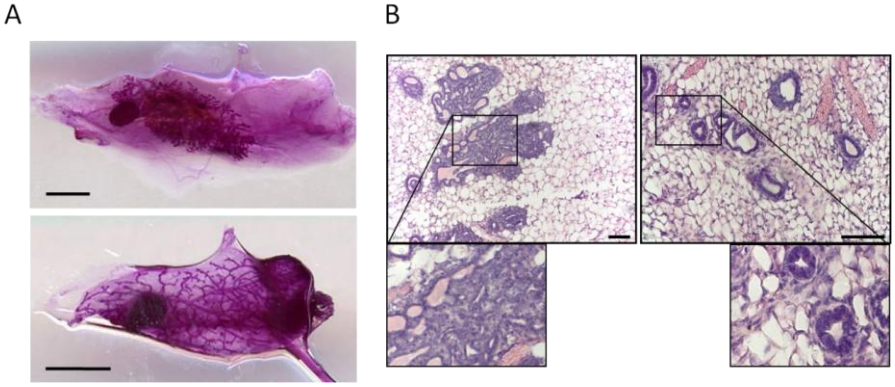

Figure 6. CAGS-CreERT2 H1047R derived mammary epithelial cells form aberrant outgrowths *in vivo*. (A) Mammary glands from donor CAGS-CreERT2 control and CAGS-CreERT2 H1047R mice were isolated and digested enzymatically. The resulting organoid suspension was injected with matrigel into cleared fat pads of three-week old Balb/c recipients. 6 weeks after transplantation the glands were harvested and prepared as whole mounts. Scale bars represent 2mm. (B) H&E sections showing outgrowth produced by CAGS-CreERT2 H1047R (left) and control epithelium (right). Scale bar represents 100 µm.

The recipient mice transplanted with control or mutant epithelium were monitored for tumor formation. As expected, mice transplanted with control tissue did not form any tumors while mice with H1047R mutant epithelium developed mammary carcinomas after 221.3 (±20.3) days. By the end of the study 16 mice that formed H1047R mutant donor epithelium outgrowths developed a mammary tumor while only 3 mice did not (Figure 7).

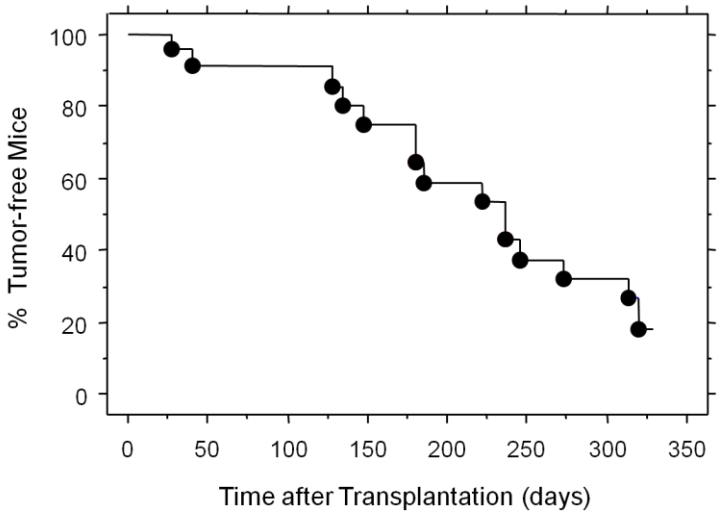

Figure 7. CAGS-CreERT2 H1047R-derived mammary epithelial cells form tumors *in vivo*. Kaplan-Meier curves showing tumor onset in Balb/c mice transplanted with CAGS-CreERT2 H1047R mutant epithelium (*n*=19). 16 mice developed palpable tumors on average 221.3 (±20.3) days after transplantation. Three mice (15.8 %) showed aberrant outgrowths but did not form a mammary tumor by the end of the study (320 days after transplantation).

Discussion and Outlook

Upon tamoxifen induction the three CAGS-CreERT2 *PIK3CA* transgenic mouse lines express either wild-type or mutant *PIK3CA* E545K or H1047R. Expression of H1047R or E545K caused premature death within one or three weeks, respectively. Since there is a certain degree of leakiness inherent to this Cre-mediated recombination system (data not shown), even CAGS-CreERT2 H1047R and E545K mice that were not induced with tamoxifen died within two or four months, respectively. We found that, starting from the age of three weeks, transgenic mice

started to develop large hematomas underneath the skin of the ears, tail, and pads (Figure 3) without the administration of tamoxifen. This suggested a coagulation problem or enhanced leakiness of blood vessels as a result of mutant p110α expression. Further analysis of the transgenic animals by Frimorfo (Marly, Switzerland), however, revealed that a platelet defect can be excluded and that bleeding time and blood coagulation are not affected in CAGS-CreERT2 H1047R mice.

Of note, CAGS-targeted expression of the transgene seems to affect various organs including liver, pancreas, and the cardiovascular system (blood vessels) as plasma levels of some liver and pancreatic enzymes and of the metabolites glucose and triglycerides are pathologic. The dramatic change in glucose and triglycerides might not be surprising given the important role of PI3K and its downstream effectors in the regulation of metabolism (Engelman, Luo et al. 2006; Manning and Cantley 2007). Recently, p110α was demonstrated to be an important mediator of insulin metabolic action in liver and glucose homeostasis and ablation of p110α in the liver caused an increase of serum glucose levels which is in line with our finding of decreased glucose levels in the *PIK3CA* H1047R mutant mice (Sopasakis, Liu et al. 2010).

In conclusion, the examination by Frimorfo shows that bleeding time and blood coagulation are not affected in CAGS-CreERT2 H1047R mice. Although *PIK3CA* H1047R expression affects plasma levels of glucose and triglycerides and causes pathological levels of some liver and pancreatic enzymes the cause for the hematomas and premature death remains unclear and merits further analysis. Of note, CAGS-CreERT2 E545K show hematomas much like CAGS-CreERT2 H1047R mice and die prematurely albeit with a longer latency. The fact that CAGS-CreERT2 E545K mice show a similar but weaker phenotype than CAGS-CreERT2 H1047R mice is interesting and is in line with the weaker potency of E545K to induce mammary carcinomas in mice as compared to H1047R mice. Once more, this raises the question about the mechanism explaining this difference in potency. The easiest explanation would be that E545K is a less potent activator of downstream signaling than H1047R. However, at least in mammary carcinomas, induced by mutant p110α, no difference in the signaling amplitude could be

detected using phosphorylation of Akt, mTOR, and S6 as read-outs. As discussed in the previous section, it might be that the two types of mutations activate a slightly different set of downstream pathways, a hypothesis that merits testing.

The observation that tamoxifen-induced CAGS-CreERT2 *PIK3CA*^{wt} mice develop mammary tumors after ~430 days is interesting for two reasons. On the one hand, this is the only obvious phenotype that we observed with any mouse model expressing wild-type *PIK3CA* (WAPiCre *PIK3CA*^{wt}, CAGS-CreERT2 *PIK3CA*^{wt}) and demonstrates that the additional copy of human *PIK3CA* on top of endogenous *PIK3CA* allows transformation and induction of mammary tumors in mice. On the other hand, we have not observed any tumors in mice expressing wild-type *PIK3CA* targeted by the WAP promoter 240 days after delivery which corresponds to ~320 days of age (see Figure 1, part II) indicating that the WAPiCre *PIK3CA*^{wt} mice might develop tumors as well as they become older. Alternatively, and more interestingly, the CAGS promoter might target *PIK3CA*^{wt} expression to a mammary epithelial subpopulation which is susceptible to *PIK3CA*^{wt}-evoked tumorigenesis but not targeted by the WAP promoter.

When cells from mammary glands of CAGS-CreERT2 *PIK3CA* mutant mice were seeded in suspension they formed more mammospheres which are generally larger than those derived from control mice. In line with the difference in tumor latency and induction of premature death, this phenotype was more pronounced in cells expressing H1047R which formed around three times more mammospheres than control cells whereas cells expressing E545K formed only twice the number of spheres than control cells. Interestingly, no difference in sphere number was observed in cells expressing wild-type *PIK3CA* as compared to control cells, suggesting that the enhanced sphere-forming capacity of cells expressing mutant *PIK3CA* is due to the oncogenic mutation rather than overexpression. The fact that after one passage the number of spheres remained the same in both control and H1047R mutant cells (Figure 4A), suggests that expression of mutant *PIK3CA* does not affect the self-renewing capacity of mutant MECs but may still affect survival of these cells. However, more and larger spheres were formed by mammary cells expressing mutant *PIK3CA* indicating that the proliferative capacity of these cells is enhanced. In concordance with our findings, Korkaya et al. found that activation of the

PI3K pathway via PTEN knockdown in human MECs increased the number and size of mammospheres in suspension (Korkaya, Paulson et al. 2009).

While control organoids reconstituted the whole fat pad, when transplanted into cleared recipient glands, CAGS-CreERT2 H1047R-derived organoids produced outgrowths that were hyperplastic and the mutant epithelium reconstituted the fat pad only partially (Figure 6A). We can only speculate why mutant mammary epithelium results in solely partial outgrowth in recipient fat pads at this stage of the study. It might be possible that expression of mutant *PIK3CA* results in a depletion of mammary stem cells (Figure 5). Alternatively, there might be a defect in cap cells which are required for the protrusion of the mammary epithelial cells through the mammary fat pad. The progression of the hyperplasias produced by H1047R mutant organoids into carcinomas is in concordance with the oncogenic potential of mutant p110α *in vivo* we and others observed (Figure 2 part I; Figure1 part II) (Adams, Xu et al. ; Bader, Kang et al. 2006; Engelman, Chen et al. 2008). It will be interesting to analyze the tumor histotypes produced by the transplanted CAGS-CreERT2 H1047R-derived organoids since the expression of *PIK3CA* H1047R is allowed in all the epithelial subpopulations. Therefore other cells (e.g. basal epithelial cells) could serve as the cell-of-origin in these glands which might result in tumor histotypes different from the ones we observed in tumors where H1047R expression was targeted to cells in which the WAP or MMTV promoter is active.

In FACS experiments, we observed a strong accumulation of cells expressing H1047R (GFP-positive cells) within the $CD24^{high}$ $Sca\text{-}1^{-}$ population. This population, at least in the normal mammary gland, is enriched in ER^{-} luminal epithelial cells and possesses limited mammary gland repopulating activity (Sleeman, Kendrick et al. 2007). In contrast, only ~15% of GFP-positive cells were found in the $CD24^{high}$ $Sca\text{-}1^{+}$ and $CD24^{med}$ $Sca\text{-}1^{-}$ population, respectively. This data indicates that in CAGS-CreERT2 H1047R transgenic mice the basal cell compartment which includes mammary stem cells and myoepithelial cells as well as the ER^{+} enriched population are depleted (Figure 5B). This finding is consistent with reports demonstrating the importance of PTEN for the maintenance of hematopoietic stem cells (HSC) as the absence of PTEN drove HSCs into cell cycle resulting in the depletion of HSCs and the initiation of leukemia

(Yilmaz, Valdez et al. 2006; Zhang, Grindley et al. 2006). In a murine model of prostate cancer, deletion of PTEN led to the expansion of a prostatic stem/progenitor cell subpopulation and tumor initiation (Wang, Garcia et al. 2006). In light of these observations, we speculate that expression of mutant H1047R results in an expansion of a mammary progenitor population that eventually gives rise to mammary carcinomas. However, this hypothesis is relying on FACS analysis based on the expression of the markers CD24 and Sca-1. Thus, we cannot exclude that mammary epithelial cells start to express different levels of CD24 and/or Sca-1 once they express H1047R, and therefore, would cause a shift in the FACS profile. Further experiments are required to confirm the depletion of basal cells and expansion of a progenitor population including transplantation assays and proper characterization and quantification of the FACS sorted populations based on the expression of differentiation markers (K14, K18, ER) and colony-forming capacity.

Summary and Outlook

We demonstrated that expression of *PIK3CA* E545K or H1047R in the mammary gland evoked heterogeneous tumors that recapitulated features of human disease and that a multipotent progenitor was likely to be the target of mutant *PIK3CA*-induced tumorigenesis. Notably, the H1047R mutant was a more potent inducer of mammary carcinomas than the E545K mutant.

We showed that whole body expression of *PIK3CA* mutants E545K or H1047R in mice resulted in premature death, however, the cause of death remains unclear. We further demonstrated that H1047R expression in all cells resulted in the formation of mammary carcinomas upon transplantation of the mutant mammary epithelium into recipient mice. Of note, expression of H1047R in all cells of the mammary gland resulted in an accumulation of a mammary epithelial cell subpopulation that is enriched in ER-negative luminal epithelial cells and we therefore speculate that cells within that mammary epithelial subpopulation are the targets of H1047R-mediated carcinogenesis.

In the future the mutant *PIK3CA* mouse models generated in the present work should be helpful for detecting collaborating pathways in mutant *PIK3CA*-induced tumorigenesis. In addition, several kinase inhibitors targeting PI3K are in clinical trials and these mouse models should help anticipate potential mechanisms of resistance and test combination therapies that may synergize with PI3K inhibition.

Material and Methods

Transgenic Mice

We constructed a vector with a transcriptional STOP sequence flanked by *loxP* sites upstream of the 5'-terminally HA-tagged human *PIK3CA* cDNA (Addgene) and an *IRES2-EGFP* reporter element (pIRES2-EGFP vector, Clontech). The resulting *loxP*-STOP-*loxP*-HA-*PIK3CA*-*IRES2-EGFP* fragment was cloned into a recombination-mediated cassette exchange (RMCE) plasmid. The vector was introduced into the modified Rosa26 locus of Balb/c mouse embryonic stem (ES) cells by RMCE and the ES cells used for blastocyst injection (Tchorz, Kinter et al. 2009). Chimeric mice were mated with Balb/c mice and transgenic mice identified by genotyping using the primers 5'-TGGCCAGTACCTCATGGATT-3' and 5'-GCAATACATCTGGGCTACTTCAT-3'. FVB/N-Tg(MMTV-Cre) and FVB/N.B6-Tg(WAPiCre) mice were described previously (Wintermantel, Mayer et al. 2002; Andrechek, White et al. 2005). Tg(MMTV-Cre) mice are in the FVB/N background and B6-Tg(WAPiCre) mice were backcrossed for five generations to an FVB/N background. MMTV-*NeuNT* (strain TG.NK) mice were purchased from Charles River (Wilmington, MA).

Immunohistochemistry

The following antibodies were used: K14 (Thermo Scientific, RB-9020, 1:1000), K18 (Fitzgerald, #GP11, 1:500), GFP (Invitrogen, A11122, 1:500), ER (Santa Cruz, SC-542, 1:1000), PR (Thermo Scientific, RM-9102, 1:200), α-SMA (Thermo Scientific, RB-9010, 1:500), cleaved caspase-3 (Cell Signaling, #9661, 1:100), and Ki-67 (Thermo Scientific, RM-9106, 1:1000).

Protein Analysis

Mouse tumors were lysed in a modified RIPA buffer [50mmol/L Tris-HCl (pH 7.5); 1% NP40; 150 mmol/L NaCl; 0.5% sodium deoxycholate; 0.1% SDS; 5 mmol/L EGTA; 2 mmol/L phenylmethylsulfonyl fluoride; 2 μg/mL each of aprotinin, leupeptin, and pepstatin; 2 mmol/L Na_3VO_4; 10mmol/L NaF; 10mmol/L β-glycerophosphate; 10mmol/L sodium pyrophosphate]. For immunoprecipitation, samples were lysed in Co-IP buffer [25mM Tris-HCl (pH 7.5); 2.5mM EGTA; 75mM NaCl; 0.75mM $MgCl_2$; 12.5mM β-glycerophosphate; 12.5mM NaF]. Antibodies were purchased from Cell Signaling except for α-GFP (MBL), α-K14 (Thermo Scientific), and α-HA (Covance).

Statistical analysis

Survival curves were generated using the Kaplan-Meier method with the software StatView.

Southern Blot

12 μg of genomic DNA isolated from mouse tails were digested with a total of 8 U of AvrII enzyme (New England Biolabs) and separated on a 1% Agarose gel. A DIG-labeled DNA probe targeting the neomycin resistance cassette was amplified using the PCR DIG Probe Synthesis Kit (Roche) and the primers ATGGGATCGGCCATTGAACAAGAT and CGGCCATTTTCCACCATGATAT.

RT-PCR

RNA was isolated from 100-200 mg of mouse tissue using Trizol (Invitrogen) according to the manufacturer's protocol. Traces of contaminating DNA were removed by a 30 minutes incubation of 5μg of RNA with TURBO DNase (Ambion) at 37°C and RT-PCR performed using the ThermoScript RT-PCR System (Invitrogen). *Taq Man* polymerase and appropriate buffers were

purchased from New England Biolabs. Human *PIK3CA* was detected using the primers CAGATCCCAGTGTGGTGGTACG and CCTCACGGAGGCATTCTAAAGT and endogenous *gapdh* was detected using the primers CATCAAGAAGGTGGTGAAGC and GGGAGTTGCTGTTGAAGTCG.

MEC isolation and mammosphere assay

Mammary glands were isolated from mice and chopped into fine pieces using a razor blade. The pieces were digested on a rotor shaker at 37 degrees in a solution containing DMEM-F12 medium (Gibco), collagenase [300 U/ml], hyualuronidase [100 U/ml], insulin [10µg/ml], hydrocortisone [0.5µg/ml], β-mercaptoethanol (1:250'000), and antibiotics (penicillin and streptomycin) for 2-3 hours. The resulting organoid suspension was incubated with red blood cell lysis buffer to remove erythrocytes. After washing with PBS, organoids were incubated for 5-10 minutes with HiQtase at 37 degrees and pipetted up and down extensively to produce single cells. After washing with 2% fetal calf serum FBS the cells were resuspended in suspension medium consisting of DMEM-F12 medium, 1X B27 supplement (Invitrogen), recombinant FGF [20ng/ml], mouse EGF [20ng/ml], and gentamycin [100 µg/ml] and filtered through a 40 µm cell strainer. 5'000 cells were seeded in 0.5 ml of suspension medium into wells of a 24-well dish. For passaging spheres were collected and digested in 0.05% Trypsin solution at 37 degrees for 5 minutes. Cells were resuspended in suspension medium, filtered through a 40 µm cell strainer, and were counted before seeding as single cells analogue to first passage.

FACS analysis

Isolation of MECs was performed according to the protocol of Sleeman and co-workers (Sleeman, Kendrick et al. 2006) with the exception of the antibody that was used to stain CD24. We used a PerCP/Cy5.5-labeled anti-mouse CD24 antibody (Biolegend, #101823, 1:33).

Acknoledgements

I would like to thank Momo for giving me the opportunity to work in his lab as one of the first PhD students. It has not always been easy to work in a new lab that was not fully running yet but it was definitely a great experience to be part of a small group that contributed to what this lab is today. I am also glad that he let me work on this exciting project generating a new mouse model and at the same time "setting up" a new research area within the lab which was challenging but also very interesting.

I want to particularly thank our technicians Heike, Urs, and Ina for their contribution to this work which would not be here in its present form without them. Thanks to the excellent lab organization of Heike the daily bench work in the Bentires lab could always be carried out smoothly and efficiently.

A big "thank you" goes to Nico and Ema who started along with me in this lab. Together we shared the experience to work in a new lab and together we went through all the ups and downs that are connected to that experience. They both were extremely helpful throughout the years in this lab which was particularly important for me at the beginning of my studies where – as a former bacteriologist - I had no clue how to do proper tissue culture. I also wanna thank Stephan for sharing his tremendous knowledge and endless list of lab protocols with me and always appreciated his advice as well as his friendly nature. Thank you also Abdullah, Nina, Adrian, Janice, and Fabienne for being my colleagues, for fruitful scientific discussion, but also for providing a friendly and relaxed atmosphere in the lab in which everyday's work was mostly a pleasure..

Among the former lab members I thank Simon and Kamal, two post-docs who always were willing to share their experience with me and with their happy personalities contributed a lot to the excellent lab atmosphere and kit we had at the very beginning.

Last but not least I wanna thank Laurent and Steven at the microscopy facility, Patrick from the imaging facility, and Sandrine & Augustyn from the histology lab for their assistance and guidance. I also would like to thank the members of my thesis committee, Nancy Hynes, Christoph Rochlitz, Michel Maira and Matthias Wymann, for their contributions and suggestions to the present work and for their guidance throughout the years. Thanks to Hubertus for his help, patience, and black tea that was needed to spend hours and days in front of the FACS sorting machine to go through the endless sortings even if sometimes the whole effort was “just” to sort a handful of cells…

References

Ackler, S., S. Ahmad, et al. (2002). "Delayed mammary gland involution in MMTV-AKT1 transgenic mice." Oncogene **21**(2): 198-206.

Adams, J. R., K. Xu, et al. "Cooperation between Pik3ca and p53 Mutations in Mouse Mammary Tumor Formation." Cancer Res **71**(7): 2706-2717.

Alessi, D. R., S. R. James, et al. (1997). "Characterization of a 3-phosphoinositide-dependent protein kinase which phosphorylates and activates protein kinase Balpha." Curr Biol **7**(4): 261-269.

Alimonti, A., A. Carracedo, et al. (2010). "Subtle variations in Pten dose determine cancer susceptibility." Nature genetics **42**(5): 454-458.

Andrechek, E. R., D. White, et al. (2005). "Targeted disruption of ErbB2/Neu in the mammary epithelium results in impaired ductal outgrowth." Oncogene **24**(5): 932-937.

Bachman, K. E., P. Argani, et al. (2004). "The PIK3CA gene is mutated with high frequency in human breast cancers." Cancer Biol Ther **3**(8): 772-775.

Bader, A. G., S. Kang, et al. (2006). "Cancer-specific mutations in PIK3CA are oncogenic in vivo." Proc Natl Acad Sci U S A **103**(5): 1475-1479.

Bader, A. G., S. Kang, et al. (2005). "Oncogenic PI3K deregulates transcription and translation." Nat Rev Cancer **5**(12): 921-929.

Barbareschi, M., F. Buttitta, et al. (2007). "Different prognostic roles of mutations in the helical and kinase domains of the PIK3CA gene in breast carcinomas." Clin Cancer Res **13**(20): 6064-6069.

Biggs, W. H., 3rd, J. Meisenhelder, et al. (1999). "Protein kinase B/Akt-mediated phosphorylation promotes nuclear exclusion of the winged helix transcription factor FKHR1." Proc Natl Acad Sci U S A **96**(13): 7421-7426.

Bondeva, T., L. Pirola, et al. (1998). "Bifurcation of lipid and protein kinase signals of PI3Kgamma to the protein kinases PKB and MAPK." Science **282**(5387): 293-296.

Booth, B. W., C. A. Boulanger, et al. (2007). "Alveolar progenitor cells develop in mouse mammary glands independent of pregnancy and lactation." J Cell Physiol **212**(3): 729-736.

Boulanger, C. A., K. U. Wagner, et al. (2005). "Parity-induced mouse mammary epithelial cells are pluripotent, self-renewing and sensitive to TGF-beta1 expression." Oncogene **24**(4): 552-560.

Boxer, R. B., D. B. Stairs, et al. (2006). "Isoform-specific requirement for Akt1 in the developmental regulation of cellular metabolism during lactation." Cell Metab **4**(6): 475-490.

Bozulic, L., B. Surucu, et al. (2008). "PKBalpha/Akt1 acts downstream of DNA-PK in the DNA double-strand break response and promotes survival." Molecular cell **30**(2): 203-213.

Broderick, D. K., C. Di, et al. (2004). "Mutations of PIK3CA in anaplastic oligodendrogliomas, high-grade astrocytomas, and medulloblastomas." Cancer Res **64**(15): 5048-5050.

Brunet, A., A. Bonni, et al. (1999). "Akt promotes cell survival by phosphorylating and inhibiting a Forkhead transcription factor." Cell **96**(6): 857-868.

Bruno, R. D. and G. H. Smith (2010). "Functional Characterization of Stem Cell Activity in the Mouse Mammary Gland." Stem Cell Rev.

Buttitta, F., L. Felicioni, et al. (2006). "PIK3CA mutation and histological type in breast carcinoma: high frequency of mutations in lobular carcinoma." J Pathol **208**(3): 350-355.

Campbell, I. G., S. E. Russell, et al. (2004). "Mutation of the PIK3CA gene in ovarian and breast cancer." Cancer Res **64**(21): 7678-7681.

Cardiff, R. D. and S. R. Wellings (1999). "The comparative pathology of human and mouse mammary glands." J Mammary Gland Biol Neoplasia **4**(1): 105-122.

Carson, J. D., G. Van Aller, et al. (2008). "Effects of oncogenic p110alpha subunit mutations on the lipid kinase activity of phosphoinositide 3-kinase." Biochem J **409**(2): 519-524.

Corvera, S. and M. P. Czech (1998). "Direct targets of phosphoinositide 3-kinase products in membrane traffic and signal transduction." Trends Cell Biol **8**(11): 442-446.

Datta, S. R., H. Dudek, et al. (1997). "Akt phosphorylation of BAD couples survival signals to the cell-intrinsic death machinery." Cell **91**(2): 231-241.

del Peso, L., M. Gonzalez-Garcia, et al. (1997). "Interleukin-3-induced phosphorylation of BAD through the protein kinase Akt." Science **278**(5338): 687-689.

Denley, A., M. Gymnopoulos, et al. (2009). "Requirement of phosphatidylinositol(3,4,5)trisphosphate in phosphatidylinositol 3-kinase-induced oncogenic transformation." Mol Cancer Res **7**(7): 1132-1138.

Deome, K. B., L. J. Faulkin, Jr., et al. (1959). "Development of mammary tumors from hyperplastic alveolar nodules transplanted into gland-free mammary fat pads of female C3H mice." Cancer Res **19**(5): 515-520.

Depowski, P. L., S. I. Rosenthal, et al. (2001). "Loss of expression of the PTEN gene protein product is associated with poor outcome in breast cancer." Mod Pathol **14**(7): 672-676.

Dhand, R., I. Hiles, et al. (1994). "PI 3-kinase is a dual specificity enzyme: autoregulation by an intrinsic protein-serine kinase activity." The EMBO journal **13**(3): 522-533.

Dijkers, P. F., K. U. Birkenkamp, et al. (2002). "FKHR-L1 can act as a critical effector of cell death induced by cytokine withdrawal: protein kinase B-enhanced cell survival through maintenance of mitochondrial integrity." J Cell Biol **156**(3): 531-542.

Dillon, R. L., R. Marcotte, et al. (2009). "Akt1 and akt2 play distinct roles in the initiation and metastatic phases of mammary tumor progression." Cancer Res **69**(12): 5057-5064.

Dontu, G., W. M. Abdallah, et al. (2003). "In vitro propagation and transcriptional profiling of human mammary stem/progenitor cells." Genes & development **17**(10): 1253-1270.

Dunlap, J., C. Le, et al. (2010). "Phosphatidylinositol-3-kinase and AKT1 mutations occur early in breast carcinoma." Breast cancer research and treatment **120**(2): 409-418.

Dupont, J., J. P. Renou, et al. (2002). "PTEN overexpression suppresses proliferation and differentiation and enhances apoptosis of the mouse mammary epithelium." J Clin Invest **110**(6): 815-825.

Easton, D., D. Ford, et al. (1993). "Inherited susceptibility to breast cancer." Cancer Surv **18**: 95-113.

Engelman, J. A., L. Chen, et al. (2008). "Effective use of PI3K and MEK inhibitors to treat mutant Kras G12D and PIK3CA H1047R murine lung cancers." Nat Med **14**(12): 1351-1356.

Engelman, J. A., J. Luo, et al. (2006). "The evolution of phosphatidylinositol 3-kinases as regulators of growth and metabolism." Nat Rev Genet **7**(8): 606-619.

Foulkes, W. D., I. M. Stefansson, et al. (2003). "Germline BRCA1 mutations and a basal epithelial phenotype in breast cancer." J Natl Cancer Inst **95**(19): 1482-1485.

Fruman, D. A., R. E. Meyers, et al. (1998). "Phosphoinositide kinases." Annual review of biochemistry **67**: 481-507.

Gaidarov, I., M. E. Smith, et al. (2001). "The class II phosphoinositide 3-kinase C2alpha is activated by clathrin and regulates clathrin-mediated membrane trafficking." Mol Cell **7**(2): 443-449.

Garami, A., F. J. Zwartkruis, et al. (2003). "Insulin activation of Rheb, a mediator of mTOR/S6K/4E-BP signaling, is inhibited by TSC1 and 2." Mol Cell **11**(6): 1457-1466.

Gonzalez-Angulo, A. M., K. Stemke-Hale, et al. (2009). "Androgen receptor levels and association with PIK3CA mutations and prognosis in breast cancer." Clin Cancer Res **15**(7): 2472-2478.

Graus-Porta, D., R. R. Beerli, et al. (1997). "ErbB-2, the preferred heterodimerization partner of all ErbB receptors, is a mediator of lateral signaling." EMBO J **16**(7): 1647-1655.

Gymnopoulos, M., M. A. Elsliger, et al. (2007). "Rare cancer-specific mutations in PIK3CA show gain of function." Proc Natl Acad Sci U S A **104**(13): 5569-5574.

Hay, N. and N. Sonenberg (2004). "Upstream and downstream of mTOR." Genes Dev **18**(16): 1926-1945.

Hennessy, B. T., A. M. Gonzalez-Angulo, et al. (2009). "Characterization of a naturally occurring breast cancer subset enriched in epithelial-to-mesenchymal transition and stem cell characteristics." Cancer Res **69**(10): 4116-4124.

Hennessy, B. T., D. L. Smith, et al. (2005). "Exploiting the PI3K/AKT pathway for cancer drug discovery." Nat Rev Drug Discov **4**(12): 988-1004.

Herschkowitz, J. I., K. Simin, et al. (2007). "Identification of conserved gene expression features between murine mammary carcinoma models and human breast tumors." Genome biology **8**(5): R76.

Holbro, T., R. R. Beerli, et al. (2003). "The ErbB2/ErbB3 heterodimer functions as an oncogenic unit: ErbB2 requires ErbB3 to drive breast tumor cell proliferation." Proc Natl Acad Sci U S A **100**(15): 8933-8938.

Howard, B. A. and B. A. Gusterson (2000). "Human breast development." J Mammary Gland Biol Neoplasia **5**(2): 119-137.

Hu, Z., C. Fan, et al. (2006). "The molecular portraits of breast tumors are conserved across microarray platforms." BMC Genomics **7**: 96.

Hutchinson, J., J. Jin, et al. (2001). "Activation of Akt (protein kinase B) in mammary epithelium provides a critical cell survival signal required for tumor progression." Mol Cell Biol **21**(6): 2203-2212.

Hutchinson, J. N., J. Jin, et al. (2004). "Activation of Akt-1 (PKB-alpha) can accelerate ErbB-2-mediated mammary tumorigenesis but suppresses tumor invasion." Cancer Res **64**(9): 3171-3178.

Hynes, N. E. and H. A. Lane (2005). "ERBB receptors and cancer: the complexity of targeted inhibitors." Nat Rev Cancer **5**(5): 341-354.

Inoki, K., Y. Li, et al. (2003). "Rheb GTPase is a direct target of TSC2 GAP activity and regulates mTOR signaling." Genes Dev **17**(15): 1829-1834.

Inoki, K., Y. Li, et al. (2002). "TSC2 is phosphorylated and inhibited by Akt and suppresses mTOR signalling." Nat Cell Biol **4**(9): 648-657.

Isakoff, S. J., J. A. Engelman, et al. (2005). "Breast cancer-associated PIK3CA mutations are oncogenic in mammary epithelial cells." Cancer Res **65**(23): 10992-11000.

Jeselsohn, R., N. E. Brown, et al. (2010). "Cyclin D1 kinase activity is required for the self-renewal of mammary stem and progenitor cells that are targets of MMTV-ErbB2 tumorigenesis." Cancer Cell **17**(1): 65-76.

Kalinsky, K., L. M. Jacks, et al. (2009). "PIK3CA mutation associates with improved outcome in breast cancer." Clin Cancer Res **15**(16): 5049-5059.

Kang, S., A. G. Bader, et al. (2005). "Phosphatidylinositol 3-kinase mutations identified in human cancer are oncogenic." Proc Natl Acad Sci U S A **102**(3): 802-807.

Kang, S., A. Denley, et al. (2006). "Oncogenic transformation induced by the p110beta, -gamma, and -delta isoforms of class I phosphoinositide 3-kinase." Proc Natl Acad Sci U S A **103**(5): 1289-1294.

Katso, R., K. Okkenhaug, et al. (2001). "Cellular function of phosphoinositide 3-kinases: implications for development, homeostasis, and cancer." Annual review of cell and developmental biology **17**: 615-675.

Kops, G. J., N. D. de Ruiter, et al. (1999). "Direct control of the Forkhead transcription factor AFX by protein kinase B." Nature **398**(6728): 630-634.

Kordon, E. C. and G. H. Smith (1998). "An entire functional mammary gland may comprise the progeny from a single cell." Development **125**(10): 1921-1930.

Korkaya, H., A. Paulson, et al. (2009). "Regulation of mammary stem/progenitor cells by PTEN/Akt/beta-catenin signaling." PLoS biology **7**(6): e1000121.

Lai, Y. L., B. L. Mau, et al. (2008). "PIK3CA exon 20 mutation is independently associated with a poor prognosis in breast cancer patients." Ann Surg Oncol **15**(4): 1064-1069.

Lam, K., C. L. Carpenter, et al. (1994). "The phosphatidylinositol 3-kinase serine kinase phosphorylates IRS-1. Stimulation by insulin and inhibition by Wortmannin." The Journal of biological chemistry **269**(32): 20648-20652.

Lee, J. W., Y. H. Soung, et al. (2005). "PIK3CA gene is frequently mutated in breast carcinomas and hepatocellular carcinomas." Oncogene **24**(8): 1477-1480.

Lee, J. Y., J. A. Engelman, et al. (2007). "Biochemistry. PI3K charges ahead." Science **317**(5835): 206-207.

Lerma, E., L. Catasus, et al. (2008). "Exon 20 PIK3CA mutations decreases survival in aggressive (HER-2 positive) breast carcinomas." Virchows Arch **453**(2): 133-139.

Levine, D. A., F. Bogomolniy, et al. (2005). "Frequent mutation of the PIK3CA gene in ovarian and breast cancers." Clin Cancer Res **11**(8): 2875-2878.

Li, G., G. W. Robinson, et al. (2002). "Conditional loss of PTEN leads to precocious development and neoplasia in the mammary gland." Development **129**(17): 4159-4170.

Li, H., R. Zhu, et al. (2010). "PIK3CA mutations mostly begin to develop in ductal carcinoma of the breast." Experimental and molecular pathology **88**(1): 150-155.

Li, J., K. DeFea, et al. (1999). "Modulation of insulin receptor substrate-1 tyrosine phosphorylation by an Akt/phosphatidylinositol 3-kinase pathway." J Biol Chem **274**(14): 9351-9356.

Li, S. Y., M. Rong, et al. (2006). "PIK3CA mutations in breast cancer are associated with poor outcome." Breast Cancer Res Treat **96**(1): 91-95.

Li, X., B. Monks, et al. (2007). "Akt/PKB regulates hepatic metabolism by directly inhibiting PGC-1alpha transcription coactivator." Nature **447**(7147): 1012-1016.

Li, Y., K. Podsypanina, et al. (2001). "Deficiency of Pten accelerates mammary oncogenesis in MMTV-Wnt-1 transgenic mice." BMC Mol Biol **2**: 2.

Liang, J., J. Zubovitz, et al. (2002). "PKB/Akt phosphorylates p27, impairs nuclear import of p27 and opposes p27-mediated G1 arrest." Nat Med **8**(10): 1153-1160.

Lim, E., F. Vaillant, et al. (2009). "Aberrant luminal progenitors as the candidate target population for basal tumor development in BRCA1 mutation carriers." Nat Med **15**(8): 907-913.

Loi, S., B. Haibe-Kains, et al. (2007). "Definition of clinically distinct molecular subtypes in estrogen receptor-positive breast carcinomas through genomic grade." J Clin Oncol **25**(10): 1239-1246.

Maehama, T., G. S. Taylor, et al. (2001). "PTEN and myotubularin: novel phosphoinositide phosphatases." Annu Rev Biochem **70**: 247-279.

Mankoo, P. K., S. Sukumar, et al. (2009). "PIK3CA somatic mutations in breast cancer: Mechanistic insights from Langevin dynamics simulations." Proteins **75**(2): 499-508.

Manning, B. D. and L. C. Cantley (2007). "AKT/PKB signaling: navigating downstream." Cell **129**(7): 1261-1274.

Maroulakou, I. G., W. Oemler, et al. (2008). "Distinct roles of the three Akt isoforms in lactogenic differentiation and involution." J Cell Physiol **217**(2): 468-477.

Maroulakou, I. G., W. Oemler, et al. (2007). "Akt1 ablation inhibits, whereas Akt2 ablation accelerates, the development of mammary adenocarcinomas in mouse mammary tumor virus (MMTV)-ErbB2/neu and MMTV-polyoma middle T transgenic mice." Cancer Res **67**(1): 167-177.

Maruyama, N., Y. Miyoshi, et al. (2007). "Clinicopathologic analysis of breast cancers with PIK3CA mutations in Japanese women." Clin Cancer Res **13**(2 Pt 1): 408-414.

Matsuzaki, H., H. Daitoku, et al. (2003). "Insulin-induced phosphorylation of FKHR (Foxo1) targets to proteasomal degradation." Proc Natl Acad Sci U S A **100**(20): 11285-11290.

Medema, R. H., G. J. Kops, et al. (2000). "AFX-like Forkhead transcription factors mediate cell-cycle regulation by Ras and PKB through p27kip1." Nature **404**(6779): 782-787.

Meyer, D. S. and M. Bentires-Alj (2010). "Can PI3K/mTOR inhibition ERase them all?" Breast Cancer Res **12:315**.

Michelucci, A., C. Di Cristofano, et al. (2009). "PIK3CA in breast carcinoma: a mutational analysis of sporadic and hereditary cases." Diagn Mol Pathol **18**(4): 200-205.

Miled, N., Y. Yan, et al. (2007). "Mechanism of two classes of cancer mutations in the phosphoinositide 3-kinase catalytic subunit." Science **317**(5835): 239-242.

Miron, A., M. Varadi, et al. (2010). "PIK3CA mutations in in situ and invasive breast carcinomas." Cancer Res **70**(14): 5674-5678.

Molyneux, G., F. C. Geyer, et al. (2010). "BRCA1 basal-like breast cancers originate from luminal epithelial progenitors and not from basal stem cells." Cell Stem Cell **7**(3): 403-417.

Nahta, R. and F. J. Esteva (2006). "HER2 therapy: molecular mechanisms of trastuzumab resistance." Breast Cancer Res **8**(6): 215.

Oakes, S. R., H. N. Hilton, et al. (2006). "The alveolar switch: coordinating the proliferative cues and cell fate decisions that drive the formation of lobuloalveoli from ductal epithelium." Breast Cancer Res **8**(2): 207.

Odorizzi, G., M. Babst, et al. (2000). "Phosphoinositide signaling and the regulation of membrane trafficking in yeast." Trends Biochem Sci **25**(5): 229-235.

Okkenhaug, K. and B. Vanhaesebroeck (2001). "New responsibilities for the PI3K regulatory subunit p85 alpha." Sci STKE **2001**(65): pe1.

Pacold, M. E., S. Suire, et al. (2000). "Crystal structure and functional analysis of Ras binding to its effector phosphoinositide 3-kinase gamma." Cell **103**(6): 931-943.

Perez-Tenorio, G., L. Alkhori, et al. (2007). "PIK3CA mutations and PTEN loss correlate with similar prognostic factors and are not mutually exclusive in breast cancer." Clin Cancer Res **13**(12): 3577-3584.

Perou, C. M. and A. L. Borresen-Dale (2011). "Systems biology and genomics of breast cancer." Cold Spring Harbor perspectives in biology **3**(2).

Perou, C. M., T. Sorlie, et al. (2000). "Molecular portraits of human breast tumours." Nature **406**(6797): 747-752.

Perren, A., L. P. Weng, et al. (1999). "Immunohistochemical evidence of loss of PTEN expression in primary ductal adenocarcinomas of the breast." Am J Pathol **155**(4): 1253-1260.

Plas, D. R. and C. B. Thompson (2003). "Akt activation promotes degradation of tuberin and FOXO3a via the proteasome." J Biol Chem **278**(14): 12361-12366.

Potter, C. J., L. G. Pedraza, et al. (2002). "Akt regulates growth by directly phosphorylating Tsc2." Nat Cell Biol **4**(9): 658-665.

Rakha, E. A., M. E. El-Sayed, et al. (2007). "Biologic and clinical characteristics of breast cancer with single hormone receptor positive phenotype." J Clin Oncol **25**(30): 4772-4778.

Ramaswamy, S., N. Nakamura, et al. (2002). "A novel mechanism of gene regulation and tumor suppression by the transcription factor FKHR." Cancer Cell **2**(1): 81-91.

Renner, O., C. Blanco-Aparicio, et al. (2008). "Activation of phosphatidylinositol 3-kinase by membrane localization of p110alpha predisposes mammary glands to neoplastic transformation." Cancer Res **68**(23): 9643-9653.

Rhei, E., L. Kang, et al. (1997). "Mutation analysis of the putative tumor suppressor gene PTEN/MMAC1 in primary breast carcinomas." Cancer Res **57**(17): 3657-3659.

Rodriguez-Viciana, P., P. H. Warne, et al. (1994). "Phosphatidylinositol-3-OH kinase as a direct target of Ras." Nature **370**(6490): 527-532.

Rodriguez-Viciana, P., P. H. Warne, et al. (1996). "Activation of phosphoinositide 3-kinase by interaction with Ras and by point mutation." EMBO J **15**(10): 2442-2451.

Rouzier, R., C. M. Perou, et al. (2005). "Breast cancer molecular subtypes respond differently to preoperative chemotherapy." Clin Cancer Res **11**(16): 5678-5685.

Ruggero, D. and N. Sonenberg (2005). "The Akt of translational control." Oncogene **24**(50): 7426-7434.

Saal, L. H., K. Holm, et al. (2005). "PIK3CA mutations correlate with hormone receptors, node metastasis, and ERBB2, and are mutually exclusive with PTEN loss in human breast carcinoma." Cancer Res **65**(7): 2554-2559.

Samuels, Y., Z. Wang, et al. (2004). "High frequency of mutations of the PIK3CA gene in human cancers." Science **304**(5670): 554.

Sarbassov, D. D., D. A. Guertin, et al. (2005). "Phosphorylation and regulation of Akt/PKB by the rictor-mTOR complex." Science **307**(5712): 1098-1101.

Schade, B., T. Rao, et al. (2009). "PTEN deficiency in a luminal ErbB-2 mouse model results in dramatic acceleration of mammary tumorigenesis and metastasis." J Biol Chem **284**(28): 19018-19026.

Schmidt, M., S. Fernandez de Mattos, et al. (2002). "Cell cycle inhibition by FoxO forkhead transcription factors involves downregulation of cyclin D." Mol Cell Biol **22**(22): 7842-7852.

Schwertfeger, K. L., J. L. McManaman, et al. (2003). "Expression of constitutively activated Akt in the mammary gland leads to excess lipid synthesis during pregnancy and lactation." J Lipid Res **44**(6): 1100-1112.

Schwertfeger, K. L., M. M. Richert, et al. (2001). "Mammary gland involution is delayed by activated Akt in transgenic mice." Mol Endocrinol **15**(6): 867-881.

Seoane, J., H. V. Le, et al. (2004). "Integration of Smad and forkhead pathways in the control of neuroepithelial and glioblastoma cell proliferation." Cell **117**(2): 211-223.

Shackleton, M., F. Vaillant, et al. (2006). "Generation of a functional mammary gland from a single stem cell." Nature **439**(7072): 84-88.

Shin, I., F. M. Yakes, et al. (2002). "PKB/Akt mediates cell-cycle progression by phosphorylation of p27(Kip1) at threonine 157 and modulation of its cellular localization." Nat Med **8**(10): 1145-1152.

Silberstein, G. B. (2001). "Postnatal mammary gland morphogenesis." Microsc Res Tech **52**(2): 155-162.

Sims, A. H., A. Howell, et al. (2007). "Origins of breast cancer subtypes and therapeutic implications." Nat Clin Pract Oncol **4**(9): 516-525.

Sleeman, K. E., H. Kendrick, et al. (2006). "CD24 staining of mouse mammary gland cells defines luminal epithelial, myoepithelial/basal and non-epithelial cells." Breast Cancer Res **8**(1): R7.

Sleeman, K. E., H. Kendrick, et al. (2007). "Dissociation of estrogen receptor expression and in vivo stem cell activity in the mammary gland." J Cell Biol **176**(1): 19-26.

Sopasakis, V. R., P. Liu, et al. (2010). "Specific roles of the p110alpha isoform of phosphatidylinsositol 3-kinase in hepatic insulin signaling and metabolic regulation." Cell metabolism **11**(3): 220-230.

Sorlie, T., C. M. Perou, et al. (2001). "Gene expression patterns of breast carcinomas distinguish tumor subclasses with clinical implications." Proc Natl Acad Sci U S A **98**(19): 10869-10874.

Sorlie, T., R. Tibshirani, et al. (2003). "Repeated observation of breast tumor subtypes in independent gene expression data sets." Proc Natl Acad Sci U S A **100**(14): 8418-8423.

Sotiriou, C., S. Y. Neo, et al. (2003). "Breast cancer classification and prognosis based on gene expression profiles from a population-based study." Proc Natl Acad Sci U S A **100**(18): 10393-10398.

Sotiriou, C. and L. Pusztai (2009). "Gene-expression signatures in breast cancer." N Engl J Med **360**(8): 790-800.

Stemke-Hale, K., A. M. Gonzalez-Angulo, et al. (2008). "An integrative genomic and proteomic analysis of PIK3CA, PTEN, and AKT mutations in breast cancer." Cancer Res **68**(15): 6084-6091.

Stingl, J. and C. Caldas (2007). "Molecular heterogeneity of breast carcinomas and the cancer stem cell hypothesis." Nat Rev Cancer **7**(10): 791-799.

Stingl, J., P. Eirew, et al. (2006). "Purification and unique properties of mammary epithelial stem cells." Nature **439**(7079): 993-997.

Takaishi, H., H. Konishi, et al. (1999). "Regulation of nuclear translocation of forkhead transcription factor AFX by protein kinase B." Proc Natl Acad Sci U S A **96**(21): 11836-11841.

Tang, E. D., G. Nunez, et al. (1999). "Negative regulation of the forkhead transcription factor FKHR by Akt." J Biol Chem **274**(24): 16741-16746.

Tchorz, J. S., J. Kinter, et al. (2009). "Notch2 signaling promotes biliary epithelial cell fate specification and tubulogenesis during bile duct development in mice." Hepatology **50**(3): 871-879.

Trimboli, A. J., C. Z. Cantemir-Stone, et al. (2009). "Pten in stromal fibroblasts suppresses mammary epithelial tumours." Nature **461**(7267): 1084-1091.

Turner, N., A. Tutt, et al. (2004). "Hallmarks of 'BRCAness' in sporadic cancers." Nat Rev Cancer **4**(10): 814-819.

Turner, N. C., J. S. Reis-Filho, et al. (2007). "BRCA1 dysfunction in sporadic basal-like breast cancer." Oncogene **26**(14): 2126-2132.

Ueda, K., M. Nishijima, et al. (1998). "Infrequent mutations in the PTEN/MMAC1 gene among primary breast cancers." Jpn J Cancer Res **89**(1): 17-21.

Viglietto, G., M. L. Motti, et al. (2002). "Cytoplasmic relocalization and inhibition of the cyclin-dependent kinase inhibitor p27(Kip1) by PKB/Akt-mediated phosphorylation in breast cancer." Nat Med **8**(10): 1136-1144.

Wang, S., A. J. Garcia, et al. (2006). "Pten deletion leads to the expansion of a prostatic stem/progenitor cell subpopulation and tumor initiation." Proceedings of the National Academy of Sciences of the United States of America **103**(5): 1480-1485.

Watson, C. J. (2006). "Involution: apoptosis and tissue remodelling that convert the mammary gland from milk factory to a quiescent organ." Breast Cancer Res **8**(2): 203.

Wintermantel, T. M., A. K. Mayer, et al. (2002). "Targeting mammary epithelial cells using a bacterial artificial chromosome." Genesis **33**(3): 125-130.

Wishart, M. J. and J. E. Dixon (2002). "PTEN and myotubularin phosphatases: from 3-phosphoinositide dephosphorylation to disease." Trends Cell Biol **12**(12): 579-585.

Yilmaz, O. H., R. Valdez, et al. (2006). "Pten dependence distinguishes haematopoietic stem cells from leukaemia-initiating cells." Nature **441**(7092): 475-482.

Yu, J., Y. Zhang, et al. (1998). "Regulation of the p85/p110 phosphatidylinositol 3'-kinase: stabilization and inhibition of the p110alpha catalytic subunit by the p85 regulatory subunit." Mol Cell Biol **18**(3): 1379-1387.

Zhang, J., J. C. Grindley, et al. (2006). "PTEN maintains haematopoietic stem cells and acts in lineage choice and leukaemia prevention." Nature **441**(7092): 518-522.

Zhang, Y., X. Gao, et al. (2003). "Rheb is a direct target of the tuberous sclerosis tumour suppressor proteins." Nat Cell Biol **5**(6): 578-581.

Zhao, H., Y. Cui, et al. (2005). "Overexpression of the tumor suppressor gene phosphatase and tensin homologue partially inhibits wnt-1-induced mammary tumorigenesis." Cancer Res **65**(15): 6864-6873.

Zhao, J. J., Z. Liu, et al. (2005). "The oncogenic properties of mutant p110alpha and p110beta phosphatidylinositol 3-kinases in human mammary epithelial cells." Proc Natl Acad Sci U S A **102**(51): 18443-18448.

Zhao, L. and P. K. Vogt (2008). "Helical domain and kinase domain mutations in p110alpha of phosphatidylinositol 3-kinase induce gain of function by different mechanisms." Proc Natl Acad Sci U S A **105**(7): 2652-2657.

Zhou, B. P., Y. Liao, et al. (2001). "HER-2/neu induces p53 ubiquitination via Akt-mediated MDM2 phosphorylation." Nat Cell Biol **3**(11): 973-982.

Appendix

Manuscript: Luminal Expression of PIK3CA Mutant H1047R in the Mammary Gland Induces Heterogeneous Tumors

Published OnlineFirst April 11, 2011; DOI:10.1158/0008-5472.CAN-10-3827

Priority Report

Cancer Research

Luminal Expression of *PIK3CA* Mutant H1047R in the Mammary Gland Induces Heterogeneous Tumors

Dominique S. Meyer[1], Heike Brinkhaus[1], Urs Müller[1], Matthias Müller[2], Robert D. Cardiff[3], and Mohamed Bentires-Alj[1]

Abstract

The phosphoinositide 3-kinase (PI3K) signaling cascade, a key mediator of cellular survival, growth, and metabolism, is frequently altered in human cancer. Activating mutations in *PIK3CA*, which encodes the α-catalytic subunit of PI3K, occur in approximately 30% of breast cancers. These mutations result in constitutive activity of the enzyme and are oncogenic, but it is not known whether they are sufficient to induce mammary carcinomas in mice. In the present study, we show that the expression of mutant *PIK3CA* H1047R in the luminal mammary epithelium evokes heterogeneous tumors that express luminal and basal markers and are positive for the estrogen receptor. Our results suggest that the *PIK3CA* H1047R oncogene targets a multipotent progenitor cell and, furthermore, show that this model recapitulates features of human breast tumors with *PIK3CA* H1047R. *Cancer Res; 71(13); 4344–51. ©2011 AACR.*

Introduction

Breast cancer is a complex and heterogeneous disease, probably due to the diversity of transforming events and mammary cells in which they occur, as well as to the cross-talk between the transformed epithelium and the surrounding stroma during breast tumorigenesis (1). Definition of the molecular and cellular alterations causing breast tumor heterogeneity should increase our understanding of breast cancer pathogenesis and support the design of optimal therapeutic strategies.

The phosphoinositide 3-kinase (PI3K) pathway, a central regulator of diverse normal cellular functions, is often subverted during neoplastic transformation (2). Mechanisms of activation of the PI3K pathway in cancer include (i) the mutation and/or amplification of *PIK3CA*, the gene encoding the α-catalytic subunit of the kinase (p110α); (ii) the loss of expression of the PTEN phosphatase that reverses PI3K action; (iii) the activation downstream of oncogenic receptor tyrosine kinases; and (iv) the mutation/amplification of Akt. A hyperactive PI3K pathway results in cancer cells that have a competitive advantage by decreasing cell death and increasing cell proliferation, migration, invasion, metabolism, angiogenesis, and resistance to chemotherapy.

PIK3CA is mutated in approximately 30% of human breast cancers with nearly 80% of the mutations occurring at 3 hotspots: E542K (∼4% of human breast cancers) and E545K (∼6%) within the helical domain; and H1047R (∼15%) within the kinase domain of p110α (3–5). These mutations result in a constitutively active enzyme that transforms cells *in vitro* and increases tumorigenicity in xenograft models (6–9). The increase in lipid kinase activity of the mutated p110α makes it a "druggable" target, and several inhibitors have entered phase I/II clinical trials (10, 11). Mutations in *PIK3CA* are more frequent in estrogen receptor (ER)-positive and HER2-positive tumors than in basal-like breast cancers (12). Reported correlations between *PIK3CA* mutations and prognosis are contradictory; studies comprising large numbers of patients have shown a paradoxical correlation of *PIK3CA* mutations with good prognosis (12–15).

PIK3CA mutations have been reported in breast ductal carcinoma *in situ* (DCIS; ref. 16), and the mutation frequencies in pure DCIS, DCIS adjacent to invasive ductal carcinoma (IDC), and IDC (17) are similar. Thus, mutations of *PIK3CA* appear to occur early in breast tumorigenesis. To test the hypothesis that *PIK3CA* mutation initiates mammary tumors, we generated a mouse model conditionally expressing *PIK3CA* H1047R. In this study, we show that the expression of this mutation in the mammary gland induces carcinomas with different phenotypes composed of cells expressing luminal markers or basal markers or both, and a significant number expressing ER.

Materials and Methods

Transgenic mice

We constructed a vector with a transcriptional STOP sequence flanked by *loxP* sites upstream of the 5′-terminally

Authors' Affiliations: [1]Friedrich Miescher Institute for Biomedical Research; [2]Developmental and Molecular Pathways, Novartis Institutes for Biomedical Research, Basel, Switzerland; and [3]Center for Comparative Medicine and Department of Pathology, University of California Davis, Davis, California

Note: Supplementary data for this article are available at Cancer Research Online (http://cancerres.aacrjournals.org/).

Corresponding Author: Mohamed Bentires-Alj, Friedrich Miescher Institute for Biomedical Research, Maulbeerstr. 66, 4058 Basel, Switzerland. Phone: 41-61-69-74048; Fax: 41-61-697-3976; E-mail: bentires@fmi.ch

doi: 10.1158/0008-5472.CAN-10-3827

©2011 American Association for Cancer Research.

Downloaded from cancerres.aacrjournals.org on July 15, 2011
Copyright © 2011 American Association for Cancer Research

Published OnlineFirst April 11, 2011; DOI:10.1158/0008-5472.CAN-10-3827

hemagglutinin (HA)-tagged human *PIK3CA* cDNA (Addgene) and an *IRES2-EGFP* reporter element (pIRES2-EGFP Vector; Clontech). The resulting *loxP*-STOP-*loxP*-HA-*PIK3CA-IRES2-EGFP* fragment was cloned into a recombination-mediated cassette exchange (RMCE) plasmid. The vector was introduced into the modified Rosa26 locus of Balb/c mouse embryonic stem (ES) cells by RMCE, and the ES cells were used for blastocyst injection (18). Chimeric mice were mated with Balb/c mice, and transgenic mice were identified by genotyping using the primers 5′-TGGCCAGTACCTCATGGATT-3′ and 5′-GCAATACATCTGGGCTACTTCAT-3′. FVB/N-Tg(MMTV-Cre) and FVB/N.B6-Tg(WAPiCre) mice have been described previously (19, 20). Tg(MMTV-Cre) mice have the FVB/N background, and B6-Tg(WAPiCre) mice were backcrossed for 5 generations to an FVB/N background. MMTV-*NeuNT* (strain TG.NK) mice were purchased from Charles River.

Immunohistochemistry

The following antibodies were used: K14 (Thermo Scientific; catalog no. RB-9020; dilution 1:1,000), K18 (Fitzgerald; catalog no. GP11; dilution 1:500), green fluorescent protein (GFP; Invitrogen; catalog no. A11122; dilution 1:500), ER (Santa Cruz Biotechnology; catalog no. SC-542; dilution 1:1,000), progesterone receptor (PR; Thermo Scientific; catalog no. RM-9102; dilution 1:200), α-smooth muscle actin (α-SMA; Thermo Scientific; catalog no. RB-9010 dilution 1:500), cleaved caspase-3 (Cell Signaling; catalog no. 9661; dilution 1:100), and Ki-67 (Thermo Scientific; catalog no. RM-9106; dilution 1:1,000).

Southern blotting

Genomic DNA from mouse tails was digested with 8 units of AvrII enzyme [New England BioLabs (NEB)] and separated on 1% agarose gel. A DIG-labeled DNA probe targeting the neomycin-resistance cassette was amplified using the PCR DIG Probe Synthesis Kit (Roche) and the primers 5′-ATGG-GATCGGCCATTGAACAAGAT-3′ and 5′-CGGCCATTTTC-CACCATGATAT-3′.

Reverse transcriptase-PCR

RNA was isolated from mouse tissue using TRIzol (Invitrogen). TaqMan polymerase and appropriate buffers were purchased from NEB. Human *PIK3CA* was detected using the primers 5′-CAGATCCCAGTGTGGTGGTACG-3′ and 5′-CCTCACGGAGGCATTCTAAAGT-3′ and endogenous *gapdh* was detected using the primers 5′-CATCAAGAAGGTGGT-GAAGC-3′ and 5′-GGGAGTTGCTGTTGAAGTCG-3′.

Results and Discussion

Expression of *PIK3CA* H1047R in luminal mammary epithelial cells induces carcinomas

To test whether *PIK3CA* H1047R evokes mammary carcinoma, we generated transgenic mice that conditionally expressed this mutation in mammary epithelium. The correct integration of the construct in ES cells conditionally expressing *PIK3CA* H1047R (Fig. 1A) was tested by Southern blotting and PCR (Fig. 1B, left; data not shown). The ES cells were used to generate the H1047R line, and the mutation was confirmed by DNA sequencing (Fig. 1B, right). Next, H1047R animals were crossed to WAPiCre mice in which expression of recombinase Cre was driven by the whey acidic protein (*WAP*) promoter, which is active in alveolar progenitor cells and differentiated secretory luminal cells (20–23). Furthermore, we crossed H1047R animals to mice expressing Cre under the control of the mouse mammary tumor virus (MMTV) long terminal repeat, which results in expression within luminal mammary epithelial cells (19).

Female bitransgenic WAPiCre H1047R mice and littermate controls (WAPiCre) were generated. Mammary glands from WAPiCre H1047R virgin mice had GFP-positive areas indicating expression of the oncogene (Fig. 1C, left). This is consistent with previous studies that reported activity of the *WAP* promoter in a fraction of mammary epithelial cells in virgin mice (21, 23). Examination of whole mounts and hematoxylin and eosin (H&E)-stained sections revealed an average of 5.7 (±2.2) neoplastic lesions in glands from 21- to 24-week-old virgin WAPiCre H1047R mice but not from WAPiCre H1047R virgin mice up to 18 weeks of age or age-matched littermate controls (Fig. 1C, right).

The WAPiCre H1047R and control mice were impregnated to achieve maximal Cre-mediated recombination, and the pups were removed the day after delivery. Although parous WAPiCre mice did not form tumors, WAPiCre H1047R mice developed mammary tumors, on average, 36.8 (±4.9) days after delivery of the pups, corresponding to an age of 140.3 (±6.9) days (Fig. 2A). Bitransgenic MMTV-Cre H1047R mice and littermate controls (MMTV-Cre) were generated and left as virgins. Surprisingly, approximately 75% of the MMTV-Cre H1047R animals died before the age of 4 months. Although we did not identify the cause of death, we consider that leakiness of the *MMTV* promoter causing deleterious H1047R expression in tissues other than the mammary gland was a likely cause (D.S. Meyer and M. Bentires-Alj, unpublished observations). However, approximately 25% of the MMTV-Cre H1047R mice were viable and formed mammary carcinomas, on average, after 214 (±22.6) days, whereas no tumors were detected in MMTV-Cre control mice (Fig. 2B).

Because the average age of tumor onset between parous WAPiCre H1047R and virgin MMTV-Cre H1047R mice differs by approximately 75 days (140.3 vs. 214 days), we sought to investigate whether pregnancy accelerates *PIK3CA* H1047R-driven tumorigenesis. To address this question, we compared tumor onset in nulliparous and parous WAPiCre H1047R mice and found tumor onset to occur significantly earlier in parous mice than in nulliparous mice (Fig. 2C). These data show that pregnancy accelerates tumor onset in WAPiCre H1047R mice.

We then comparatively assessed the mechanisms underlying the accelerated tumor onset seen in parous against those in nulliparous WAPiCre H1047R mice. Fluorescence images and Western blot analysis showed enhanced GFP expression in glands from parous mice, indicating an increase in the number of cells that underwent Cre-mediated recombination and thus expressed H1047R (Supplementary Fig. S1). In addition, whole mounts of the involuting glands revealed a dramatic delay in involution in mice expressing *PIK3CA* H1047R compared with control animals (Supplementary Fig. S2A), which is in line with

Downloaded from cancerres.aacrjournals.org on July 15, 2011
Copyright © 2011 American Association for Cancer Research

Published OnlineFirst April 11, 2011; DOI:10.1158/0008-5472.CAN-10-3827

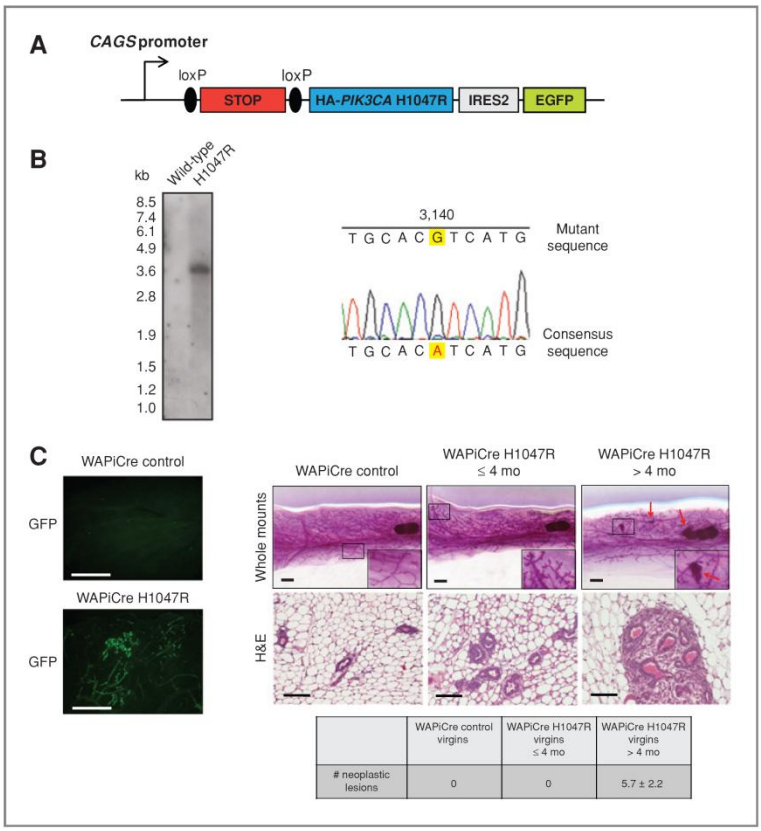

	WAPiCre control virgins	WAPiCre H1047R virgins ≤ 4 mo	WAPiCre H1047R virgins > 4 mo
# neoplastic lesions	0	0	5.7 ± 2.2

Figure 1. Targeted expression of mutant p110α in luminal mammary epithelial cells. A, schematic of the construct used for generating transgenic mice conditionally expressing *PIK3CA* H1047R. The *PIK3CA* cDNA is flanked by a floxed STOP cassette upstream and an IRES2-EGFP reporter element downstream. Expression of *PIK3CA* H1047R is driven by a chicken β-actin (*CAGS*) promoter. B, Southern blotting of genomic DNA from wild-type (WT) and *PIK3CA* H1047R mice (left) and sequencing of genomic DNA from H1047R transgenic mice harboring an A–G mutation at nucleotide 3140 (right). C, left, fluorescence images of glands from virgin WAPiCre control and virgin WAPiCre H1047R mice showing GFP expression; right, representative images of mammary glands from WAPiCre control mice (left), WAPiCre H1047R virgin mice between 12 and 18 weeks of age (middle), and WAPiCre H1047R virgin mice between 21 and 24 weeks of age (right). Images show whole-mount preparations (top) and H&E-stained sections (bottom). The red arrows indicate neoplastic lesions. Inserts show the indicated areas at higher magnification. Table (bottom) shows quantification of neoplastic lesions. Scale bars, 1 mm (whole mounts, fluorescence images); 100 μm (H&E images).

previous reports of a delayed involution when the PI3K pathway is hyperactivated (24, 25). Immunostaining for cleaved caspase-3 revealed a reduction in the number of apoptotic cells in involuting glands from WAPiCre H1047R mice compared with control mice, suggesting that reduced cell death is the cause of the delayed involution (Supplementary Fig. S2B and C). Our results suggest, therefore, that the acceleration of tumor onset is most likely due to an increase in the number of cells expressing *PIK3CA* H1047R in parous glands and to impaired cell death in involuting glands with the H1047R mutation. Indeed, pregnancy-induced proliferation could facilitate the acquirement of further genomic alterations and, therefore, accelerate tumorigenesis.

Analysis of RNA and proteins from WAPiCre H1047R and MMTV-Cre H1047R-induced tumors confirmed that mutant *PIK3CA* was expressed in the bitransgenic mice (Fig. 3A and B). In addition, tumors from both WAPiCre H1047R and MMTV-Cre H1047R mice showed 3-fold and 8-fold higher phospho-Akt (p-Akt) levels than mammary tumors from the MMTV-NeuNT model, respectively. In contrast, activation of the Erk1/2 pathway in *PIK3CA* H1047R tumors tended to be weaker than in tumors from MMTV-NeuNT mice (Fig. 3C).

Our results show that luminal expression of *PIK3CA* H1047R induces mammary tumor formation. This is consistent with the observation that conditional expression of mutant *PIK3CA* H1047R in type II lung alveolar epithelial cells causes lung adenocarcinomas in transgenic mice (26) and suggests that this mutation plays a causal role in epithelial cancers.

WAPiCre H1047R and MMTV-Cre H1047R–evoked mammary tumors are heterogeneous

To gain insight into significant pathophysiologic features, 22 WAPiCre H1047R and 21 MMTV-Cre H1047R-induced mammary tumors were characterized histologically. MMTV-Cre H1047R-caused tumors showed multiple adenomyoepitheliomas, with clusters of well-delineated polypoid tumors composed of a mixture of glandular epithelium and interstitial fusiform cells having abundant polar cytoplasm (Fig. 4A, top left). Similar tumors have been reported in MMTV-Cre/Pten$^{fl/fl}$/ErbB2^{KI} mice, suggesting that an activated PI3K pathway mediates this histotype (27).

Downloaded from cancerres.aacrjournals.org on July 15, 2011
Copyright © 2011 American Association for Cancer Research

Published OnlineFirst April 11, 2011; DOI:10.1158/0008-5472.CAN-10-3827

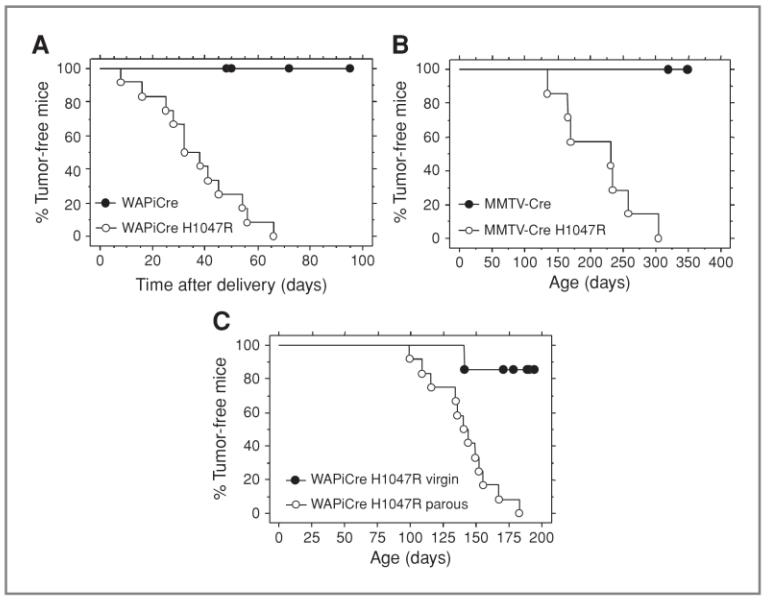

Figure 2. WAPiCre H1047R and MMTV-Cre H1047R mice develop mammary tumors. A, Kaplan–Meier curves showing tumor onset in bitransgenic WAPiCre H1047R mice ($n = 12$) and WAPiCre littermate controls ($n = 7$). The mice were impregnated and the pups removed from the mothers the day after delivery. Bitransgenic animals developed palpable tumors, on average, 36.8 (±4.9) days after delivery, corresponding to age 140.3 (±6.9) days. B, Kaplan–Meier curves showing tumor onset in double transgenic MMTV-Cre H1047R mice ($n = 7$) and MMTV-Cre littermate controls ($n = 8$). MMTV-Cre H1047R mice developed palpable tumors, on average, within 214 (±22.6) days. C, Kaplan–Meier curves showing tumor onset in virgin WAPiCre H1047R ($n = 7$) and parous WAPiCre H1047R mice ($n = 12$). Parous animals developed palpable tumors, on average, at 140.3 (±6.9) days and all animals had at least 1 tumor within 183 days of age. In contrast, by 170 days, only 1 out of 7 virgin WAPiCre H1047R mice developed a tumor (at 141 days). The difference in tumor latency between parous and virgin animals is statistically significant ($P = 0.0006$).

In contrast, the WAPiCre H1047R mice formed a more diverse spectrum of tumors with 5 distinct histotypes. The most prevalent tumor phenotypes found are adenosquamous carcinomas (54.6%) and adenomyoepitheliomas (22.7%). Furthermore, adenocarcinomas with squamous metaplasia (13.6%) and adenocarcinomas (9.1%) were observed, albeit at lower frequencies (Fig. 4A and B). All the glands surrounding the tumors displayed diffuse adenocarcinomatosis with invasive periductal cords of neoplastic epithelial cells in dense connective tissue (Fig. 4A, top right).

To further characterize H1047R-induced carcinomas, tumors were stained for luminal cytokeratin 18 (K18), basal/myoepithelial cytokeratin 14 (K14), and myoepithelial α-SMA markers, as well as for ER and PR. Notably, approximately 18% to 26% of the tumor cells of the adenomyopitheliomas from both transgenic mice expressed ER and approximately 16% expressed PR in the luminal cells (Fig. 4A; Supplementary Table S1; Supplementary Fig. S3A). In addition, other tumor histotypes contained ER-positive cells although at lower frequencies (<5%; Fig. 4A; Supplementary Table S1). WAPiCre- and MMTV-Cre H1047R tumors were positive for both luminal K18 and basal K14. The relative tumor area positive for K14 was approximately 15% in adenomyoepitheliomas and adenocarcinomatosis, whereas in the other phenotypes it ranged between 26% and 43%. The percentage of K18-positive tumor area was 25% in adenocarcinomatosis and ranged between 36% and 45% in the other tumor histotypes (Fig. 4A; Supplementary Table S1). Although the majority of tumor cells expressed either K18 or K14, some cells were positive for both K14 and K18 (Fig. 4C). As expected, the K14-positive cells within WAPiCre- and MMTV-Cre H1047R adenomyoepitheliomas were also α-SMA-positive (Fig. 4A). In contrast, the K14-positive cells within adenosquamous carcinomas observed in WAPiCre H1047R mice were largely negative for α-SMA, a characteristic of human metaplastic breast cancer in which *PIK3CA* is mutated in approximately 50% of cases (28). Interestingly, all tumors showed very low rates of apoptosis (0.2%–1.4%; Supplementary Table S1; Supplementary Fig. S3A), most likely due to the antiapoptotic effect of an activated PI3K pathway. Furthermore, we found the percentage of Ki-67–positive cells to be lower in adenomyoepitheliomas and adenocarcinomatosis than in all other tumor phenotypes (Supplementary Table S1; Supplementary Fig. S3A).

These data show that luminal expression of *PIK3CA* H1047R can induce mammary tumors expressing the basal marker K14. To exclude the possibility that luminal *PIK3CA* H1047R induces expression of paracrine factors that transform basal cells, we analyzed K14-positive cancer cells for GFP expression

Downloaded from cancerres.aacrjournals.org on July 15, 2011
Copyright © 2011 American Association for Cancer Research

Published OnlineFirst April 11, 2011; DOI:10.1158/0008-5472.CAN-10-3827

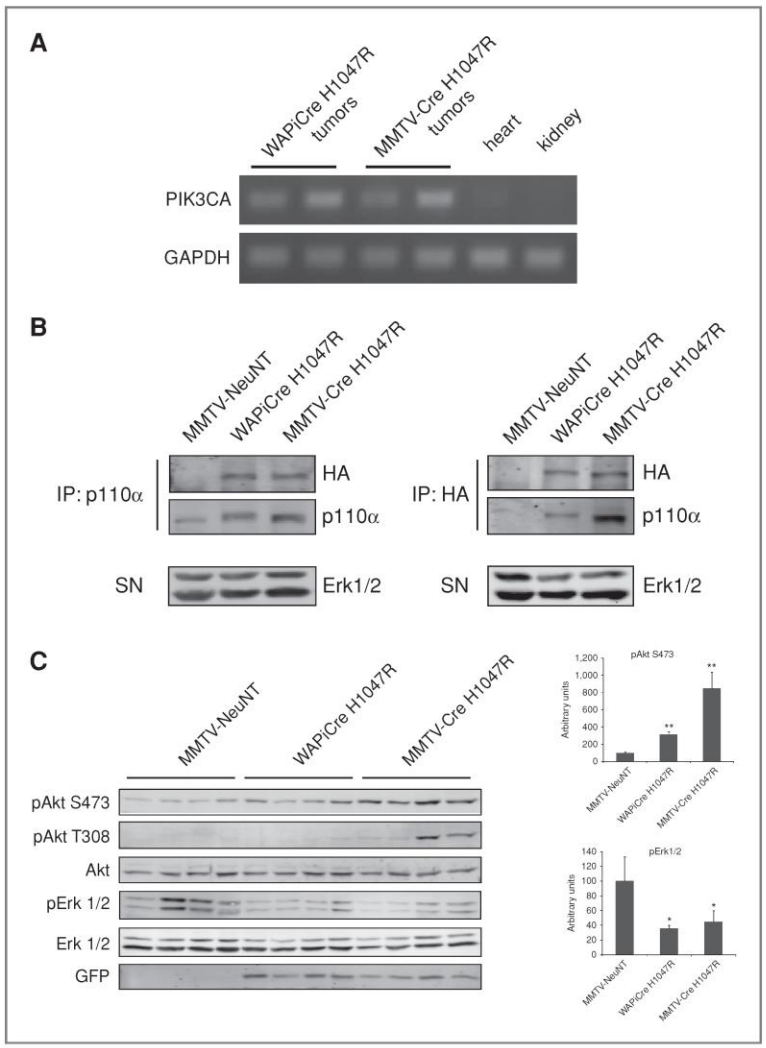

Figure 3. Tumors from WAPiCre H1047R and MMTV-Cre H1047R mice express mutant *PIK3CA*. A, RT-PCR showing expression of *PIK3CA* H1047R in WAPiCre H1047R and MMTV-Cre H1047R mammary tumors but not in heart or kidney tissues of a WAPiCre H1047R animal. B, expression of exogenous p110α as indicated by p110α-immunoprecipitation (IP) from MMTV-NeuNT, WAPiCre H1047R, and MMTV-Cre H1047R tumor lysates using anti-p110α (left) or anti-HA antibodies (right). C, immunoblotting of mammary tumor lysates from the indicated genotypes using the specified antibodies (left) and quantification of pAkt S473 and pErk1/2 signals (right). *, not significant; **, $P < 0.01$; SN: supernatant.

by immunostaining and fluorescence-activated cell sorting (FACS). There was a significant overlap between K14 and GFP expression (Fig. 4D; data not shown), suggesting that some K14-positive cancer cells within the WAPiCre H1047R and MMTV-Cre H1047R tumors resulted from expression of the oncogene in luminal cells. This supports the emerging notion that certain tumors with basal characteristics arise from luminal cells (29, 30).

Taken together, our results show that luminal expression of *PIK3CA* H1047R evokes mammary tumors, recapitulating the heterogeneity of human breast cancer. These results lead to major conclusions. The finding that *PIK3CA* H1047R causes ER- and PR-positive tumors suggests that PI3K activity expands ER-positive mammary cells, consistent with the presence of *PIK3CA* H1047R mutations in human ER-positive tumors (4).

The presence of cancer cells expressing luminal and basal markers in WAPiCre- and MMTV-Cre H1047R–evoked tumors suggests, in both models, that multipotent progenitor cells are the targets of H1047R-mediated transformation. The *WAP* promoter is active in a multipotent progenitor population, the parity-identified mammary epithelial cells (PI-MEC)—present in nulliparous mice, and expanded after pregnancy (21, 23). Tumors that developed in WAPiCre H1047R nullipar-

Downloaded from cancerres.aacrjournals.org on July 15, 2011
Copyright © 2011 American Association for Cancer Research

Published OnlineFirst April 11, 2011; DOI:10.1158/0008-5472.CAN-10-3827

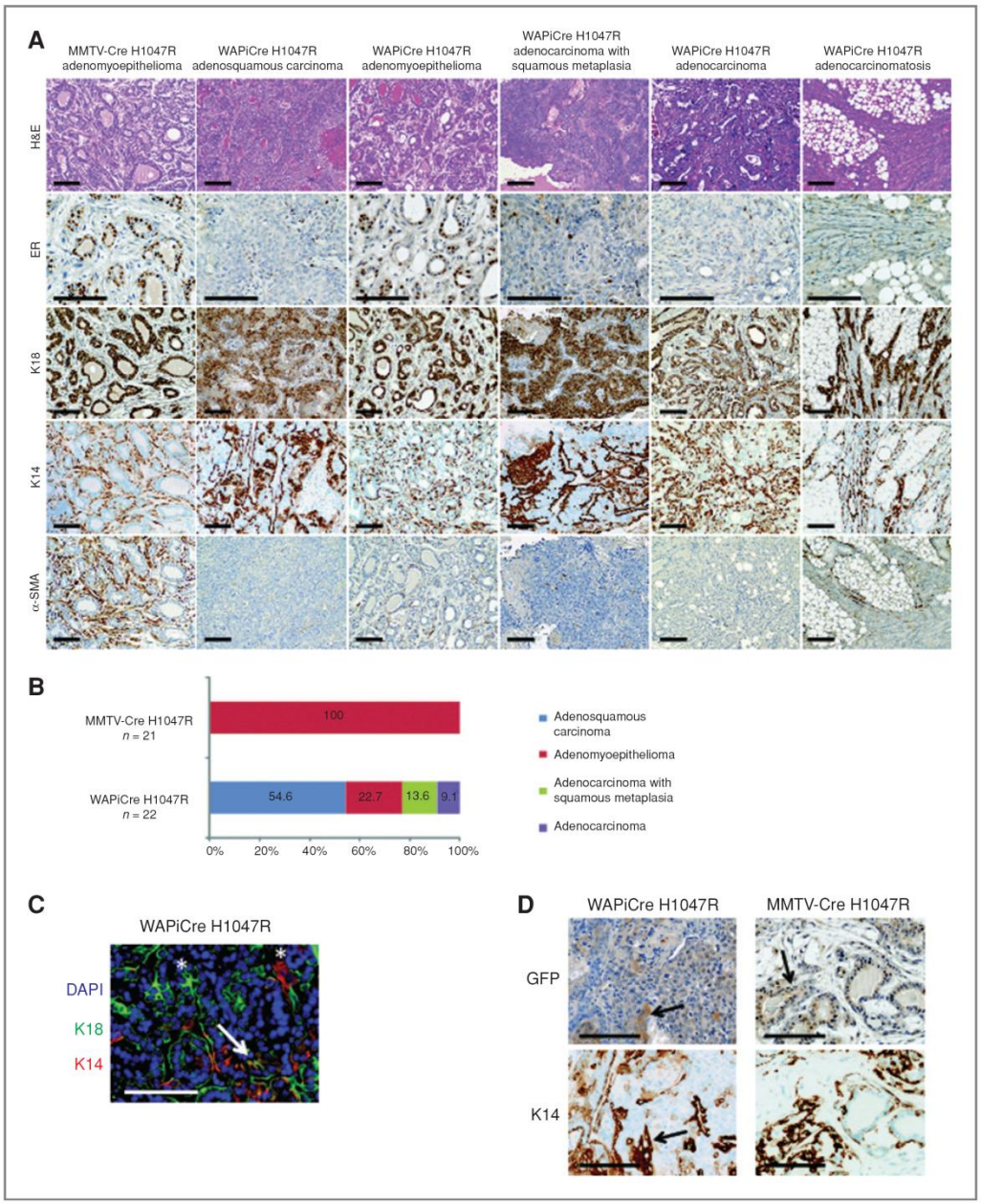

Figure 4. WAPiCre H1047R- and MMTV-Cre H1047R–evoked tumors express basal markers. A, H&E-stained sections and immunostainings for ER, K18, K14, and α-SMA from MMTV-Cre H1047R adenomyoepithelioma and different WAPiCre H1047R tumor histotypes as indicated. B, relative prevalence of adenosquamous carcinoma (blue), adenomyoepithelioma (red), adenocarcinoma with squamous metaplasia (green), and adenocarcinoma (purple) among MMTV-Cre H1047R- and WAPiCre H1047R–evoked tumors. C, fluorescence image of 4′,6-diamidino-2-phenylindole (DAPI) staining (blue) and immunostaining of K18 (green) and K14 (red) in a WAPiCre H1047R tumor section. The arrow indicates K14/K18 double-positive cells. *, K14 and K18 single-positive cells. D, images of immunostaining for GFP and K14 in WAPiCre H1047R (left) and MMTV-Cre H1047R tumor sections (right). Arrows indicate areas of K14/GFP double-positive cells. Scale bars, 100 μm.

Downloaded from cancerres.aacrjournals.org on July 15, 2011
Copyright © 2011 American Association for Cancer Research

Published OnlineFirst April 11, 2011; DOI:10.1158/0008-5472.CAN-10-3827

ous mice most likely derived from PI-MECs because this is the cell population that expresses WAP-driven Cre in glands from nulliparous mice (21). Recently, PI-MECs were shown to be the target of MMTV-NeuNT-driven carcinogenesis (21, 31). Therefore, it is plausible that PI-MECs are the cells of origin of cancer in both WAPiCre- and MMTV-Cre H1047R–evoked tumors; however, at this stage, we cannot completely exclude the possibility that expression of *PIK3CA* H1047R in more differentiated cells also contributes to tumor formation in these models.

The observation of different histotypes between WAPiCre H1047R- and MMTV-Cre H1047R-derived tumors has several possible explanations. First, WAPiCre H1047R, but not MMTV-Cre H1047R, mice underwent pregnancy. Second, it is possible that the cellular targets of MMTV and WAP are overlapping but not congruent.

The fact that tumors from MMTV-Cre H1047R, but not MMTV-NeuNT, mice express K14 (Supplementary Fig. S3B) suggests a model in which *PIK3CA* H1047R transforms multipotent progenitors, allowing differentiation along the luminal and basal lineages. In contrast, the *NeuNT* oncogene favors luminal differentiation resulting in K18-positive, but not K14-positive, tumors. An alternative and more interesting explanation is that the *MMTV* promoter is active in differentiated luminal cells and H1047R causes their dedifferentiation to multipotent progenitor cells, which then give rise to K14- and/or K18-positive cancer cells. This would suggest a role for *PIK3CA* H1047R in cancer cell plasticity, a hypothesis that merits testing.

Disclosure of Potential Conflicts of Interest

No potential conflicts of interest were disclosed.

Acknowledgments

We thank N. Hynes (FMI) for helpful comments on the manuscript, W.J. Muller (McGill University) for providing the MMTV-Cre line, members of the Bentires-Alj lab for advice and discussions, Corinne Haller, Thierry Doll, and Marianne Lemaistre for excellent technical assistance, and various colleagues for provision of reagents.

Grant Support

Research conducted in the laboratory of M. Bentires-Alj is supported by the Novartis Research Foundation, the European Research Council (ERC starting grant 243211-PTPsBDC), the Swiss Cancer League, and the Krebsliga Beider Basel.

Received October 27, 2010; revised March 4, 2011; accepted March 28, 2011; published OnlineFirst April 11, 2011.

References

1. Polyak K. Breast cancer: origins and evolution. J Clin Invest 2007;117:3155–63.
2. Engelman JA, Luo J, Cantley LC. The evolution of phosphatidylinositol 3-kinases as regulators of growth and metabolism. Nat Rev Genet 2006;7:606–19.
3. Samuels Y, Wang Z, Bardelli A, Silliman N, Ptak J, Szabo S, et al. High frequency of mutations of the PIK3CA gene in human cancers. Science 2004;304:554.
4. Saal LH, Holm K, Maurer M, Memeo L, Su T, Wang X, et al. PIK3CA mutations correlate with hormone receptors, node metastasis, and ERBB2, and are mutually exclusive with PTEN loss in human breast carcinoma. Cancer Res. 2005;65:2554–9.
5. Bader AG, Kang S, Zhao L, Vogt PK. Oncogenic PI3K deregulates transcription and translation. Nat Rev Cancer 2005;5:921–9.
6. Kang S, Bader AG, Vogt PK. Phosphatidylinositol 3-kinase mutations identified in human cancer are oncogenic. Proc Natl Acad Sci U S A 2005;102:802–7.
7. Isakoff SJ, Engelman JA, Irie HY, Luo J, Brachmann SM, Pearline RV, et al. Breast cancer-associated PIK3CA mutations are oncogenic in mammary epithelial cells. Cancer Res 2005;65:10992–1000.
8. Zhao JJ, Liu Z, Wang L, Shin E, Loda MF, Roberts TM. The oncogenic properties of mutant p110alpha and p110beta phosphatidylinositol 3-kinases in human mammary epithelial cells. Proc Natl Acad Sci U S A 2005;102:18443–8.
9. Chakrabarty A, Rexer BN, Wang SE, Cook RS, Engelman JA, Arteaga CL. H1047R phosphatidylinositol 3-kinase mutant enhances HER2-mediated transformation by heregulin production and activation of HER3. Oncogene 2010;29:5193–203.
10. Di Cosimo S, Baselga J. Management of breast cancer with targeted agents: importance of heterogeneity. Nat Rev Clin Oncol 2010;7:139–47.
11. Engelman JA. Targeting PI3K signalling in cancer: opportunities, challenges and limitations. Nat Rev Cancer 2009;9:550–62.
12. Carvalho S, Schmitt F. Potential role of PI3K inhibitors in the treatment of breast cancer. Future Oncol 2010;6:1251–63.
13. Meyer DS, Bentires-Alj M. Can PI3K/mTOR inhibition ERase them all? Breast Cancer Res 2010;12:315.
14. Loi S, Haibe-Kains B, Majjaj S, Lallemand F, Durbecq V, Larsimont D, et al. PIK3CA mutations associated with gene signature of low mTORC1 signaling and better outcomes in estrogen receptor-positive breast cancer. Proc Natl Acad Sci U S A 2010;107:10208–13.
15. Kalinsky K, Jacks LM, Heguy A, Patil S, Drobnjak M, Bhanot UK, et al. PIK3CA mutation associates with improved outcome in breast cancer. Clin Cancer Res 2009;15:5049–59.
16. Dunlap JB, Le C, Patterson J, Presnell A, Heinrich MC, Corless CL, et al. PI3 kinase mutations occur early in breast carcinoma. Laboratory Investigation 2007;87:29a-a.
17. Miron A, Varadi M, Carrasco D, Li H, Luongo L, Kim HJ, et al. PIK3CA mutations in *in situ* and invasive breast carcinomas. Cancer Res 2010;70:5674–8.
18. Tchorz JS, Kinter J, Muller M, Tornillo L, Heim MH, Bettler B. Notch2 signaling promotes biliary epithelial cell fate specification and tubulogenesis during bile duct development in mice. Hepatology 2009;50:871–9.
19. Andrechek ER, White D, Muller WJ. Targeted disruption of ErbB2/Neu in the mammary epithelium results in impaired ductal outgrowth. Oncogene 2005;24:932–7.
20. Wintermantel TM, Mayer AK, Schutz G, Greiner EF. Targeting mammary epithelial cells using a bacterial artificial chromosome. Genesis 2002;33:125–30.
21. Bruno RD, Smith GH. Functional characterization of stem cell activity in the mouse mammary gland. Stem Cell Rev 2011;7:238–47.
22. Boulanger CA, Wagner KU, Smith GH. Parity-induced mouse mammary epithelial cells are pluripotent, self-renewing and sensitive to TGF-beta1 expression. Oncogene 2005;24:552–60.
23. Booth BW, Boulanger CA, Smith GH. Alveolar progenitor cells develop in mouse mammary glands independent of pregnancy and lactation. J Cell Physiol 2007;212:729–36.
24. Schwertfeger KL, Richert MM, Anderson SM. Mammary gland involution is delayed by activated Akt in transgenic mice. Mol Endocrinol 2001;15:867–81.
25. Li G, Robinson GW, Lesche R, Martinez-Diaz H, Jiang Z, Rozengurt N, et al. Conditional loss of PTEN leads to precocious development

Downloaded from cancerres.aacrjournals.org on July 15, 2011
Copyright © 2011 American Association for Cancer Research

Published OnlineFirst April 11, 2011; DOI:10.1158/0008-5472.CAN-10-3827

and neoplasia in the mammary gland. Development 2002;129:4159–70.

26. Engelman JA, Chen L, Tan X, Crosby K, Guimaraes AR, Upadhyay R, et al. Effective use of PI3K and MEK inhibitors to treat mutant Kras G12D and PIK3CA H1047R murine lung cancersNat Med 2008;14:1351–6.
27. Schade B, Rao T, Dourdin N, Lesurf R, Hallett M, Cardiff RD, et al. PTEN deficiency in a luminal ErbB-2 mouse model results in dramatic acceleration of mammary tumorigenesis and metastasis. J Biol Chem 2009;284:19018–26.
28. Hennessy BT, Gonzalez-Angulo AM, Stemke-Hale K, Gilcrease MZ, Krishnamurthy S, Lee JS, et al. Characterization of a naturally occurring breast cancer subset enriched in epithelial-to-mesenchymal transition and stem cell characteristics. Cancer Res 2009;69:4116–24.
29. Lim E, Vaillant F, Wu D, Forrest NC, Pal B, Hart AH, et al. Aberrant luminal progenitors as the candidate target population for basal tumor development in BRCA1 mutation carriers. Nat Med 2009;15:907–13.
30. Molyneux G, Geyer FC, Magnay FA, McCarthy A, Kendrick H, Natrajan R, et al. BRCA1 basal-like breast cancers originate from luminal epithelial progenitors and not from basal stem cells. Cell Stem Cell 2010;7:403–17.
31. Jeselsohn R, Brown NE, Arendt L, Klebba I, Hu MG, Kuperwasser C, et al. Cyclin D1 kinase activity is required for the self-renewal of mammary stem and progenitor cells that are targets of MMTV-ErbB2 tumorigenesis. Cancer Cell 2010;17:65–76.

Downloaded from cancerres.aacrjournals.org on July 15, 2011
Copyright © 2011 American Association for Cancer Research

Viewpoint: Can phosphatidylinositol 3-kinase/mammalian target of rapamycin inhibition Erase them all?

Meyer and Bentires-Alj *Breast Cancer Research* 2010, **12**:315
http://breast-cancer-research.com/content/12/5/315

Breast Cancer RESEARCH

VIEWPOINT

Can phosphatidylinositol 3-kinase/mammalian target of rapamycin inhibition ERase them all?

Dominique S Meyer and Mohamed Bentires-Alj*

Abstract

Seventy percent of breast tumors are estrogen receptor (ER) positive. Although endocrine therapy is successful for the majority of patients with ER-positive tumors, approximately 30% show *de novo* or acquired resistance and the underlying molecular mechanisms and biomarkers that predict such resistance remain elusive. Two recent papers report that hyperactivation of the phosphatidylinositol 3-kinase (PI3K) pathway produces resistance to tamoxifen. This raises the possibility that combining endocrine therapy and PI3K inhibition may be more effective than monotherapy for treating ER-positive breast tumors, either as first-line therapy for tumors with high PI3K activity or after the development of resistance to endocrine therapy.

Background

Tamoxifen, which interferes with estrogen for receptor binding, was the first successful targeted therapy and has been the treatment of choice for estrogen receptor (ER)-positive breast cancers for more than two decades. Unfortunately, resistance occurs in approximately 30% of patients and the mechanisms of resistance act directly on the ER pathway and/or activate parallel pathways that block the anti-proliferative and pro-apoptotic actions of tamoxifen [1,2]. For example, increased mitogen-activated protein kinase (MAPK) and phosphatidylinositol 3-kinase (PI3K) signaling downstream of growth factor receptors (for example, ERBB2 and Insulin-like growth factor 1 receptor (IGF-1R)) has been implicated in a crosstalk with ER and in resistance to endocrine therapy [1-3].

The PI3K pathway, a central regulator of diverse normal cellular functions, is very often subverted during neoplastic transformation and contributes to several hallmarks of cancer that result in a competitive advantage for cancer cells [4-6]. Not surprisingly, the PI3K cascade is an attractive therapeutic target and several inhibitors are currently in phase I/II clinical trials. Preclinical studies have shown that PI3K inhibition circumvents resistance to trastuzumab in ERBB2-positive breast cancers and this has led to clinical trials combining anti-ERBB2 and anti-PI3K therapies [7]. Although PI3K has been implicated in resistance to endocrine therapy of ER-positive tumors, several questions remain unanswered. Is PI3K inhibition, alone or in combination with tamoxifen, effective in tamoxifen-resistant ER-positive cancer cells? Does PI3K inhibition block the emergence of tamoxifen resistance? Does a PI3K hyperactivation signature in human tumors predict tamoxifen sensitivity? Two recent papers now provide some answers to these outstanding questions.

The articles

Creighton and colleagues [8] investigated the relationship between the PI3K pathway and ER levels and activity using breast cancer cell lines and data sets of human breast tumors, and they defined proteomic and transcriptomic signatures of a hyperactivated PI3K pathway. These signatures negatively correlate with ER levels within ER-positive human breast tumors and are associated with the luminal B breast cancer subtype, the more aggressive subtype of ER-positive tumors. In addition, the transcriptomic signature was shown to predict the worst prognosis in ER-positive tumors. Treatment with the dual PI3K/mammalian target of rapamycin (mTOR) inhibitor BEZ235 increased ER expression in a number of ER-positive breast cancer cell lines. Interestingly, treatment of two luminal B ER-positive cell lines simultaneously with tamoxifen and BEZ-235 reduced cell proliferation more than with either inhibitor alone. Of note, luminal A tumors might also benefit from PI3K inhibition as the luminal A cell lines used by Creighton and colleagues [8] and by Miller and colleagues [9] are also sensitive to BEZ235.

Whether hyperactivation of the PI3K pathway contributes to tamoxifen resistance after chronic tamoxifen treatment was not addressed by this study, but was

*Correspondence: bentires@fmi.ch
Friedrich Miescher Institute for Biomedical Research, Maulbeerstr. 66, 4058 Basel, Switzerland

BioMed Central © 2010 BioMed Central Ltd

answered by Miller and colleagues [9], who generated estrogen-independent breast cancer cell lines from estrogen-dependent ER-positive lines by long-term estrogen deprivation (LTED). Unbiased phosphoprotein microarrays, immunocapture arrays and transcription profiling revealed an increase in PI3K/mTOR signaling as a consequence of higher phosphorylation of the insulin receptor and/or IGF-1R in LTED cells compared with parental cells. Inhibition of PI3K/mTOR using BEZ235 [10] reduced cell growth in both parental and LTED cells and increased apoptosis in most of them. It remains unclear whether LTED cells are more reliant on the PI3K pathway for survival than their parental counterparts as BEZ235 caused a similar level of apoptosis in the two lines. Finally, the authors found that the protein signature of activated PI3K signaling predicted disease outcome after adjuvant endocrine therapy [9].

The viewpoint

Both studies highlight the role of the PI3K pathway in resistance to tamoxifen. Creighton and colleagues [8] suggest that this effect is caused by PI3K-mediated down-regulation of ER. This is also supported by the observation of Miller and colleagues [9] that PI3K pathway activation is inversely correlated with expression of ER in 64 human ER-positive breast tumors. As two lines (MCF7-LTED, HCC1428-LTED) used by Miller and colleagues showed a hyperactivated PI3K pathway compared with parental cells, but no decrease in ER expression, it is conceivable that further mechanisms account for PI3K-mediated resistance [9]. Altogether, the two studies suggest that targeting PI3K/mTOR and ER should be effective in ER-positive tumors and warrant complementary studies using *in vivo* models. Indeed, the interaction of cancer cells with the stroma might modulate estrogen sensitivity and lead to different mechanisms of resistance [2].

Although these studies might suggest that ER-positive tumors with a hyperactivated PI3K pathway should correlate with poor prognosis, this does not seem to be the case, at least for tumors showing activation of the PI3K pathway driven by *PIK3CA* mutations. Indeed, three recent studies reported that mutations of *PIK3CA*, in particular the catalytic domain mutation H1047R, are associated with better prognosis in ER-positive breast cancers [11-13]. This is surprising given the transforming effect of *PIK3CA* mutations in experimental systems. One possible explanation for this '*PIK3CA* paradox' is that most experimental models assess effects on primary tumor growth and not metastases and long-term survival. Alternatively, *PIK3CA* mutations might only moderately activate the pathway and/or constitutive activity of mutant *PIK3CA* may induce negative feedback loops that preclude a more pronounced activation of the pathway [14]. In fact, several cell lines with *PIK3CA* mutations (MCF-7, BT-483, MB-361) [15] were associated with a low/intermediate PI3K score in the proteomic signature of Creighton and colleagues [8]. Therefore, better experimental models and systems biology-like assessment of the PI3K network, including the activities of all intermediates of the pathway, associated feedback loops and collaborating oncogenic pathways, may be needed to solve the '*PIK3CA* paradox'.

In summary, these two studies suggest hyperactivation of PI3K as a mechanism of resistance to tamoxifen, which may have clinical impact. It is reasonable to conclude that the combination of endocrine therapy and inhibition of PI3K in ER-positive tumors with a hyperactive PI3K pathway may be more effective than monotherapy. Studies on *in vivo* breast cancer models with alterations in the PI3K pathway should increase our understanding of this complex but fascinating signaling network, test the validity of this speculation and optimize combination therapies. Ultimately, clinical trials testing combinations of anti-ER and anti-PI3K therapies may finally lead to relapse-free therapy for patients with ER-positive tumors.

Abbreviations

ER, estrogen receptor; IGF-1R, Insulin-like growth factor 1 receptor; LETD, long-term estrogen deprivation; mTOR, mammalian target of rapamycin; PI3K, phosphatidylinositol 3-kinase.

Competing interests

The authors declare that they have no competing interests.

Acknowledgements

We thank various colleagues for helpful comments on the manuscript. Research in the lab of MB-A is supported by the Novartis Research Foundation, the European Research Council (ERC starting grant 243211-PTPsBDC), the Swiss Cancer League and the Krebsliga Beider Basel.

Published: 20 October 2010

References

1. Shou J, Massarweh S, Osborne CK, Wakeling AE, Ali S, Weiss H, Schiff R: **Mechanisms of tamoxifen resistance: increased estrogen receptor-HER2/neu cross-talk in ER/HER2-positive breast cancer.** *J Natl Cancer Inst* 2004, **96:**926-935.
2. Musgrove EA, Sutherland RL: **Biological determinants of endocrine resistance in breast cancer.** *Nat Rev Cancer* 2009, **9:**631-643.
3. Miller TW, Pérez-Torres M, Narasanna A, Guix M, Stål O, Pérez-Tenorio G, Gonzalez-Angulo AM, Hennessy BT, Mills GB, Kennedy JP, Lindsley CW, Arteaga CL: **Loss of Phosphatase and Tensin homologue deleted on chromosome 10 engages ErbB3 and insulin-like growth factor-I receptor signaling to promote antiestrogen resistance in breast cancer.** *Cancer Res* 2009, **69:**4192-4201.
4. Cantley LC: **The phosphoinositide 3-kinase pathway.** *Science* 2002, **296:**1655-1657.
5. Bader AG, Kang S, Zhao L, Vogt PK: **Oncogenic PI3K deregulates transcription and translation.** *Nat Rev Cancer* 2005, **5:**921-929.
6. Engelman JA, Luo J, Cantley LC: **The evolution of phosphatidylinositol 3-kinases as regulators of growth and metabolism.** *Nat Rev Genet* 2006, **7:**606-619.
7. Junttila TT, Akita RW, Parsons K, Fields C, Lewis Phillips GD, Friedman LS, Sampath D, Sliwkowski MX: **Ligand-independent HER2/HER3/PI3K complex is disrupted by trastuzumab and is effectively inhibited by the PI3K inhibitor GDC-0941.** *Cancer Cell* 2009, **15:**429-440.
8. Creighton CJ, Fu X, Hennessy BT, Casa AJ, Zhang Y, Gonzalez-Angulo AM,

Lluch A, Gray JW, Brown PH, Hilsenbeck SG, Osborne CK, Mills GB, Lee AV, Schiff R: **Proteomic and transcriptomic profiling reveals a link between the PI3K pathway and lower estrogen-receptor (ER) levels and activity in ER+ breast cancer.** *Breast Cancer Res*, **12:**R40.

9. Miller TW, Hennessy BT, Gonzalez-Angulo AM, Fox EM, Mills GB, Chen H, Higham C, Garcia-Echeverria C, Shyr Y, Arteaga CL: **Hyperactivation of phosphatidylinositol-3 kinase promotes escape from hormone dependence in estrogen receptor-positive human breast cancer.** *J Clin Invest*, **120:**2406-2413.
10. Maira SM, Stauffer F, Brueggen J, Furet P, Schnell C, Fritsch C, Brachmann S, Chène P, De Pover A, Schoemaker K, Fabbro D, Gabriel D, Simonen M, Murphy L, Finan P, Sellers W, García-Echeverría C: **Identification and characterization of NVP-BEZ235, a new orally available dual phosphatidylinositol 3-kinase/mammalian target of rapamycin inhibitor with potent in vivo antitumor activity.** *Mol Cancer Ther* 2008, **7:**1851-1863.
11. Loi S, Haibe-Kains B, Majjaj S, Lallemand F, Durbecq V, Larsimont D, Gonzalez-Angulo AM, Pusztai L, Symmans WF, Bardelli A, Ellis P, Tutt AN, Gillett CE, Hennessy BT, Mills GB, Phillips WA, Piccart MJ, Speed TP, McArthur GA, Sotiriou C: **PIK3CA mutations associated with gene signature of low mTORC1 signaling and better outcomes in estrogen receptor-positive breast cancer.** *Proc Natl Acad Sci U S A*, **107:**10208-10213.
12. Kalinsky K, Jacks LM, Heguy A, Patil S, Drobnjak M, Bhanot UK, Hedvat CV, Traina TA, Solit D, Gerald W, Moynahan ME: **PIK3CA mutation associates with improved outcome in breast cancer.** *Clin Cancer Res* 2009, **15:**5049-5059.
13. Ellis MJ, Lin L, Crowder R, Tao Y, Hoog J, Snider J, Davies S, DeSchryver K, Evans DB, Steinseifer J, Bandaru R, Liu W, Gardner H, Semiglazov V, Watson M, Hunt K, Olson J, Baselga J: **Phosphatidyl-inositol-3-kinase alpha catalytic subunit mutation and response to neoadjuvant endocrine therapy for estrogen receptor positive breast cancer.** *Breast Cancer Res Treat*, **119:**379-390.
14. Li J, DeFea K, Roth RA: **Modulation of insulin receptor substrate-1 tyrosine phosphorylation by an Akt/phosphatidylinositol 3-kinase pathway.** *J Biol Chem* 1999, **274:**9351-9356.
15. Hollestelle A, Elstrodt F, Nagel JH, Kallemeijn WW, Schutte M: **Phosphatidylinositol-3-OH kinase or RAS pathway mutations in human breast cancer cell lines.** *Mol Cancer Res* 2007, **5:**195-201.

doi:10.1186/bcr2718
Cite this article as: Meyer DS, Bentires-Alj M: **Can phosphatidylinositol 3-kinase/mammalian target of rapamycin inhibition ERase them all?** *Breast Cancer Research* 2010, **12:**315.

Frimorfo Report

frimorfo®

CONFIDENTIAL

Phenotyping of mice

Study for Dominique Meyer,
FMI Basel

Experiment 112/10

June 30, 2010

Definitive report

Frimorfo Inc.
Ch.du Musée 12
PO BOX 191
CH – 1705 Fribourg
Switzerland
T. +41 26 300 85 30
F. +41 26 300 96 68

info@frimorfo.com
www.frimorfo.com

frimorfo®

1. Summary

Mice with a conditional expression of a transgene induced upon tamoxifen administration die within 6-7 days. The major visible phenotype is the appearance of hematomas.

Hematological and clinico-chemical parameters were measured and selected organs were studied histologically.

No difference between WT and TG mice was found in the blood smear, platelet count and in bleeding and coagulation tests. The histology of the vessels was not overtly pathologic, but neo-vascularization was observed. Clinical chemistry parameters indicate liver (and pancreas) derangements.

Date work performed:	January - June 2010

Frimorfo Inc.
Ch.du Musée 12
PO BOX 191
CH – 1705 Fribourg
Switzerland
T. +41 26 300 85 30
F. +41 26 300 96 68

info@frimorfo.com
www.frimorfo.com

frimorfo®

2. Contents

1. Summary 2
2. Contents 3
3. Introduction 4
4. Materials and Methods 4
5. Results 5
6. Discussion 10
7. Comments 10

Frimorfo Inc.
Ch.du Musée 12
PO BOX 191
CH – 1705 Fribourg
Switzerland
T. +41 26 300 85 30
F. +41 26 300 96 68

info@frimorfo.com
www.frimorfo.com

frimorfo®

3. Introduction

Dominique Meyer asked Frimorfo to clarify the bleeding phenotype of a transgene mouse line. Bleeding- and coagulation test, blood smears as well as blood chemistry and histology were performed.

4. Materials and Methods

4.1 Tissue samples

Animal	Genome	Received	Bleeding time	Hematology	Clinical chemistry	Histology
1	WT	27.1.10	X	X		X
2	WT	"	X	X		
3	WT	"	X	X		
4	Tg	"	Died early	(X)		X
5	Tg	"	X	X		X
6	Tg	"	X	X		X
7	Tg	"	X	X		
1a	WT	18.2.10		X	X	X
2a	WT	"			X	
3a	WT	"	X	X	X	X
4a	Tg	"		X	X	
5a	Tg	"		X	X	X
6a	Tg	"	X	X	X	X
7a	Tg	"			X	X
8	Tg	27.5		X autom	X	X
9	Tg	"		X autom	X	X
10	Tg	"		X autom	X	
11	WT	"		X autom	X	X
12	WT	"		X autom	X	
13	WT	"		X autom	X	

Table 1: Animal identification: summary of the studied mice and of the test performed.

Frimorfo Inc.
Ch.du Musée 12
PO BOX 191
CH – 1705 Fribourg
Switzerland
T. +41 26 300 85 30
F. +41 26 300 96 68

info@frimorfo.com
www.frimorfo.com

4.2 Bleeding time

Bleeding time was studied by the tail cutting method (Duke method), always comparing in parallel one WT and one Tg mouse.

4.3 Coagulation tests

The Quick-test and the partial thromboplastin time (PTT) were measured in the pooled blood of WT (1a-3a) and Tg (4a-7a) mice. Fibrinogen concentration was assessed in the plasma of mice 8 to 13.

frimorfo®

4.4 Hematology

Parameters concerning red and white blood corpuscle as well as thrombocytes were evaluated on separate blood smears of each animal. Hematology was repeated on animals 8-13 with a Abbott "CELL-DYN Sapphire" automat.

4.5 Clinical chemistry

The serum of 3 WT and 4 Tg mice of the second shipment was pooled to allow determination of 21 parameters at the same time. The pathologic parameters were measured again, but separately in the plasma of mice 8-13.

4.6 Histology

Tissue and organ pieces, some containing visible hematomas, were dissected, fixed with 4% buffered formalin and embedded in Paraffin. 3 μm sections were cut with a microtome and stained with Hematoxylin-Eosin and for elastin. For mice 8-13, the bone marrow of the sternum was evaluated histopathologically.

5. Results

General Observations:

At their arrival the transgenic mice could be recognized by their unhealthy appearance. One died after a few hours (number 4). All the others were sacrificed one day later.

Frimorfo Inc.
Ch.du Musée 12
PO BOX 191
CH – 1705 Fribourg
Switzerland
T. +41 26 300 85 30
F. +41 26 300 96 68

info@frimorfo.com
www.frimorfo.com

5.1 Bleeding time

The bleeding time with the Duke (dabbing away) method was of 7 +/- 2 minutes in both WT and Tg mice.

5.2 Coagulation

No differences between WT and Tg were found either in the Quick-test, nor in the activated PTT (Table 2).

frimorfo®

	WT	Tg
TP % Quick	> 130	> 130
TP INR	<1.0	<1.0
PTT sec	39.8	36.5

Table 2: Quick-test and partial thomboplastin time (PTT). INR: international normalized ratio.

5.3 Hematology

No major differences between WT and Tg mouse were found by visual inspection of the blood smears (*see Table 3 of the previous, preliminary report*). This test was repeated in the 6 last animals using an automated Abbot-system (Table 3).

	Tg			WT		
	8	**9**	**10**	**11**	**12**	**13**
Leucocytes (G/l)	3.8	6.7	6.8	3.87	6	6.87
Erythrocytes (T/l)	8.19	8.64	8.73	8.46	8.43	8.73
Haemoglobin (g/l)	134	148	141	142	140	146
Haematocrit (l/l)	0.41	0.44	0.43	0.44	0.44	0.46
MCV (fl)	50	51	50	51	52	52
MCH (pg)	16	17	16	17	17	17
MCHC (g/l)	330	335	326	327	321	321
RDW (% anisocytose)	11	12	12	12	13	12
Platelets (G/l)	1131	1080	1035	1167	1116	1218

Table 3: Hematologic analysis of the blood of mice 8-13 with an Abbot Cell-Dyn Sapphyre automate.

5.4 Clinical chemistry

Major differences were detected in liver (GOT, GPT) and pancreas parameters (amylase) of the pooled plasma of animals 1a-3a, respectively 4a-7a (Table 4).

	WT Pooled	**Tg pooled**	**Units**
Cl	110.5	116.5	mmol/L
K	4.3	3.7	mmol/L
Na	151	156	mmol/L
BiliT	1.3	0.8	µmol/L
ALB	26.7	29.8	g/L

Frimorfo Inc.
Ch.du Musée 12
PO BOX 191
CH – 1705 Fribourg
Switzerland
T. +41 26 300 85 30
F. +41 26 300 96 68

info@frimorfo.com
www.frimorfo.com

frimorfo®

Amyl	1411	**2062**	U/L
Ca	2.27	2.56	mmol/L
Chol	2	2.7	mmol/L
CK	505	300	U/L
Glu	15.3	**7.3**	mmol/L
GOT	77	**139**	U/L
GPT	36	**85**	U/L
Lip	23	33	U/L
P	2.55	3.07	mmol/L
Mg	0.96	1.07	mmol/L
Trig	4.2	**0.68**	mmol/L
Uree	6.5	6.7	mmol/L
Uacid	35	27	µmol/L
CreaJ	<18	<18	µmol/L
LDH	355	346	U/L
PAL	330	334	U/L

Table 4: Values of different enzymes, ions and other components in the pooled plasma of Wt (1a-3a) and transgenic (4a-7a) mice. The lower glucose and triglyceride level may be explained by the experimental situation.

These results, measured in the pooled plasma, were repeated on separate plasma samples (Table 5)

	Tg			WT			
	8	**9**	**10**	**11**	**12**	**13**	**Units**
GLU	3.62	4.96	4.62	7.89	10.26	10.08	mM
TRIG	0.52	0.36	0.7	2.64	2.77	1.98	mM
GOT	132	81	107	66	50	42	U/L
GPT	66	30	77	26	28	19	U/L
AMYL	11'365	1834	4322	1922	1799	1802	mmol/L

Table 5: Values of different liver and pancreas enzymes. The results of the single blood samples confirm the results gained with the pooled blood.

The concentration of Fibrinogen in the mice plasma of the last shipment was:

	Value	**Genotype**	**Units**
8	2.3	Tg	g/L
9	3.1		
10	1		
11	1	WT	
12	1.5		
13	1.5		

Frimorfo Inc.
Ch.du Musée 12
PO BOX 191
CH – 1705 Fribourg
Switzerland
T. +41 26 300 85 30
F. +41 26 300 96 68

info@frimorfo.com
www.frimorfo.com

frimorfo®

5.5 Histology

Hematomas were mainly observed in the skin (ear [Fig. 1 B and 1D], tail, nose), but also found in the nasal cavity, in the intestinal wall, uterine tube, brain (Fig. 1F) and liver. Histologically fresh and old hematomas were observed. Both cases are depicted in the following pictures (Figs 1B and 1D). Besides focal hemorrhages and hematoma, ectatic vessels (probably venous vessels) were noted in the mice Tg-1, -6 and -7. Individual vessels were affected to different degree. Changes varied from slight to pronounced, cystic dilation. In mouse Tg-6 there was suspicion of remnants of a vessel wall in the area of the hematoma suggesting rupture of an affected vessel.

Fig 1A: Ear lobe of mouse WT 1. Axially located cartilage surrounded by skin. X100

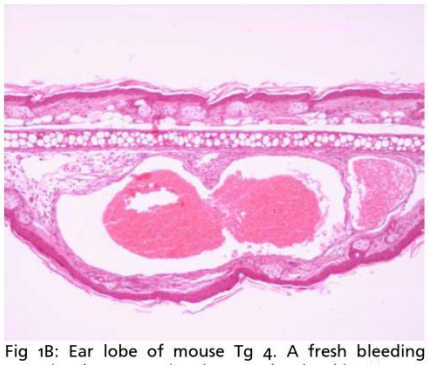

Fig 1B: Ear lobe of mouse Tg 4. A fresh bleeding occupies the connective tissue under the skin. X100

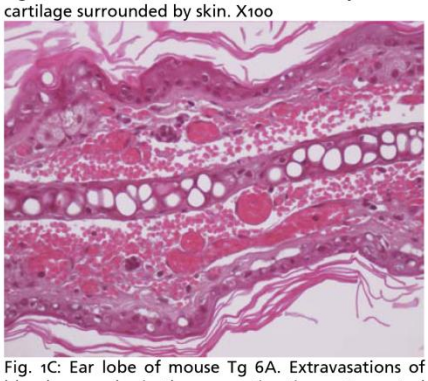

Fig. 1C: Ear lobe of mouse Tg 6A. Extravasations of blood-corpuscles in the connective tissue. Congested veins. X400.

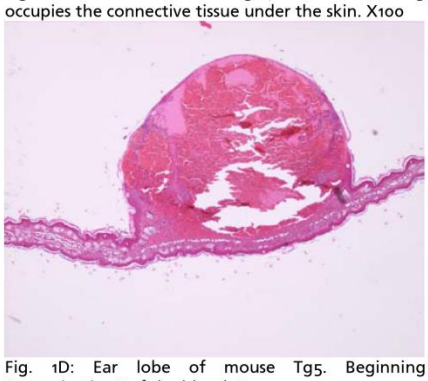

Fig. 1D: Ear lobe of mouse Tg5. Beginning "organization" of the blood. X 100

Frimorfo Inc.
Ch.du Musée 12
PO BOX 191
CH – 1705 Fribourg
Switzerland
T. +41 26 300 85 30
F. +41 26 300 96 68

info@frimorfo.com
www.frimorfo.com

frimorfo®

Fig. 1E: Liver of mouse Tg 5. Congested veins. X 100

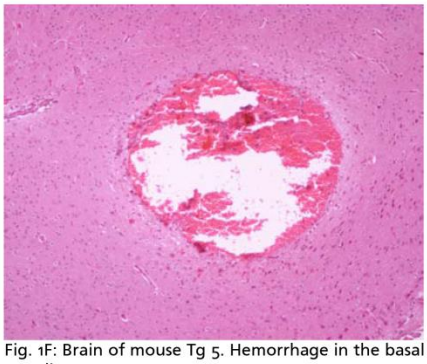

Fig. 1F: Brain of mouse Tg 5. Hemorrhage in the basal ganglia

In the last group of Tg animals (8-10; Figs. 1G and 1H) the vascular lesions consisted of angiectasia, thrombi formation and focal angiomatous hyperplasia. Most of the thrombi were in the stage of organization. The angiomatous hyperplasia noted in 2 mice might be a consequence of neovascularization of thrombotic vessels.

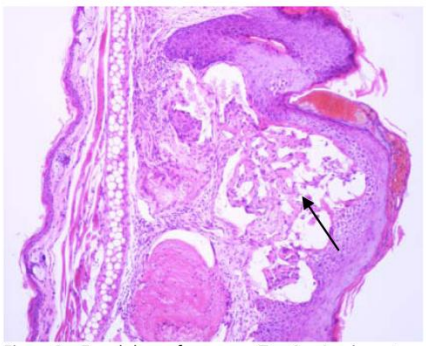

Fig. 1G: Ear lobe of mouse Tg 8. Angiomatous hyperplasia (arrow).

Fig. 1H: Ear lobe of mouse Tg 9. Angiomatous hyperplasia (arrow).

The bone marrows examined, particularly the megakaryoblasts, were histopathologically unremarkable.

Frimorfo Inc.
Ch.du Musée 12
PO BOX 191
CH – 1705 Fribourg
Switzerland
T. +41 26 300 85 30
F. +41 26 300 96 68

info@frimorfo.com
www.frimorfo.com

frimorfo®

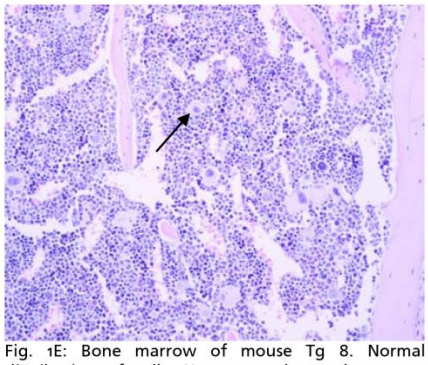

Fig. 1E: Bone marrow of mouse Tg 8. Normal distribution of cells. Note normal megakaryocytes (arrow). HE-stain X 100

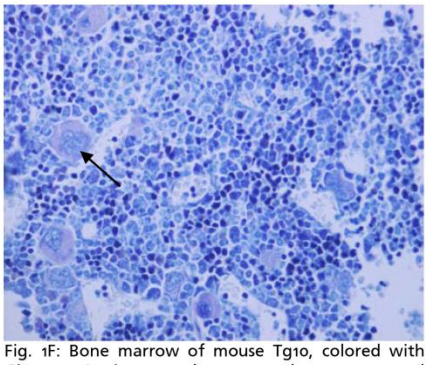

Fig. 1F: Bone marrow of mouse Tg10, colored with Giemsa. Again, megakaryocytes have a normal structure (arrow).

6. Discussion

A platelet problem is to exclude in view of their normal percentage in blood smear, a bleeding time in the normal range and the normal bone marrow histology. The coagulation cascade is also not involved since Quick-time and TPP are comparable in Tg and WT mice. The fibrinogen concentration is higher in Tg mice (2 out of 3) than in WT-mice. Clinical chemical analysis of plasma has revealed pathologic values for liver (and pancreas) enzymes. Histology has not shown major anomalies in the vessel wall. In the animals of the last shipment a neovascularization of thrombotic vessels was taking place. A cause of the vascular dilation (vessel wall weakness, right heart failure?) in certain cases could not be identified.

Frimorfo Inc.
Ch.du Musée 12
PO BOX 191
CH – 1705 Fribourg
Switzerland
T. +41 26 300 85 30
F. +41 26 300 96 68

info@frimorfo.com
www.frimorfo.com

7. Comments

Our examination allows concluding that bleeding time and blood coagulation are not affected in these mice. The activation of the transgene seems to affect various organs (liver, pancreas, cardiovascular system [blood vessels]). The cause for the hematomas and of the premature death remains unclear.

Curriculum Vitae

CURRICULUM VITAE Dominique Meyer

PERSONAL INFORMATION

Office address: Friedrich Miescher Institute for Biomedical Research
Maulbeerstrasse 66
CH-4058 Basel (Switzerland)
Mail: dominique.meyer@fmi.ch
Phone: +41 61 697 66 92

Date of Birth: 29.07.1981
Citizenship: Swiss
Marital status: Single

EDUCATION

2006-present **Ph.D. Biochemistry, Department of Signaling & Cancer**, Friedrich Miescher Institute for Biomedical Research, Basel, Switzerland; Research Topic: **The Role of Mutant p110α in Mammary Tumorigenesis**. Supervision: Dr. Mohamed Bentires-Alj.

2004-2005 M.Sc. Molecular Biology, Department of Microbiology, Biozentrum, Basel, Switzerland; Research Topic: Characterization of a Gene Cluster Involved in *C. crescentus* Holdfast Formation and Timing During Development. Supervision: Prof. Dr. Urs Jenal.

2001-2004 B.Sc. Biology, Major in Molecular Biology, University of Basel, Basel, Switzerland

ADDITIONAL TRAINING

Education for persons carrying out animal experiments (FELASA-Category B)

Biosafety course (2007), at the FMI, Basel, Switzerland

Instruction course in “Immunohistochemistry basics” (2009), at the FMI, Basel, Switzerland

Instruction course in statistical analysis using R (2009), at the FMI, Basel, Switzerland

Introduction course into MATLAB (2011), at the FMI, Basel, Switzerland

LANGUAGES

German: first language
English: very good knowledge
French: good knowledge

CONFERENCES ATTENDED

FMI Annual Meeting 2007-2010, Switzerland

ENBDC Workshop 2010, Lucerne, Switzerland

Targeting the PI3-Kinase Pathway in Cancer 2008, Cambridge MA, USA

Targeting the Kinome 2006, Basel, Switzerland

PUBLICATIONS

Meyer DS, Brinkhaus H, Müller U, Müller M, Cardiff RD, Bentires-Alj M.: **Luminal Expression of *PIK3CA* Mutant H1047R in the Mammary Gland Induces Heterogeneous Tumors.** Cancer Res. 2011 Apr 11. PMID:21482677

Meyer DS, Bentires-Alj M.: **Can phosphatidylinositol 3-kinase/mammalian target of rapamycin inhibition ERase them all?** Breast Cancer Res. 2010 Oct 20;12(5):315. PMID:21062517

Meyer DS, Brinkhaus H, Müller U, Müller M, Cardiff RD, Bentires-Alj M.: **Role of *PIK3CA* Mutant E545K in Mammary Gland Tumorigenesis**. In preparation.

Meyer DS, Brinkhaus H, Müller U, Bentires-Alj M.: **The Receptor Protein Tyrosine Phosphatase Alpha is Dispensable for ErbB2-Induced Mammary Tumorigenesis**. In preparation.

WORKING EXPERIENCE

- Broad range of techniques in molecular biology and biochemistry
- Cell culture (monolayer, three-dimensional cell cultures and suspension cultures)
- Experience in mouse genetics: Generation and characterization of novel mouse models of breast cancer
- Experience in mouse experiments: Fat pad clearing, mammary gland transplantation, and orthotopic xenografting of human breast cancer cells
- Immunohistochemistry and analysis/quantification of immunostained tumor sections
- Microarray and pathway analysis using Ingenuity
- Microsoft Office programs, Endnote, Adobe Photoshop and Illustrator, VectorNTI, and imaging softwares including AxioVision and Image-Pro

REFERENCES

Mohamed Bentires-Alj, Ph.D.
Friedrich Miescher Institute for Biomedical Research
Maulbeerstrasse 66
P.O. Box 2543
CH-4002 Basel / Switzerland
T: +41 61 697 40 48, Fax: +41 61 697 39 76
bentires@fmi.ch

Nancy E. Hynes, Ph.D., Prof.
Friedrich Miescher Institute for Biomedical Research
Maulbeerstrasse 66
P.O. Box 2543
CH-4002 Basel / Switzerland
T: +41 61 697 81 07, Fax: +41 61 697 39 76
nancy.hynes@fmi.ch

Christoph Rochlitz, M.D., Prof.
Department of Biomedicine
University Hospital Basel
Hebelstrasse 20
CH-4031 Basel / Switzerland
T: +41 61 265 50 59, Fax: +41 61 265 53 16
crochlitz@uhbs.ch

Saskia Brachmann, Ph.D.
Novartis Pharma AG, Werk Klybeck
Postfach
CH-4002 Basel / Switzerland
T: +41 61 696 40 63
saskia.brachmann@novartis.com